A low-energy effective Hamiltonian for Landau quasiparticles

Pierre-Louis Taillat[1⋆], Hadrien Kurkjian[1†]

1 Laboratoire de Physique Théorique de la Matière Condensée, Sorbonne Université, CNRS, 75005, Paris, France

⋆ pierre-louis.taillat@sorbonne-universite.fr , † hadrien.kurkjian@cnrs.fr

November 21, 2025

Abstract

We introduce a new renormalisation scheme to construct the Landau quasiparticles of Fermi fluids. The scheme relies on an energy cutoff Λ which removes the quasi-resonant couplings, enabling the dressing of the particles into quasiparticles via a unitary transformation. The dynamics of the quasiparticles is then restricted to low-energy transitions and is fully determined by an effective Hamiltonian which unifies the Landau interaction function f and the collision amplitude in a single amplitude $\mathcal{A}$ regularized by Λ. Our effective theory captures all the low-energy physics of Fermi fluids that support Landau quasiparticles, from the equation of state to the transport properties, both in the normal and in the superfluid phase. We apply it to an atomic Fermi gas with contact interaction to compute the speed of zero sound in function of the scattering length a. We also recover the Gork'ov-Melik Barkhudarov correction to the superfluid gap and critical temperature as a direct consequence of the dressing of particles into Landau quasiparticles.

Contents

Introduction

Originally formulated as a phenomenological theory, Fermi liquid theory is based on a quadratic action [1], in which fermionic quasiparticles are described by a semiclassical density field δn fluctuating about the Fermi sea and interacting through a static interaction function f. The physical origin of quasiparticles is not elucidated; their existence is merely justified by the heuristic assumption that the noninteracting states can be adiabatically followed when interactions are switched on [2]. When Landau's semi-classical action becomes insufficient—for instance to describe the transport phenomena or the superfluid transition—additional phenomenological parameters are introduced [3], such as a collision or pairing amplitude. Microscopic approaches were later proposed [4–6] to interpret the parameters of Landau's theory in terms of two-particle correlation functions, which relies in particular on the introduction of a quasiparticle residue.

In a more modern perspective, Landau's theory has been reinterpreted as a low-energy effective theory emerging from a renormalization process [7–12]. This moves beyond the phenomenological nature of the theory and provides it with a fundamental justification. In the renormalization picture, the quasiparticle energies and interactions arise from the progressive integration of the high-energy degrees of freedom. Although the renormalization group generates in principle a complete effective action for the quasiparticle field, in practice one follows Landau's original formulation by concentrating on specific "interaction channels", i.e., restrictions of the quasiparticle scattering processes to specific geometries [13, 14]. The forward-scattering channel collects the collisions in which the scattering angle tends to zero; the pairing or Bardeen–Cooper–Schrieffer (BCS) channel describes head-on collisions, where the angle of incidence approaches π. Restricting the attention to such channels is insufficient in three-dimensional (3D) Fermi liquids, where resonant collisions between quasiparticles of the Fermi surface are not limited to small momentum transfers nor to small center-of-mass momenta. In 3D, the collision probability depends on two independent angles, in contrast to the static interaction function f, which depends only on the angle between the quasiparticle momenta $\mathbf{p}$ and $\mathbf{p}'$. In this respect, the 3D case is fundamentally different from its 2D counterpart, where resonant collisions depend on a single angle and thus fall into either one of the two channels [15, 16]. Although effective-theory approaches are a natural starting point to derive the quasiparticle transport equation, and thus access the density and polarization response functions, they are often restricted to the collisionless regime, neglecting the ergodic processes contained in the collision integral. An effective theory that fully captures the Boltzmann equation of the Fermi liquid would then be particularly valuable, for instance to assess the corrections to transport properties beyond the Born–Markov approximation [17].

In fact, a convincing low-energy effective theory should be able to describe, within a unified formalism, all low-energy phenomena, from the low-temperature thermodynamics to the hydrodynamic equations, in both the normal and superfluid phases (provided that superfluidity itself remains a low-energy phenomenon). In this work, we construct an effective Hamiltonian that captures the full dynamics of Landau quasiparticles, and thereby the whole low-energy physics of fermionic fluids in which these quasiparticles are well defined. Our formalism relies on a unitary transformation that connects the quasiparticle states to the noninteracting Fock states; such unitary transformations are common in atomic physics [18–20] when one applies a perturbation to multiplets of quasidegenerate energy levels. Our construction of the quasiparticle states thus excludes from the dressing any quasidegenerate state in a narrow energy band of width Λ. The unitary operator $\exp(\hat{S})$ of this dressing block-diagonalizes the Hamiltonian, thereby decoupling levels whose energy separation exceeds Λ. This is not the same as introducing a momentum cutoff [7–12], and the renormalization group generated by infinitesimal variations of Λ is different. To ensure that the physical quantities predicted by the effective theory are independent of Λ, the cutoff must be small compared to the Fermi energy ϵ_{F} yet remain large compared to the typical evolution frequencies of the fluid, such as the quasiparticle damping rate Γ in the normal phase, or the gap Δ in the superfluid phase. In Heisenberg picture, the transformation generated by $\hat{S}$ relates particle operators to their quasiparticle counterparts; this allows us in particular to construct the quasiparticle annihilation operator $\hat{\gamma}$ [6].

The adiabaticity condition usually invoked to justify the existence of the quasiparticles translates, in our formalism, into a condition of weak mixing between (significantly coupled) energy levels. Two quasiparticle states must be resonant at the scale Λ if and only if the corresponding particle states are resonant as well. In a generic many-body system, this condition would restrict the theory to the lowest orders of perturbation theory. In a Fermi liquid, it remains valid all the way to the strongly interacting regime, and the dressed states, free from low-energy couplings, can be followed adiabatically. The conservation of a spectrum that vanishes linearly at the Fermi level thus appears as a necessary condition to the existence of Landau quasiparticles.

Our unitary transformation constructs the low-energy effective theory by a direct renormalisation of the underlying microscopic theory, without introducing emergent degrees of freedom. The renormalisation group emerging from the infinitesimal generator $\hat{S}(\Lambda)-\hat{S}(\Lambda-\mathrm{d}\Lambda)$ [21, 22] acts on the full Hamiltonian. It is not restricted to a gradient expansion, nor to an expansion in powers of the quasiparticle field $\hat{\gamma}$. Only after the renormalization procedure do we expand the Hamiltonian in powers of the fluctuations $\delta(\hat{\gamma}^\dagger\hat{\gamma})$ of the density field about its expectation value in the quasiparticle Fermi sea (defined as the image of the non-interacting Fermi sea through the unitary transform). The effective Hamiltonian obtained in this way is not limited to specific interaction channels: its diagonal part in the Fock basis coincides with Landau's semi-classical Hamiltonian, but its off-diagonal part contains the generic collision amplitude. It allows us to derive the Boltzmann equation—including the collision integral—without leaving the effective picture, i.e., without returning to particle Green's functions and without using the quasiparticle residue. The Born–Markov approximation can be used to truncate the Bogoliubov–Born–Green–Kirkwood–Yvon (BBGKY) hierarchy in the quasiparticle picture, even though the problem is strongly correlated in the particle picture.

Our construction of an effective Hamiltonian for Fermi fluids is motivated by experimental considerations, particularly in the context of ultracold atomic gases. The Fermi gas with contact interactions, long considered as an academic model [23–25], can nowadays be prepared and manipulated with great flexibility using laser trapping techniques [26–30]. At low temperature, its microscopic physics is fully characterized by the scattering length a of the contact interactions, which therefore fixes all the parameters of our low-energy effective theory. While it supports Landau quasiparticles only in the weakly-interacting regime ($a \to 0$), the contact gas gives access to several observables whose dependence on a is highly nontrivial. The Landau quasiparticles are then a powerful, and likely inevitable, heuristic tool to derive quantitatively predictions of mesurable quantities such as the velocity and damping of zero sound [31], the transport coefficients [24, 32], or the collective modes of the superfluid [33, 34].

This article is divided into three sections.

In Section 1, we construct the low-energy effective theory of Landau quasiparticles. We introduce the unitary transformation that allows us to define the quasiparticle Fock states, the operators acting on these states, and in particular their effective Hamiltonian. We illustrate our formalism by applying it perturbatively to the Fermi gas with contact interactions. We compute to second order in $k_\mathrm{F}a$ the effective parameters of the theory: the quasiparticle energy, the interaction functions, and the collision amplitude. Finally, we return to a more general framework and derive the quasiparticle Boltzmann equation from the effective Hamiltonian.

In Section 2, we study the density and spin responses of the contact Fermi gas. In particular, we analyze the collisionless regime and compute the expansion of the zero-sound velocity c_0 in powers of the interaction strength $k_\mathrm{F}a$. A major result is the presence of a log-perturbative correction in the deviation c_0-v_F between this velocity and the Fermi velocity v_F, which results into a prefactor $\exp(6)$ for the density mode and $\exp(-2)$ for the spin mode. We further investigate the role of collisions on zero sound and show that they lead to a collisional damping proportional to $1/\tau$, where τ is the mean collision time. This damping is universal in the sense that its dependence on $k_\mathrm{F}a$ enters only through τ. Finally, we present a numerical method that solves the transport equation exactly throughout the crossover from the hydrodynamic to the collisionless regime.

In Section 3, we show that the effective theory describes the superfluid instability and the paired ground state. We express the zero-temperature order parameter Δ and the critical temperature T_c in terms of a parameter $\alpha_{\uparrow\downarrow}$ appearing in the effective Hamiltonian, which corresponds to the residual value of the collision amplitude $\mathcal{A}_{\uparrow\downarrow}$ regularized of its logarithmic divergence in Λ [7, 10, 35, 36]. We then apply this result to the contact gas: by computing the pairing parameter $\alpha_{\uparrow\downarrow}$ to order $(k_F a)^2$, we obtain a log-perturbative correction to the BCS gap and critical temperature, a correction that coincides with the result of Gor'kov and Melik-Barkhudarov [37].

1 The low-energy effective Hamiltonian of Fermi liquids

We consider a 3D fluid made of N spin-1/2 fermionic particles evolving in a volume $\mathcal{V}$ under the Hamiltonian

$$\hat{H} = \hat{H}_0 + \hat{V} \tag{1}$$

This section will discuss the construction of the Landau quasiparticles on general grounds, so we make minimal assumptions on the form of $\hat{H}$. We write the generic noninteracting Hamiltonian and the generic two-body interaction between opposite spin fermions as

$$\hat{H}_0 = \sum_{\alpha\in\mathcal{D}\sigma} \omega_{\alpha\sigma} \hat{a}^\dagger_{\alpha\sigma} \hat{a}_{\alpha\sigma} \tag{2}$$

$$\hat{V} = \sum_{\alpha\beta\gamma\delta\in\mathcal{D}} V(\alpha,\beta|\gamma,\delta) \hat{a}^\dagger_{\alpha\uparrow} \hat{a}^\dagger_{\beta\downarrow} \hat{a}_{\gamma\downarrow} \hat{a}_{\delta\uparrow} \tag{3}$$

where $\hat{a}_{\alpha\uparrow}$ annihilates a fermion of spin σ in mode α. We use $\hbar = k_B = 1$ throughout this article. This implies that momenta p and wavenumber k are not differentiated, in particular $p_F = k_F$ for the Fermi momentum/wavenumber.

1.1 Landau quasiparticles in quasi-degenerate perturbation theory

The quasiparticles states are often viewed [2, 38] as the states in which the eigenstates of $\hat{H}_0$ evolve after an adiabatic ramp of the interactions of the form $\hat{V}(t) = \lambda(t)\hat{V}$, with $\lambda(0) = 0$ and $\lambda(t_f) = 1$. It is then argued that the ramping time t_f [2] should be long enough to ensure an adiabatic evolution, but short enough to prevent the quasiparticle decay. This picture is problematic since the existence of a finite time t_f fulfilling the adiabatic theorem [39] is questionable in a gapless, strongly-interacting fluid. Instead, we develop here a rigorous method to construct the quasiparticles states from the eigenstates of $\hat{H}_0$, and to continuously follow them from the non-interacting to the strongly-interacting regime.

Given an eigenstate $|n\rangle_0$ of $\hat{H}_0$, we decompose the rest of the eigenstates of $\hat{H}_0$ into *quasidegenerate* and *energetically well-separated* states. An eigenstate $|m\rangle_0$ is quasidegenerate with $|n\rangle_0$ if its energy E_m^0 is within a narrow energy band Λ, $|E_n^0 - E_m^0| \ll \Lambda$, and it is well-separated if $|E_n^0 - E_m^0| \gg \Lambda$. One can then construct the quasiparticle states by a unitary transformation $|n\rangle = e^{\hat{S}}|n\rangle_0$, where we impose that the hermitian operator $\hat{S}$ has no matrix elements between quasidegenerate states. This construction is similar to the van Vleck transformation in quasi-degenerate perturbation theory [18–20, 40].

Rather than an adiabaticity condition, the possibility of such a construction is tied to a *non-crossing* condition: the only level crossings[1] that occur as interactions are increased should be between states $|n\rangle$ and $|m\rangle$ that are already quasidegenerate in the non-interacting state, *i.e.*

$$|E_n - E_m| \ll \Lambda \iff |E_n^0 - E_m^0| \ll \Lambda \tag{4}$$

This is a reformulation of the usual assumption that the (low-energy) quasiparticles have a gapless spectrum similar to the spectrum of the particles in the ideal Fermi gas.

[1] Our acceptation of level crossings is restricted to states $|n\rangle_0$ and $|m\rangle_0$ that are significantly coupled by $\hat{V}$. In the thermodynamic limit, this excludes in particular states with different densities of excitation.

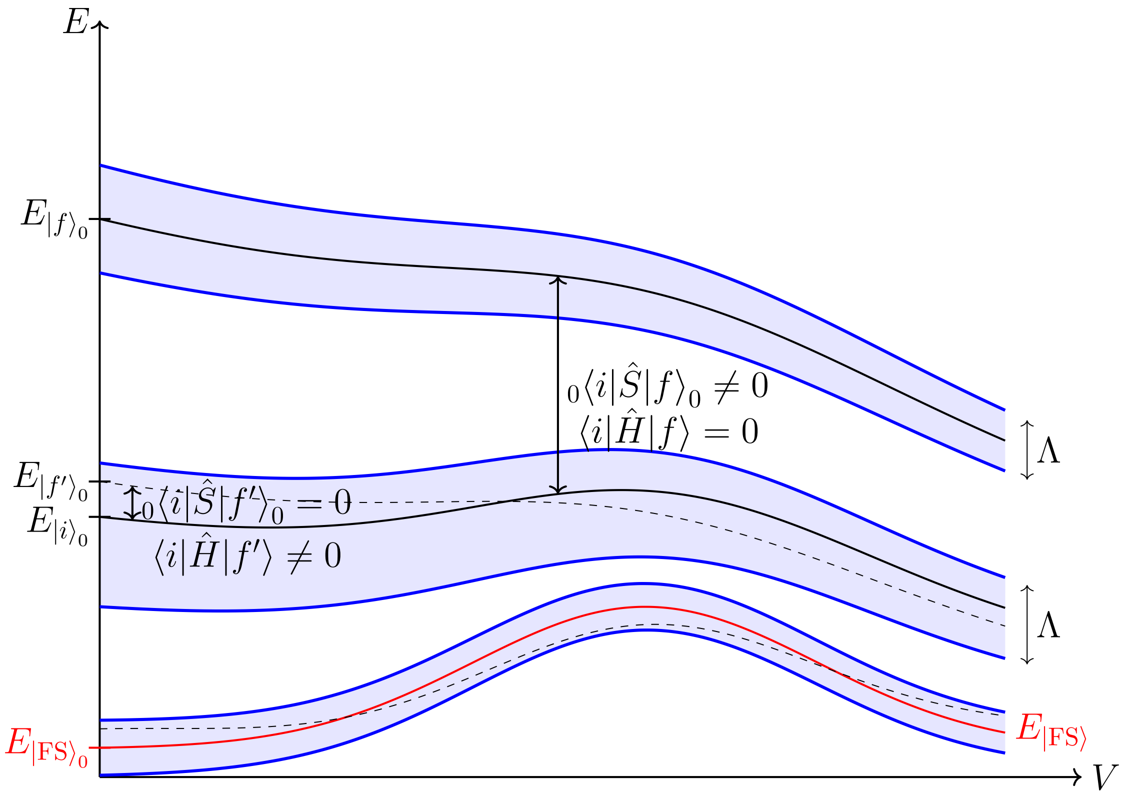

Figure 1: Construction of the quasiparticle states within quasi-degenerate perturbation theory. An unpertubed Fock state $|i\rangle_0$ is dressed via the operator $\hat{S}$ by its interactions with the off-resonant states $|f\rangle_0$, whose unperturbed energy verifies $|E_{|f\rangle_0} - E_{|i\rangle_0}| > \Lambda$ (here $E_{|\psi\rangle_0} = {}_0\langle\psi|\hat{H}_0|\psi\rangle_0$). The dressed state $|i\rangle$ can then be followed adiabatically as the interaction strength V increases. However, due to its incomplete dressing, it is not an eigenstate of $\hat{H}$, and it remains coupled to the nearly degenerate states $|f'\rangle$ of energies $|E_{|f'\rangle} - E_{|i\rangle}| < \Lambda$, (here $E_{|\psi\rangle} = \langle\psi|\hat{H}|\psi\rangle$). This construction applies in particular to the particle Fermi sea $|\mathrm{FS}\rangle_0$, which evolves into a quasiparticle Fermi sea $|\mathrm{FS}\rangle$ (red curve). In general the quasiparticle Fermi sea is not the ground state of $\hat{H}$, and therefore not the ground state of our effective Hamiltonian.

Clearly, the quasiparticle states $|n\rangle$ are not the exact eigenstates of $\hat{H}$ since there remain quasi on-shell couplings between them, $\langle n|\hat{H}|m\rangle \neq 0$ if $|E_n - E_m| \ll \Lambda$. These coupling ensure that the quasiparticle states, which are described by the same quantum numbers as the noninteracting states (*i.e.* the set of fermionic occupation numbers $\{n_{\alpha\sigma}\}_{\alpha\sigma}$), decay to the ergodic eigenstates. In this picture the eigenstates appear as ergodic mixtures of all quasiparticle states at energy E, in accordance with the Eigenstate Thermalization Hypothesis [41].

The cutoff Λ used to construct the quasiparticle description should be tuned so that all physical quantities are independent of it. This constrains it to a plateau between a low- and a high-energy bound. As an upper bound we want Λ to single-out the low-energy region, and incorporate in it the off-resonant couplings from the high-energy part of the spectrum. This is achieved by

$$\Lambda \ll \epsilon_{\mathrm{F}} \tag{5}$$

As a lower-bound, we want the couplings between quasiparticle states to vary smoothly over the frequencies at which the system evolves. In the case of an isolated system prepared in some excited quasiparticle state, the evolution frequencies are set by the intrinsic decay rate

$\Gamma_{\rm typ}$ of the quasiparticles. In the case of a system driven at frequency $\omega_{\rm ext}$ by an external force, all the transitions due to the external force should remain in the same Λ shell:

$$\Gamma_{\rm typ},\ \omega_{\rm ext} \ll \Lambda \tag{6}$$

This inequality, combined with Eq. (5), constrains the states and the frequencies that one can excite without breaking the quasiparticle description.

1.1.1 Partition of the Hilbert space and unitary transformation

To classify the quasidegenerate and well-separated states, we introduce the projector

$$\hat{P}_\Lambda(E) = \sum_{|n\rangle_0} \Pi_\Lambda(E - \hat{H}_0)|n\rangle_0\langle n|_0 \tag{7}$$

where the summation runs over the eigenstates $|n\rangle_0$ of $\hat{H}_0$. As long as the filtering function $\Pi_\Lambda(E)$ verifies that $\Pi_\Lambda(E \ll \Lambda) = 1$ and $\Pi_\Lambda(E \gg \Lambda) = 0$, its precise shape does not matter. We shall thus use

$$\Pi_\Lambda(E) = \begin{cases} 1 & \text{if } |E| \leq \Lambda \\ 0 & \text{else} \end{cases} \tag{8}$$

To defined the properties of the quasiparticles, we will focus on the energy shell centered around the energy E_0^0 of the particle Fermi sea $|\mathrm{FS}\rangle_0$ (the ground state of $\hat{H}_0$ at fixed chemical potential μ). However, we want our description to apply to states, such as thermal or superfluid states, that have a macroscopic excitation or condensation energy, obtained through the excitation of a macroscopic number of low-energy quasiparticles. We therefore slice the whole spectrum into Λ shells centered around $E_n = E_0^0 + 2n\Lambda$ with $n \in \mathbb{Z}$. The projector onto the n-th energy window is

$$\hat{P}_n = \hat{P}_\Lambda(E_n) \tag{9}$$

with $\hat{P}_0$ projecting onto the shell of the Fermi sea.

We then construct an antihermitian operator $\hat{S}$

$$\hat{S}^\dagger = -\hat{S} \tag{10}$$

which generates the quasiparticle states by a unitary transform applied to the eigenstates $|n\rangle_0$ of $\hat{H}_0$:

$$|n\rangle = \mathrm{e}^{\hat{S}}|n\rangle_0 \tag{11}$$

This is the unitary, or canonical, van Vleck transformation [19] known in atomic and molecular physics [18, 20, 40]. The operator $\hat{S}$ couples only well-separated states, *i.e.* all its diagonal blocks vanish

$$\hat{P}_n\hat{S}\hat{P}_n = 0, \quad \text{for all } n \tag{12}$$

To construct the off-diagonal blocks $\hat{P}_m\hat{S}\hat{P}_n$, $m \neq n$, we impose that the couplings between transformed states vanish, $\langle m|\hat{H}|n\rangle = 0$, if $|n\rangle$ and $|m\rangle$ belong to different energy shells, that is, if $|E_n^0 - E_m^0| \gg \Lambda$. In other words, we impose that the effective Hamiltonian

$$\hat{H}_{\rm eff} = \mathrm{e}^{-\hat{S}}\hat{H}\mathrm{e}^{\hat{S}} \tag{13}$$

is block-diagonal:

$$\hat{P}_m\hat{H}_{\rm eff}\hat{P}_n = 0,\ n \neq m \tag{14}$$

At this stage, we view the effective Hamiltonian as the operator which, acting on the unperturbed basis, provides the matrix elements of $\hat{H}$ in the transformed basis:

$$\langle n|\hat{H}|m\rangle = {}_0\langle n|\hat{H}_{\rm eff}|m\rangle_0 \tag{15}$$

Using Baker-Campbell-Hausdorff formula, $\hat{H}_{\text{eff}}$ is expressed in terms of iterated commutators between $\hat{H}$ and $\hat{S}$:

$$\hat{H}_{\text{eff}} = \hat{H} + [\hat{H},\hat{S}] + \frac{1}{2}\big[[\hat{H},\hat{S}],\hat{S}\big] + \ldots \tag{16}$$

1.1.2 Perturbative calculation of $\hat{S}$ and $\hat{H}_{\text{eff}}$

When $\hat{V}$ is controlled by a small parameter, one can construct $\hat{S}$ and $\hat{H}_{\text{eff}}$ order-by-order in $\hat{V}$:

$$\hat{S} = \hat{S}_1 + \hat{S}_2 + \ldots \quad \text{where} \quad \hat{S}_1 = O(V),\ \hat{S}_2 = O(V^2), \ldots \tag{17}$$

Expanding condition (14) to first order in V, we obtain for example

$$\hat{P}_m \left(\hat{V} + [\hat{H}_0,\hat{S}_1]\right)\hat{P}_n = 0 \tag{18}$$

This relation provides the elements of $\hat{S}_1$ in the unperturbed basis:

$$_0\langle f|\hat{S}_1|i\rangle_0 = \begin{cases} \frac{_0\langle f|\hat{V}|i\rangle_0}{E_i^0 - E_f^0} & \text{if } |E_i^0 - E_f^0| \gg \Lambda \\ 0 & \text{if } |E_i^0 - E_f^0| \ll \Lambda \end{cases} \tag{19}$$

One can also express the restriction of $\hat{S}_1$ to a given energy shell $\hat{P}_n$ in terms of the unperturbed resolvent $\hat{G}_0(E) = 1/(E - \hat{H}_0)$ evaluated at the corresponding energy E_n of the shell:

$$\hat{S}_1\hat{P}_n \simeq \hat{Q}_n\left[\hat{G}_0(E_n)\hat{V}\right]\hat{P}_n \tag{20}$$

where $\hat{Q}_n = 1 - \hat{P}_n$ projects orthogonally to the shell. Note however that $\hat{S}$, unlike $\hat{G}_0$, does not depend on energy and allows to (block) diagonalize the whole spectrum, not just the vicinity of a particular energy level.

Injecting expansion (17) of $\hat{S}$, we obtain[2] a perturbative expression of the effective Hamiltonian:

$$\hat{P}_n\hat{H}_{\text{eff}}\hat{P}_n = \hat{P}_n\left(\hat{H}_0 + \hat{V} + \frac{1}{2}[\hat{V},\hat{S}_1] + O(V^3)\right)\hat{P}_n \tag{21}$$

1.1.3 Quasiparticle operators

The quasiparticle states are deduced from the particle Fock states $|\{n_{\alpha\sigma}\}\rangle_0$ through Eq. (11)

$$|\{n_{\alpha\sigma}\}\rangle = \mathrm{e}^{\hat{S}}|\{n_{\alpha\sigma}\}\rangle_0 \tag{22}$$

Switching to Heisenberg picture, $\hat{S}$ can be used to construct the operators acting on this new basis. Consider an operator $\hat{O}$ whose action is known in the unperturbed basis $|\{n_{\alpha\sigma}\}\rangle_0$. The operator $\hat{O}_\gamma$ having the same action in quasiparticle basis $|\{n_{\alpha\sigma}\}\rangle$ is then

$$\hat{O}_\gamma = \mathrm{e}^{\hat{S}}\hat{O}\mathrm{e}^{-\hat{S}} \tag{23}$$

Annihilation operator The most straightforward example is the quasiparticle annihilation operator $\hat{\gamma}$ which we construct from the particle annihilation operator $\hat{a}$ through

$$\hat{\gamma}_{\alpha\sigma} = \mathrm{e}^{\hat{S}}\hat{a}_{\alpha\sigma}\mathrm{e}^{-\hat{S}} = \hat{a}_{\alpha\sigma} + [\hat{S}_1,\hat{a}_{\alpha\sigma}] + [\hat{S}_2,\hat{a}_{\alpha\sigma}] + \frac{1}{2}\big[\hat{S}_1,[\hat{S}_1,\hat{a}_{\alpha\sigma}]\big] + O(\hat{V}^3) \tag{24}$$

Since $\hat{\gamma}$ follows from $\hat{a}$ through a unitary transformation, it automatically obeys fermionic anticommutation relations

$$\{\hat{\gamma}_{\alpha\sigma},\hat{\gamma}^\dagger_{\alpha'\sigma'}\} = \delta_{\alpha\alpha'}\delta_{\sigma\sigma'}, \qquad \{\hat{\gamma}_{\alpha\sigma},\hat{\gamma}_{\alpha'\sigma'}\} = 0 \tag{25}$$

[2] We have used that $\hat{P}_n[\hat{H}_0,\hat{S}_1+\hat{S}_2]\hat{P}_n = 0$ since $\hat{S}$ is block off-diagonal and P_n commutes with $\hat{H}_0$, together with Eq. (18) to simplify to double commutator $\hat{P}_n\big[[\hat{H}_0,\hat{S}_1],\hat{S}_1\big]\hat{P}_n = -\hat{P}_n\big[\hat{V},\hat{S}_1\big]\hat{P}_n$.

Hamiltonian Another example is the operator $\hat{H}_\gamma$ which acts on the quasiparticle states as $\hat{H}$ acts on the particle states:

$$\hat{H}_\gamma = \mathrm{e}^{\hat{S}}\hat{H}\mathrm{e}^{-\hat{S}} = \sum_{\alpha\sigma}\omega_{\alpha\sigma}\gamma^\dagger_{\alpha\sigma}\gamma_{\alpha\sigma} + \sum_{\alpha\beta\gamma\delta\in\mathcal{D}} V(\alpha,\beta|\gamma\delta)\hat{\gamma}^\dagger_{\alpha\uparrow}\hat{\gamma}^\dagger_{\beta\downarrow}\hat{\gamma}_{\gamma\downarrow}\hat{\gamma}_{\delta\uparrow} \tag{26}$$

The quasiparticle states, like any other state, do not evolve under the Hamiltonian $\hat{H}_\gamma$ but under the true Hamiltonian $\hat{H}$. Inverting Eq. (26) to express $\hat{H}$ in terms of $\hat{H}_\gamma$ allows us to reinterpret the effective Hamiltonian which appeared in Eq. (16):

$$\hat{H} = \mathrm{e}^{-\hat{S}}\hat{H}_\gamma\mathrm{e}^{\hat{S}} = \hat{H}_{\mathrm{eff},\gamma} \tag{27}$$

In other words, $\hat{H}$ is written in terms of the $\hat{\gamma}$ operators exactly like $\hat{H}_{\mathrm{eff}}$ is written in terms of the $\hat{a}$ operators.

Number operator A third example is the quasiparticle number operator

$$\hat{N}_\gamma = \mathrm{e}^{\hat{S}}\hat{N}\mathrm{e}^{-\hat{S}} = \sum_{\alpha\sigma}\hat{\gamma}^\dagger_{\alpha\sigma}\hat{\gamma}_{\alpha\sigma} \quad \text{with} \quad \hat{N} = \sum_{\alpha\sigma}\hat{a}^\dagger_{\alpha\sigma}\hat{a}_{\alpha\sigma} \tag{28}$$

This case is special since $\hat{N}$ commutes separately with $\hat{H}_0$ and $\hat{V}$. One can then show (order-by-order in $\hat{V}$) that it commutes with $\hat{S}$. We recover in this way the Luttinger theorem

$$\hat{N}_\gamma = \hat{N} \tag{29}$$

Projectors Finally, in the quasiparticle picture, the projector onto an energy-shell becomes

$$\hat{P}_{\Lambda,\gamma}(E) = \mathrm{e}^{\hat{S}}\hat{P}_\Lambda(E)\mathrm{e}^{-\hat{S}} = \sum_{\{n_{\alpha\sigma}\}}\Pi_\Lambda(E-\hat{H}_{0,\gamma})|\{n_{\alpha\sigma}\}\rangle\langle\{n_{\alpha\sigma}\}| \tag{30}$$

and correspondingly $\hat{P}_{n,\gamma} = \hat{P}_{\Lambda,\gamma}(E_n)$. The operators $\hat{P}_\gamma$ thus project the quasiparticle states $|\{n_{\alpha\sigma}\}\rangle$ according to their *unperturbed energy* $\sum_{\alpha\sigma}\omega_{\alpha\sigma}n_{\alpha\sigma}$, rather than their full energy $\langle\{n_{\alpha\sigma}\}|\hat{H}|\{n_{\alpha\sigma}\}\rangle$. In a generic many-fermion system, this would render this van Vleck transformation useless. In a Fermi liquid, this limitation is lifted by the non-crossing condition Eq. (4), which we may rewrite has

$$\left|\langle n|\hat{H}|n\rangle - \langle m|\hat{H}|m\rangle\right| \ll \Lambda \iff \left|{}_0\langle n|\hat{H}_0|n\rangle_0 - {}_0\langle m|\hat{H}_0|m\rangle_0\right| \ll \Lambda \tag{31}$$

1.1.4 Energy, residue and interaction functions of the quasiparticles

In Ref. [32], we related the energy of the quasiparticles to the average value of $\hat{H}$ in quasiparticle states with one or two excitations above the Fermi sea. Let us here generalize this definition to any quasiparticle reference state $|\psi\rangle$. To this aim, we introduce states with either one quasiparticle or one quasihole (depending on whether $n^{|\psi\rangle}_{\alpha\sigma} = \langle\psi|\hat{\gamma}^\dagger_{\alpha\sigma}\hat{\gamma}_{\alpha\sigma}|\psi\rangle = 0$ or 1) added to $|\psi\rangle$ in mode $\alpha\sigma$

$$|\alpha\sigma,\psi\rangle \equiv \begin{cases} |\psi\rangle & \text{if } n^{|\psi\rangle}_{\alpha\sigma} = 1 \\ \hat{\gamma}^\dagger_{\alpha\sigma}|\psi\rangle & \text{else} \end{cases} \qquad |\overline{\alpha\sigma},\psi\rangle \equiv \begin{cases} |\psi\rangle & \text{if } n^{|\psi\rangle}_{\alpha\sigma} = 0 \\ \hat{\gamma}_{\alpha\sigma}|\psi\rangle & \text{else} \end{cases} \tag{32}$$

The energy $\epsilon^{|\psi\rangle}_{\alpha\sigma}$ of the quasiparticle $\alpha\sigma$ is then a functional of $|\psi\rangle$ (more precisely of its occupations numbers in modes $\alpha'\sigma' \neq \alpha\sigma$):

$$\epsilon^{|\psi\rangle}_{\alpha\sigma} \equiv \langle\alpha\sigma,\psi|\hat{H}|\alpha\sigma,\psi\rangle - \langle\overline{\alpha\sigma},\psi|\hat{H}|\overline{\alpha\sigma},\psi\rangle \tag{33}$$

To define the interaction functions f in an arbitrary state $|\psi\rangle$, one should iterate the notation Eq. (32) to allow for the creation or annihilation of two (or more) quasiparticles[3]

$$|\alpha\sigma,\alpha_1\sigma_1,\ldots,\alpha_n\sigma_n,\overline{\beta_1\sigma_1},\ldots,\overline{\beta_m\sigma_m},\psi\rangle = \begin{cases} |\alpha_1\sigma_1,\ldots,\alpha_n\sigma_n,\overline{\beta_1\sigma_1},\ldots,\overline{\beta_m\sigma_m},\psi\rangle & \text{if } n_{\alpha\sigma}^{|\psi\rangle}=1 \\ \hat{\gamma}^\dagger_{\alpha\sigma}|\alpha_1\sigma_1,\ldots,\alpha_n\sigma_n,\overline{\beta_1\sigma_1},\ldots,\overline{\beta_m\sigma_m},\psi\rangle & \text{else} \end{cases} \tag{34}$$

We can now define the interaction functions as functionals of $|\psi\rangle$:

$$\mathcal{V}f_{\sigma\sigma'}^{|\psi\rangle}(\alpha,\beta) = E_{|\alpha\sigma,\beta\sigma'\psi\rangle} + E_{|\overline{\alpha\sigma},\overline{\beta\sigma'}\psi\rangle} - E_{|\overline{\alpha\sigma},\beta\sigma'\psi\rangle} - E_{|\alpha\sigma,\overline{\beta\sigma'}\psi\rangle} \tag{35}$$

where $E_{|\psi\rangle} = \langle\psi|\hat{H}|\psi\rangle$ and the volume factor $\mathcal{V}$ makes sure that $f_{\sigma\sigma'}$ has a finite thermodynamic limit. Our definition is a quantum version of the semi-classical definition of f as a second derivative $f_{\sigma\sigma'}^{|\psi\rangle}(\alpha,\beta) = \partial^2 E_{|\psi\rangle}/\partial n_{\alpha\sigma}\partial n_{\beta\sigma'}$

In the same spirit, one can define the residue of the quasiparticle as the variation of the number $\hat{a}^\dagger_{\alpha\sigma}\hat{a}_{\alpha\sigma}$ of particle in mode $\alpha\sigma$ when the quasiparticle $\alpha\sigma$ is added to the fluid:

$$Z_{\alpha\sigma}^{|\psi\rangle} \equiv \langle\alpha\sigma,\psi|\hat{a}^\dagger_{\alpha\sigma}\hat{a}_{\alpha\sigma}|\alpha\sigma,\psi\rangle - \langle\overline{\alpha\sigma},\psi|\hat{a}^\dagger_{\alpha\sigma}\hat{a}_{\alpha\sigma}|\overline{\alpha\sigma},\psi\rangle \tag{36}$$

Although conceptually important to identify the origin of the quasiparticles, the residue breaks the low-energy effective description, as it involves measuring a microscopic quantity $\hat{a}^\dagger_{\alpha\sigma}\hat{a}_{\alpha\sigma}$, unlike *e.g.* $\epsilon_{\alpha\sigma}$ which involves only the energy. All the low-energy properties should then be formulated without it.

Using the unitary transformation of the operators Eq. (23), there a dual interpretation of the residue as the variation of the number of quasiparticle in $\alpha\sigma$ upon adding the corresponding particle:

$$Z_{\alpha\sigma}^{|\psi\rangle} = {}_0\langle\alpha\sigma,\psi|\hat{\gamma}^\dagger_{\alpha\sigma}\hat{\gamma}_{\alpha\sigma}|\alpha\sigma,\psi\rangle_0 - {}_0\langle\overline{\alpha\sigma},\psi|\hat{\gamma}^\dagger_{\alpha\sigma}\hat{\gamma}_{\alpha\sigma}|\overline{\alpha\sigma},\psi\rangle_0 \tag{37}$$

In the case of an homogeneous system (where α stands for the wavevector $\mathbf{p}$), we will relate the residue, as defined in Eq. (36), to the discontinuity of the momentum distribution at the Fermi level (see Sec. 1.2.5). We already note that the leading term in $1-Z_{\alpha\sigma}^{|\psi\rangle}$ is of second order in V, in contrast to the leading term in $\epsilon_{\alpha\sigma}^{|\psi\rangle} - \omega_{\alpha\sigma}$ which is of order V. This is because $\hat{a}^\dagger_{\alpha\sigma}\hat{a}_{\alpha\sigma}$ (unlike $\hat{H}$) commutes with the projectors $\hat{P}_n$.

1.1.5 Collision amplitudes

Contrarily to a widespread believe, the effective description of the Fermi fluid is not exhaustive if we restrict ourselves to the eigenenergy $\epsilon_{\alpha\sigma}$ and interaction functions $f_{\sigma\sigma'}$ defined above. In fact these two quantities characterize only the diagonal elements of $\hat{H}$, while for many equilibrium and dynamical properties, a knowledge of the off-diagonal elements is required:

$$\mathcal{A}_{i\to f} \equiv \langle f|\hat{H}|i\rangle \tag{38}$$

Even though it is restricted to quasi on-shell couplings ($\mathcal{A}_{i\to f} \neq 0$ only if $|E_i - E_f| \ll \Lambda$), $\hat{H}$ can generate high-order collisions between quasiparticules. From Eq. (16), one can easily count that there are up to $n+1 \longleftrightarrow n+1$ quasiparticle collisions if $\hat{V}$ describes $2 \longleftrightarrow 2$ particles collisions and $\hat{H}_{\text{eff}}$ is truncated to order $\hat{V}^n$. However, we shall see that $2 \longleftrightarrow 2$ quasiparticle collisions remain the more likely if excited quasiparticles are confined to a low-energy shell about the Fermi level.

Just like the interaction functions $f_{\sigma\sigma'}$, the $2 \longleftrightarrow 2$ transitions amplitudes depend on the reference state $|\psi\rangle$ in which we compute them. Let $|i\rangle = |\overline{\alpha\sigma},\overline{\beta\sigma'},\gamma\sigma',\delta\sigma,\psi\rangle$ be a reference

[3] Together with this piling rule, the states obey a fermionic permutation rule: $|\overline{\alpha'\sigma'},\alpha\sigma\rangle = -|\alpha\sigma,\overline{\alpha'\sigma'}\rangle$.

state in which we made sure that quasiparticles are absent in $\alpha\sigma, \beta\sigma'$ and present in $\gamma\sigma', \delta\sigma$. Then let

$$|f\rangle = \hat{\gamma}^\dagger_{\alpha\sigma}\hat{\gamma}^\dagger_{\beta\sigma'}\hat{\gamma}_{\gamma\sigma'}\hat{\gamma}_{\delta\sigma}|i\rangle \qquad (\alpha\sigma,\beta\sigma') \neq (\delta\sigma,\gamma\sigma'), (\gamma\sigma',\delta\sigma) \tag{39}$$

be the final state not proportional to $|i\rangle$. We then define the collision amplitude $\mathcal{A}_{\sigma\sigma'}$ between σ and σ' quasiparticles through

$$\mathcal{A}_{i\to f} \equiv \frac{\mathcal{A}^{|i\rangle}_{\sigma\sigma'}(\alpha\beta|\gamma\delta)}{\mathcal{V}} \tag{40}$$

From the fermionic commutation relation and the hermiticity of the Hamiltonian, these amplitudes verify the relations

$$\mathcal{A}^{|i\rangle}_{\sigma\sigma'}(\delta\gamma|\beta\alpha) = \mathcal{A}^{|i\rangle}_{\sigma\sigma'}(\alpha\beta|\gamma\delta) \tag{41}$$

$$\mathcal{A}^{|i\rangle}_{\uparrow\uparrow}(\beta\alpha|\gamma\delta) = \mathcal{A}^{|i\rangle}_{\uparrow\uparrow}(\alpha\beta|\delta\gamma) = -\mathcal{A}^{|i\rangle}_{\uparrow\uparrow}(\alpha\beta|\gamma\delta) \tag{42}$$

In a spin-symmetric fluid, they verify in addition

$$\mathcal{A}^{|i\rangle}_{\sigma\sigma'}(\beta\alpha|\delta\gamma) = \mathcal{A}^{|i\rangle}_{\sigma\sigma'}(\alpha\beta|\gamma\delta) \tag{43}$$

Note that our van Vleck transformation a priori restricts $\mathcal{A}^{|i\rangle}_{\sigma\sigma'}(\alpha\beta|\gamma\delta)$ to transitions between quasi-degenerate states $|E_f - E_i| \ll \Lambda$. Comparing $E_i = \langle i|\hat{H}|i\rangle$ and $E_f = \langle f|\hat{H}|f\rangle$, this can be turned in the thermodynamic limit[4] into a resonance condition on the energies (in $|i\rangle$) of the colliding quasiparticles:

$$\left|\epsilon^{|i\rangle}_{\alpha\sigma} + \epsilon^{|i\rangle}_{\beta\sigma'} - \epsilon^{|i\rangle}_{\gamma\sigma'} - \epsilon^{|i\rangle}_{\delta\sigma}\right| \ll \Lambda \tag{44}$$

1.1.6 Low-energy effective Hamiltonian in the vicinity of the quasiparticle Fermi sea

So far, we have described the matrix elements of $\hat{H}$ between arbitrary quasiparticle states, noticing that even if we restrict to few-quasiparticle transitions the matrix elements retain a dependance on the reference state $|\psi\rangle$. This can be seen as a consequence of Eq. (27), where the expression of $\hat{H}$ (at strong coupling) contains an infinite number of $\hat{\gamma}$.

One can however derive a tractable truncation of $\hat{H}$, containing few operators $\hat{\gamma}$, and valid for quasiparticle states $|\{n_{\alpha\sigma}\}\rangle$ and $|\{m_{\alpha\sigma}\}\rangle$ that deviate from each other only at low energy ($n_{\alpha\sigma} \neq m_{\alpha\sigma}$ only when $|\omega_{\alpha\sigma} - \epsilon_{\rm F}| < \Lambda$). One truncation plays a special role, this is the one based on the quasiparticle Fermi sea:

$$|{\rm FS}\rangle = e^{\hat{S}}|{\rm FS}\rangle_0 \tag{45}$$

$$E_{\rm FS} \equiv \langle {\rm FS}|\hat{H}|{\rm FS}\rangle \tag{46}$$

Note that $|{\rm FS}\rangle$ is in general not the ground state of $\hat{H}$, such that $E_{\rm FS}$ is larger than the ground state energy E_0. In the following, we drop the $|{\rm FS}\rangle$ superscript when using the Fermi sea as the reference state: $\epsilon_{\alpha\sigma} \equiv \epsilon^{|{\rm FS}\rangle}_{\alpha\sigma}$, $f_{\sigma\sigma'} \equiv f^{|{\rm FS}\rangle}_{\sigma\sigma'}$ and $\mathcal{A}_{\sigma\sigma'} \equiv \mathcal{A}^{|{\rm FS}\rangle}_{\sigma\sigma'}$.

As the main result of this section we write this truncation of the Hamiltonian in the vicinity of the quasiparticle Fermi sea, including the collision amplitudes between resonant states. The truncation is written in terms of the fluctuations of the quasiparticle-hole operator,

$$\delta(\hat{\gamma}^\dagger_{\alpha\sigma}\hat{\gamma}_{\beta\sigma}) \equiv \hat{\gamma}^\dagger_{\alpha\sigma}\hat{\gamma}_{\beta\sigma} - n^0_{\alpha\sigma}\delta_{\alpha\beta} \tag{47}$$

$$\delta\hat{n}_{\alpha\sigma} \equiv \delta(\hat{\gamma}^\dagger_{\alpha\sigma}\hat{\gamma}_{\alpha\sigma}) \tag{48}$$

[4] One can show that $E_f - E_i = \epsilon^{|i\rangle}_{\alpha\sigma} + \epsilon^{|i\rangle}_{\beta\sigma'} - \epsilon^{|i\rangle}_{\gamma\sigma'} - \epsilon^{|i\rangle}_{\delta\sigma'} + O\left(\frac{1}{\mathcal{V}}\right)$

where $n^0_{\alpha\sigma} = \langle \mathrm{FS}|\hat{\gamma}^\dagger_{\alpha\sigma}\hat{\gamma}_{\alpha\sigma}|\mathrm{FS}\rangle$ is the Fermi sea occupation of mode $\alpha\sigma$. The fluctuation of the quasiparticle number $\delta\hat{n}$ can be viewed as the quantum version of the classical field δn (the semi-classical "number of quasiparticles") in which Fermi liquid theory is often formulated. Restricting to terms quadratic in $\delta(\hat{\gamma}^\dagger\hat{\gamma})$, we can write

$$\hat{H} = E_{\mathrm{FS}}+\sum_{\alpha\sigma}\epsilon_{\alpha\sigma}\delta\hat{n}_{\alpha\sigma}+\frac{1}{2\mathcal{V}}\sum_{\substack{\alpha\beta\gamma\delta\in\mathcal{D}\\ \sigma\sigma'=\uparrow\downarrow}}\delta^{\gamma+\delta}_{\alpha+\beta}\mathcal{B}_{\sigma\sigma'}(\alpha\beta|\gamma\delta)\delta(\gamma^\dagger_{\alpha\sigma}\gamma_{\delta\sigma})\delta(\gamma^\dagger_{\beta\sigma'}\gamma_{\gamma\sigma'})+O(\delta(\hat{\gamma}^\dagger\hat{\gamma})^3) \tag{49}$$

The function $\mathcal{B}_{\uparrow\downarrow}$ is straighforwardly related to $f_{\uparrow\downarrow}$ and $\mathcal{A}_{\uparrow\downarrow}$ by

$$\mathcal{B}_{\uparrow\downarrow}(\alpha,\beta|\beta,\alpha) = f_{\uparrow\downarrow}(\alpha,\beta) \tag{50}$$

$$\mathcal{B}_{\uparrow\downarrow}(\alpha,\beta|\gamma,\delta) = \mathcal{A}_{\uparrow\downarrow}(\alpha,\beta|\gamma,\delta),\ \alpha\neq\delta \tag{51}$$

Conversely, the indistinguishability of the colliding $\sigma\sigma$ quasiparticles leaves us some freedom in the choice of $\mathcal{B}_{\sigma\sigma}$. Without affecting the matrix element of $\hat{H}$, we can constrain $\mathcal{B}_{\sigma\sigma}$ by the following conditions[5]:

$$\mathcal{B}_{\sigma\sigma}(\alpha,\beta|\alpha,\beta) = 0 \tag{52}$$

$$\mathcal{B}_{\sigma\sigma}(\beta,\alpha|\delta,\gamma) = \mathcal{B}_{\sigma\sigma}(\alpha,\beta|\gamma,\delta) \tag{53}$$

While these choices may seem arbitrary at this stage, we will show in the next subsection that these constraints arise naturally in perturbative calculations of the truncated Hamiltonian. To reproduce $f_{\sigma\sigma}$ and $\mathcal{A}_{\sigma\sigma}$, the function $\mathcal{B}_{\sigma\sigma}$ must now satisfy

$$\mathcal{B}_{\sigma\sigma}(\alpha,\beta|\beta,\alpha) = f_{\sigma\sigma}(\alpha,\beta) \tag{54}$$

$$\mathcal{B}_{\sigma\sigma}(\alpha,\beta|\gamma,\delta)-\mathcal{B}_{\sigma\sigma}(\beta,\alpha|\gamma,\delta) = \mathcal{A}_{\sigma\sigma}(\alpha,\beta|\gamma,\delta),\ \ \alpha\neq\gamma,\delta \tag{55}$$

Eq. (49) is exact for the matrix elements between $|\mathrm{FS}\rangle$ and states connected to $|\mathrm{FS}\rangle$ by up to 4 operators $\hat{\gamma}$. It is valid up to corrections in $O(\epsilon_0)$ for states $|\psi\rangle$, whose excited quasiparticles are contained in a low-energy shell

$$\langle\psi|\delta\hat{n}_{\alpha\sigma}|\psi\rangle = 0 \text{ if } |\epsilon_{\alpha\sigma}-\mu| > \epsilon_0 \tag{56}$$

with

$$\epsilon_0 < \Lambda \ll \epsilon_{\mathrm{F}} \tag{57}$$

The omission of terms cubic or higher in $\delta(\hat{\gamma}^\dagger\hat{\gamma})$ in Eq. (49) then leads to errors in the energy and transition amplitudes controlled by $\epsilon_0/\epsilon_{\mathrm{F}}$.

We recover the usual semi-classical Hamiltonian of Fermi liquid theory

$$E = E + \sum_{\alpha\sigma}\epsilon_{\alpha\sigma}\delta n_{\alpha\sigma} + \frac{1}{2\mathcal{V}}\sum_{\substack{\alpha\beta\in\mathcal{D}\\ \sigma\sigma'=\uparrow\downarrow}} f_{\sigma\sigma'}(\alpha,\beta)\delta n_{\alpha\sigma}\delta n_{\beta\sigma'} + O(\delta n)^3 \tag{58}$$

as the restriction of Eq. (49) to terms $\alpha=\delta$, *i.e.* to terms diagonal in the basis of quasiparticle Fock states. The off-diagonal elements $\alpha\neq\delta$ in Eq. (49) are however crucial to accurately describe quasiparticle collisions. Thus, unless we are interested only in the collisionless dynamics of the Fermi liquid, our effective theory should specify not only $f_{\sigma\sigma'}(\alpha,\beta)$, but also $\mathcal{B}_{\sigma\sigma'}(\alpha,\beta|\gamma,\delta)$ for $\alpha\neq\delta$.

[5] The first constraint ensures that the particle-hole operators $\delta(\gamma^\dagger_{\alpha\uparrow}\gamma_{\delta\uparrow})$ and $\delta(\gamma^\dagger_{\beta\uparrow}\gamma_{\gamma\uparrow})$ commute in Eq. (49), and the second constraint ensures the symmetry with respect to the double exchange $\alpha\leftrightarrow\beta$, $\gamma\leftrightarrow\delta$.

In fluids where the index α describes a continuous sets of modes, one may think, looking at Eqs. (50) and (54), that the Landau functions $f_{\sigma\sigma'}$ are continuously connected to the amplitude $\mathcal{B}_{\sigma\sigma'}(\alpha,\beta|\beta-\mathrm{d}\alpha,\alpha+\mathrm{d}\alpha)$ as $\mathrm{d}\alpha\to 0$. However, the energy cutoff Λ separates two limits:

$$\lim_{\substack{\mathrm{d}\alpha\to 0\\ |\epsilon_\alpha-\epsilon_{\alpha+\mathrm{d}\alpha}|\gg\Lambda}} \mathcal{B}_{\sigma\sigma'}(\alpha,\beta|\beta-\mathrm{d}\alpha,\alpha+\mathrm{d}\alpha) \equiv \mathcal{B}^{\text{forward}}_{\sigma\sigma'}(\alpha,\beta) \tag{59}$$

$$\lim_{\substack{\mathrm{d}\alpha\to 0\\ |\epsilon_\alpha-\epsilon_{\alpha+\mathrm{d}\alpha}|\ll\Lambda}} \mathcal{B}_{\sigma\sigma'}(\alpha,\beta|\beta-\mathrm{d}\alpha,\alpha+\mathrm{d}\alpha) = f_{\sigma\sigma'}(\alpha,\beta) \tag{60}$$

The amplitude $\mathcal{B}^{\text{forward}}_{\sigma\sigma'}$ obtained for energy transfer $\epsilon_\alpha-\epsilon_{\alpha+\mathrm{d}\alpha}$ large compared to Λ but small compared to ϵ_F is called the forward-scattering amplitude. It is related to $f_{\sigma\sigma'}$ by a Bethe-Salpeter equation [4], which was understood, within the functional renormalization group approach [10–12], as a fixed point of the renormalization group equation. In our formalism, an equivalent equation could be obtained by computing the change of $\mathcal{B}$ under the action of the infinitesimal generator $\hat{S}(\Lambda-\mathrm{d}\Lambda)-\hat{S}(\Lambda)$ of the continuous unitary transform [21,22].

The forward-scattering approximation, common in the literature on ^{3}He, consists in replacing the full amplitude $\mathcal{B}(\alpha,\beta|\gamma,\delta)$ by $\mathcal{B}^{\text{forward}}_{\sigma\sigma'}(\alpha,\beta)$. This uncontrolled approximation compensates the lack of knowledge on the collision amplitude. In ^{3}He where the Landau function f has a large isotropic component ($F^+_{l=0}\geq 10$), the Bethe-Salpeter equation is particularly useful to obtain a correct order of magnitude of the scattering amplitudes.

Finally, in fluids where the modes are indexed by a 3D wavevector $\mathbf{p}$, we may rewrite Eq. (49) in real space by performing a Wigner transform of the quasiparticle distribution

$$\delta\hat{n}_{\mathbf{p}\sigma}(\mathbf{r})\equiv\sum_{\mathbf{q}}\mathrm{e}^{-\mathrm{i}\mathbf{q}\cdot\mathbf{r}}\delta(\hat{\gamma}^\dagger_{\mathbf{p}+\frac{\mathbf{q}}{2}\sigma}\hat{\gamma}_{\mathbf{p}-\frac{\mathbf{q}}{2}\sigma}) \tag{61}$$

In terms of $\delta\hat{n}(\mathbf{r})$, we have

$$\hat{H}=E_\mathrm{FS}+\sum_{\mathbf{p}\sigma}\int\frac{\mathrm{d}^3r}{\mathcal{V}}\epsilon_{\mathbf{p}\sigma}\delta\hat{n}_{\mathbf{p}\sigma}(\mathbf{r})+\frac{1}{2}\sum_{\substack{\mathbf{p}\mathbf{p}'\in\mathcal{D}\\ \sigma\sigma'=\uparrow\downarrow}}\int\frac{\mathrm{d}^3r_1\mathrm{d}^3r_2}{\mathcal{V}^2}\mathcal{B}_{\sigma\sigma'}(\mathbf{p},\mathbf{p}'|\mathbf{r}_1-\mathbf{r}_2)\delta\hat{n}_{\mathbf{p}\sigma}(\mathbf{r}_1)\delta\hat{n}_{\mathbf{p}'\sigma'}(\mathbf{r}_2) + O(\delta\hat{n})^3 \tag{62}$$

The Wigner transform of the amplitude $\mathcal{B}$ is

$$\mathcal{B}_{\sigma\sigma'}(\mathbf{p},\mathbf{p}'|\mathbf{r}_1-\mathbf{r}_2)=\frac{1}{\mathcal{V}}\sum_{\mathbf{q}}\mathrm{e}^{\mathrm{i}\mathbf{q}\cdot(\mathbf{r}_1-\mathbf{r}_2)}\mathcal{B}_{\sigma\sigma'}\left(\mathbf{p}-\frac{\mathbf{q}}{2},\mathbf{p}'+\frac{\mathbf{q}}{2}\middle|\mathbf{p}'-\frac{\mathbf{q}}{2},\mathbf{p}+\frac{\mathbf{q}}{2}\right) \tag{63}$$

It plays the role of a finite-range interaction potential between $\mathbf{p}\sigma$ and $\mathbf{p}'\sigma'$ quasiparticles. A gradient expansion [13] would replace this finite-range interaction by a short-range one.

1.2 Application to an homogeneous Fermi gas with contact interactions

We now evaluate the truncated Hamiltonian Eq. (49) in a 3D homogeneous Fermi gas with contact interactions. In this system, contrarily to most Fermi liquids, one can compute the effective parameters ϵ_σ and $\mathcal{B}_{\sigma\sigma'}$ in function of a unique microscopic parameter: the s-wave scattering length a. Here, we perform a perturbative calculation of ϵ_σ and $\mathcal{B}_{\sigma\sigma'}$ to second-order in $k_\mathrm{F}a$.

1.2.1 The lattice model for contact interactions

The kinetic and interaction Hamiltonian which describe our Fermi gas are:

$$\hat{H}_0 = \sum_{\mathbf{p}\in\mathcal{D},\sigma} \omega_{\mathbf{p}} \hat{a}^\dagger_{\mathbf{p}\sigma}\hat{a}_{\mathbf{p}\sigma} \tag{64}$$

$$\hat{V} = \frac{g_0}{L^3} \sum_{\mathbf{p}_1,\mathbf{p}_2,\mathbf{p}_3,\mathbf{p}_4\in\mathcal{D}} \delta^{\mathbf{p}_3+\mathbf{p}_4}_{\mathbf{p}_1+\mathbf{p}_2} \hat{a}^\dagger_{\mathbf{p}_1\uparrow}\hat{a}^\dagger_{\mathbf{p}_2\downarrow}\hat{a}_{\mathbf{p}_3\downarrow}\hat{a}_{\mathbf{p}_4\uparrow} \tag{65}$$

where $\omega_{\mathbf{p}} = p^2/2m$. We assume that the gas is held in a cubic volume $\mathcal{V} = L^3$ (with $L \to +\infty$ in the thermodynamic limit). To regularize the UV divergences inherent to the contact potential, we have discretized real space [42] into a cubic lattice of step l, thereby restricting the set of momenta $\mathbf{p}$ to $\mathcal{D} = (2\pi\mathbb{Z}/L)^3 \cap [-\pi/l, \pi/l[^3$. Solving the two-body problem, we express g_0 in terms of a through the Lippman-Schwinger equation

$$\frac{1}{g_0} = \frac{1}{g} - \int_{[-\pi/l,\pi/l[^3} \frac{\mathrm{d}^3 p}{(2\pi)^3}\frac{m}{p^2} \tag{66}$$

where $g = 4\pi a/m$.

1.2.2 Expansion of the quasiparticle annihilation operator

The ground state of $\hat{H}_0$ at fixed density ρ is the particle Fermi sea

$$|\mathrm{FS}\rangle_0 = \prod_{\substack{\mathbf{p}\in\mathcal{D}\\ \sigma=\uparrow,\downarrow}} \Theta(p_\mathrm{F}-p)\hat{a}^\dagger_{\mathbf{p}\sigma}|0\rangle_0 \tag{67}$$

where $p_\mathrm{F} = (3\pi^2\rho)^{1/3}$ is the Fermi momentum and $|0\rangle_0$ the particle vacuum. The occupation numbers of $|\mathrm{FS}\rangle$ are then

$$n^0_{\mathbf{p}} = \Theta(p_\mathrm{F}-p), \qquad \bar{n}^0_{\mathbf{p}} = 1 - n^0_{\mathbf{p}} = \Theta(p-p_\mathrm{F}) \tag{68}$$

Eq. (18) and Eq. (24) applied to the contact interaction potential $\hat{V}$ provides the expression of $\hat{S}$ and $\hat{\gamma}$. To first order in g, we have:

$$\hat{S}_1 = \frac{g_0}{L^3}\sum_{\mathbf{p}_\alpha\mathbf{p}_\beta\mathbf{p}_\gamma\mathbf{p}_\delta\in\mathcal{D}} \hat{a}^\dagger_{\mathbf{p}_\alpha\uparrow}\hat{a}^\dagger_{\mathbf{p}_\beta\downarrow}\hat{a}_{\mathbf{p}_\gamma\downarrow}\hat{a}_{\mathbf{p}_\delta\uparrow}\delta^{\mathbf{p}_\gamma+\mathbf{p}_\delta}_{\mathbf{p}_\alpha+\mathbf{p}_\beta}\,\mathcal{P}_\Lambda\left(\frac{1}{\omega_{\mathbf{p}_\gamma}+\omega_{\mathbf{p}_\delta}-\omega_{\mathbf{p}_\alpha}-\omega_{\mathbf{p}_\beta}}\right) \tag{69}$$

$$\hat{\gamma}_{\mathbf{p}\uparrow} = \hat{a}_{\mathbf{p}\uparrow} + \frac{g_0}{V}\sum_{\mathbf{p}_\beta\mathbf{p}_\gamma\mathbf{p}_\delta\in\mathcal{D}} \delta^{\mathbf{p}_\gamma+\mathbf{p}_\delta}_{\mathbf{p}+\mathbf{p}_\beta}\,\mathcal{P}_\Lambda\left(\frac{1}{\omega_{\mathbf{p}_\gamma}+\omega_{\mathbf{p}_\delta}-\omega_{\mathbf{p}}-\omega_{\mathbf{p}_\beta}}\right)\hat{a}^\dagger_{\mathbf{p}_\beta\downarrow}\hat{a}_{\mathbf{p}_\gamma\downarrow}\hat{a}_{\mathbf{p}_\delta\uparrow} + O(g)^2 \tag{70}$$

In these expressions, the function

$$\mathcal{P}_\Lambda\left(\frac{1}{E}\right) = \frac{1-\Pi_\Lambda(E)}{E} \tag{71}$$

originates in the projectors $\hat{P}_\Lambda$ and prevents the denominators from vanishing. Eq. (70) is a rigorous formulation of the standard first-order picture of the spin $\uparrow$ quasiparticle as a cloud of spin $\downarrow$ particle surrounding a spin $\uparrow$ particle. It is reminiscent of the Chevy Ansatz for polarons [43].

1.2.3 Expression of the Hamiltonian in terms of $\hat{\gamma}$

To avoid carrying along a quasi-resonance condition, we define an Hamiltonian $\hat{H}'$ where the energy constraint has been released

$$\hat{H}' = \hat{H}_{0,\gamma} + \hat{V}_\gamma + \frac{1}{2}[\hat{V}_\gamma, S_{1,\gamma}] + O(g)^3 \tag{72}$$

$$\hat{H} = \sum_{n=-\infty}^{+\infty} \hat{P}_{n,\gamma}\hat{H}'\hat{P}_{n,\gamma} + O(g^3) \tag{73}$$

Injecting in Eq. (72) the expressions of $\hat{H}_{0,\gamma}$, $\hat{V}_\gamma$ and $\hat{S}_{1,\gamma}$, we obtain

$$\begin{aligned}\hat{H}' = \sum_{\mathbf{p}\sigma} \omega_\mathbf{p} \gamma^\dagger_{\mathbf{p}\sigma}\gamma_{\mathbf{p}\sigma} + \frac{g_0}{L^3}\sum_{\mathbf{p}_\alpha\mathbf{p}_\beta\mathbf{p}_\gamma\mathbf{p}_\delta\in\mathcal{D}} \delta^{\mathbf{p}_\gamma+\mathbf{p}_\delta}_{\mathbf{p}_\alpha+\mathbf{p}_\beta}\hat{\gamma}^\dagger_{\mathbf{p}_\alpha\uparrow}\hat{\gamma}^\dagger_{\mathbf{p}_\beta\downarrow}\hat{\gamma}_{\mathbf{p}_\gamma\downarrow}\hat{a}_{\mathbf{p}_\delta\uparrow} \\ + \frac{1}{2}\left(\frac{g_0}{L^3}\right)^2 \sum_{\substack{\mathbf{p}_\alpha\mathbf{p}_\beta\mathbf{p}_\gamma\mathbf{p}_\delta\in\mathcal{D}\\ \mathbf{p}_a\mathbf{p}_b\mathbf{p}_c\mathbf{p}_d\in\mathcal{D}}} \delta^{\mathbf{p}_\gamma+\mathbf{p}_\delta}_{\mathbf{p}_\alpha+\mathbf{p}_\beta}\delta^{\mathbf{p}_c+\mathbf{p}_d}_{\mathbf{p}_a+\mathbf{p}_b}\mathcal{P}_\Lambda\left(\frac{1}{\omega_{\mathbf{p}_a}+\omega_{\mathbf{p}_b}-\omega_{\mathbf{p}_c}-\omega_{\mathbf{p}_d}}\right) \\ \times\left[\hat{\gamma}^\dagger_{\mathbf{p}_\alpha\uparrow}\hat{\gamma}^\dagger_{\mathbf{p}_\beta\downarrow}\hat{\gamma}_{\mathbf{p}_\gamma\downarrow}\hat{\gamma}_{\mathbf{p}_\delta\uparrow}, \hat{\gamma}^\dagger_{\mathbf{p}_d\uparrow}\hat{\gamma}^\dagger_{\mathbf{p}_c\downarrow}\hat{\gamma}_{\mathbf{p}_b\downarrow}\hat{\gamma}_{\mathbf{p}_a\uparrow}\right] + O(g)^3\end{aligned} \tag{74}$$

This Hamiltonian truncated to second order in $\hat{V}$ is thus sextic in $\hat{\gamma}$, with up to $3 \longleftrightarrow 3$ transitions as discussed above.

We proceed to linearizing $\hat{H}'$ in the vicinity of the quasiparticle Fermi sea $|\mathrm{FS}\rangle$, using the expansion Eq. (48) of the particle-hole operators about their average value in $|\mathrm{FS}\rangle$. We note that there is no ambiguity in the pairing of the $\hat{\gamma}$ operators, since the window function $\mathcal{P}_\Lambda$ guarantees that $a \neq d$, $b \neq c$ and thus

$$(\hat{\gamma}^\dagger_{\mathbf{p}_\alpha\uparrow}\hat{\gamma}^\dagger_{\mathbf{p}_\beta\downarrow}\hat{\gamma}_{\mathbf{p}_\gamma\downarrow}\hat{\gamma}_{\mathbf{p}_\delta\uparrow})(\hat{\gamma}^\dagger_{\mathbf{p}_d\uparrow}\hat{\gamma}^\dagger_{\mathbf{p}_c\downarrow}\hat{\gamma}_{\mathbf{p}_b\downarrow}\hat{\gamma}_{\mathbf{p}_a\uparrow}) = (\hat{\gamma}^\dagger_{\mathbf{p}_\alpha\uparrow}\hat{\gamma}_{\mathbf{p}_a\uparrow})(\hat{\gamma}^\dagger_{\mathbf{p}_\beta\downarrow}\hat{\gamma}_{\mathbf{p}_b\downarrow})(\hat{\gamma}_{\mathbf{p}_\gamma\downarrow}\hat{\gamma}^\dagger_{\mathbf{p}_c\downarrow})(\hat{\gamma}_{\mathbf{p}_\delta\uparrow}\hat{\gamma}^\dagger_{\mathbf{p}_d\uparrow}) \tag{75}$$

The expansion of the unconstrained Hamiltonian $\hat{H}'$ in powers of $\delta(\hat{\gamma}^\dagger\hat{\gamma})$ has the form of Eq. (49):

$$\hat{H}' = E_{\mathrm{FS}} + \sum_{\mathbf{p}\sigma}\epsilon_\mathbf{p}\delta\hat{n}_{\mathbf{p}\sigma} + \frac{1}{2L^3}\sum_{\substack{\mathbf{p}_\alpha\mathbf{p}_\beta\mathbf{p}_\gamma\mathbf{p}_\delta\in\mathcal{D}\\ \sigma\sigma'=\uparrow\downarrow}} \delta^{\mathbf{p}_\gamma+\mathbf{p}_\delta}_{\mathbf{p}_\alpha+\mathbf{p}_\beta}\mathcal{B}'_{\sigma\sigma'}(\mathbf{p}_\alpha\mathbf{p}_\beta|\mathbf{p}_\gamma\mathbf{p}_\delta)\delta(\hat{\gamma}^\dagger_{\mathbf{p}_\alpha\sigma}\hat{\gamma}_{\mathbf{p}_\delta\sigma})\delta(\hat{\gamma}^\dagger_{\mathbf{p}_\beta\sigma'}\hat{\gamma}_{\mathbf{p}_\gamma\sigma'}) + O(\delta(\hat{\gamma}^\dagger\hat{\gamma})^3) \tag{76}$$

and the expansion of the true Hamiltonian $\hat{H}$ follows from Eq. (76) simply by replacing the unconstrained amplitudes $\mathcal{B}'$ by the constrained ones

$$\mathcal{B}_{\sigma\sigma'}(\mathbf{p}_\alpha\mathbf{p}_\beta|\mathbf{p}_\gamma\mathbf{p}_\delta) = \mathcal{B}'_{\sigma\sigma'}(\mathbf{p}_\alpha\mathbf{p}_\beta|\mathbf{p}_\gamma\mathbf{p}_\delta)\Pi_\Lambda(\epsilon_{\mathbf{p}_\alpha}+\epsilon_{\mathbf{p}_\beta}-\epsilon_{\mathbf{p}_\gamma}-\epsilon_{\mathbf{p}_\delta}) \tag{77}$$

The term of order $\delta(\hat{\gamma}^\dagger\hat{\gamma})^0$ in Eq. (76) is the energy of the quasiparticle Fermi sea

$$\begin{aligned}E_{\mathrm{FS}} = \sum_{\mathbf{p}\in\mathcal{D},\sigma}\omega_\mathbf{p} n^0_p + \frac{g}{L^3}\sum_{\mathbf{p},\mathbf{p}'\in\mathcal{D}} n^0_\mathbf{p} n^0_{\mathbf{p}'} \\ + \left(\frac{g}{L^3}\right)^2\sum_{\mathbf{p}_\alpha\mathbf{p}_\beta\mathbf{p}_\gamma\mathbf{p}_\delta\in\mathcal{D}} \delta^{\mathbf{p}_\gamma+\mathbf{p}_\delta}_{\mathbf{p}_\alpha+\mathbf{p}_\beta} n^0_{\mathbf{p}_\alpha} n^0_{\mathbf{p}_\beta}(\bar{n}^0_{\mathbf{p}_\gamma}\bar{n}^0_{\mathbf{p}_\delta}-1)\mathcal{P}_\Lambda\left(\frac{1}{\omega_{\mathbf{p}_\alpha}+\omega_{\mathbf{p}_\beta}-\omega_{\mathbf{p}_\gamma}-\omega_{\mathbf{p}_\delta}}\right) + O(g^3)\end{aligned} \tag{78}$$

Note that we have used the standard perturbative renormalization procedure [25, 32] to replace g_0 by g, such that Eq. (78) is free from UV divergence when $l \to 0$. The explicit of calculation of $E_{\rm FS}(k_{\rm F}a)$ from Eq. (78) leads to the Lee-Huang-Yang equation of state to second order in $k_{\rm F}a$ [25].

Then, the eigenenergy of the quasiparticles in Eq. (76) is

$$\begin{aligned}\epsilon_{\mathbf{p}} &= \omega_{\mathbf{p}} + \frac{g_0}{L^3}\sum_{\mathbf{p}'\in\mathcal{D}} n^0_{\mathbf{p}'} \\ &+ \left(\frac{g_0}{L^3}\right)^2 \sum_{\mathbf{p}_2\mathbf{p}_3\mathbf{p}_4\in\mathcal{D}} \delta^{\mathbf{p}_3+\mathbf{p}_4}_{\mathbf{p}+\mathbf{p}_2}\left[n^0_{\mathbf{p}_2}\bar{n}^0_{\mathbf{p}_3}\bar{n}^0_{\mathbf{p}_4} + \bar{n}^0_{\mathbf{p}_2} n^0_{\mathbf{p}_3} n^0_{\mathbf{p}_4}\right]\mathcal{P}_\Lambda\left(\frac{1}{\omega_{\mathbf{p}}+\omega_{\mathbf{p}_2}-\omega_{\mathbf{p}_3}-\omega_{\mathbf{p}_4}}\right) + O(g)^3\end{aligned} \tag{79}$$

Since the quasiparticle dynamics is restricted to the vicinity of the Fermi level, this eigenenergy can be expanded in powers of $p - p_{\rm F}$.

$$\epsilon_{\mathbf{p}} - \mu = \frac{p_{\rm F}}{m^*}(p-p_{\rm F}) + O(p-p_{\rm F})^2 \tag{80}$$

An explicit expression of the effective mass m^* in powers of $k_{\rm F}a$ was computed by Galitskii [44].

Finally, the (unconstrained) collision amplitudes $\mathcal{B}'$ are

$$\begin{aligned}\mathcal{B}'_{\sigma\sigma}(\mathbf{p}_\alpha\mathbf{p}_\beta|\mathbf{p}_\gamma\mathbf{p}_\delta) &= \frac{g^2}{2L^3}\sum_{\mathbf{p}_1\mathbf{p}_2\in\mathcal{D}}\left[n^0_{\mathbf{p}_1}\bar{n}^0_{\mathbf{p}_2} - \bar{n}^0_{\mathbf{p}_1}n^0_{\mathbf{p}_2}\right] \\ &\times\left[\mathcal{P}_\Lambda\left(\frac{1}{\omega_{\mathbf{p}_\alpha}+\omega_{\mathbf{p}_2}-\omega_{\mathbf{p}_\gamma}-\omega_{\mathbf{p}_1}}\right)\delta^{\mathbf{p}_2+\mathbf{p}_\alpha}_{\mathbf{p}_1+\mathbf{p}_\gamma} + \mathcal{P}_\Lambda\left(\frac{1}{\omega_{\mathbf{p}_\beta}+\omega_{\mathbf{p}_2}-\omega_{\mathbf{p}_\delta}-\omega_{\mathbf{p}_1}}\right)\delta^{\mathbf{p}_2+\mathbf{p}_\beta}_{\mathbf{p}_1+\mathbf{p}_\delta}\right] + O(g)^3\end{aligned} \tag{81}$$

$$\begin{aligned}\mathcal{B}'_{\uparrow\downarrow}(\mathbf{p}_\alpha\mathbf{p}_\beta|\mathbf{p}_\gamma\mathbf{p}_\delta) - \mathcal{B}'_{\sigma\sigma}(\mathbf{p}_\alpha\mathbf{p}_\beta|\mathbf{p}_\gamma\mathbf{p}_\delta) &= g + \frac{g^2}{2L^3}\sum_{\mathbf{p}_1\mathbf{p}_2\in\mathcal{D}}\left[\bar{n}^0_{\mathbf{p}_1}\bar{n}^0_{\mathbf{p}_2} - n^0_{\mathbf{p}_1}n^0_{\mathbf{p}_2} - 1\right]\delta^{\mathbf{p}_1+\mathbf{p}_2}_{\mathbf{p}_\alpha+\mathbf{p}_\beta} \\ &\times\left[\mathcal{P}_\Lambda\left(\frac{1}{\omega_{\mathbf{p}_\alpha}+\omega_{\mathbf{p}_\beta}-\omega_{\mathbf{p}_1}-\omega_{\mathbf{p}_2}}\right) + \mathcal{P}_\Lambda\left(\frac{1}{\omega_{\mathbf{p}_\gamma}+\omega_{\mathbf{p}_\delta}-\omega_{\mathbf{p}_1}-\omega_{\mathbf{p}_2}}\right)\right] + O(g)^3\end{aligned} \tag{82}$$

Remark that we have symmetrized $\mathcal{B}_{\sigma\sigma}$ towards the full exchange $\mathcal{B}_{\sigma\sigma}(\beta,\alpha|\delta,\gamma) = \mathcal{B}_{\sigma\sigma}(\alpha,\beta|\gamma,\delta)$, and that the function $\mathcal{P}_\Lambda$ imposes $\mathcal{B}_{\sigma\sigma}(\mathbf{p}\mathbf{p}'|\mathbf{p}\mathbf{p}') = 0$, in accordance with the constraints (52)–(53). The Landau interaction function $f_{\sigma\sigma'}$ are simply the value of $\mathcal{B}_{\sigma\sigma'}$ for $\mathbf{p} = \mathbf{p}_\alpha = \mathbf{p}_\delta$ and $\mathbf{p}' = \mathbf{p}_\beta = \mathbf{p}_\gamma$:

$$f_{\sigma\sigma}(\mathbf{p},\mathbf{p}') = \frac{g^2}{L^3}\sum_{\mathbf{p}_1\mathbf{p}_2\in\mathcal{D}}\left[n^0_{\mathbf{p}_1}\bar{n}^0_{\mathbf{p}_2} - \bar{n}^0_{\mathbf{p}_1}n^0_{\mathbf{p}_2}\right]\delta^{\mathbf{p}'+\mathbf{p}_1}_{\mathbf{p}+\mathbf{p}_2}\mathcal{P}_\Lambda\left(\frac{1}{\omega_{\mathbf{p}}+\omega_{\mathbf{p}_2}-\omega_{\mathbf{p}'}-\omega_{\mathbf{p}_1}}\right) + O(g)^3 \tag{83}$$

$$\begin{aligned}f_{\uparrow\downarrow}(\mathbf{p},\mathbf{p}') - f_{\sigma\sigma}(\mathbf{p},\mathbf{p}') &= g + \frac{g^2}{L^3}\sum_{\mathbf{p}_1\mathbf{p}_2\in\mathcal{D}}\left[\bar{n}^0_{\mathbf{p}_1}\bar{n}^0_{\mathbf{p}_2} - n^0_{\mathbf{p}_1}n^0_{\mathbf{p}_2} - 1\right]\delta^{\mathbf{p}_1+\mathbf{p}_2}_{\mathbf{p}_\alpha+\mathbf{p}_\beta} \\ &\times\mathcal{P}_\Lambda\left(\frac{1}{\omega_{\mathbf{p}_\alpha}+\omega_{\mathbf{p}_\beta}-\omega_{\mathbf{p}_1}-\omega_{\mathbf{p}_2}}\right) + O(g)^3\end{aligned} \tag{84}$$

1.2.4 Explicit expressions of the collision amplitudes with the Λ dependence

To illustrate the role of the cutoff Λ in connecting the collision amplitudes $\mathcal{A}_{\sigma\sigma'}$ to the interaction functions $f_{\sigma\sigma'}$, we return to the explicit expressions obtained in Ref. [32]. We parametrize the Λ dependence through

$$\epsilon_\Lambda = \frac{\Lambda}{4E_\mathrm{F}} \tag{85}$$

and we are interested in the limit $\epsilon_\Lambda \to 0$. Restricting to wavevectors of the Fermi surface ($p_1 = p_2 = p_3 = p_4 = p_\mathrm{F}$), the amplitude $\mathcal{B}$ depends only on the angles $\theta_{ij} = (\widehat{\mathbf{p}_i, \mathbf{p}_j})$:

$$\frac{\mathcal{B}'_{\uparrow\downarrow}(\mathbf{p}_1,\mathbf{p}_2|\mathbf{p}_3,\mathbf{p}_4)}{g} = 1 + \frac{2k_\mathrm{F}a}{\pi}[I_\Lambda(\theta_{12}) + J_\Lambda(\theta_{13})] + O(a^2) \tag{86}$$

$$\frac{\mathcal{B}'_{\uparrow\uparrow}(\mathbf{p}_1,\mathbf{p}_2|\mathbf{p}_3,\mathbf{p}_4)}{g} = \frac{2k_\mathrm{F}a}{\pi}J_\Lambda(\theta_{13}) + O(a^3) \tag{87}$$

The functions I_Λ and J_Λ that characterize the crossed Λ,θ dependence of $\mathcal{B}$ are depicted on Figs. 2–3, and explicit expressions are given in Appendix A.

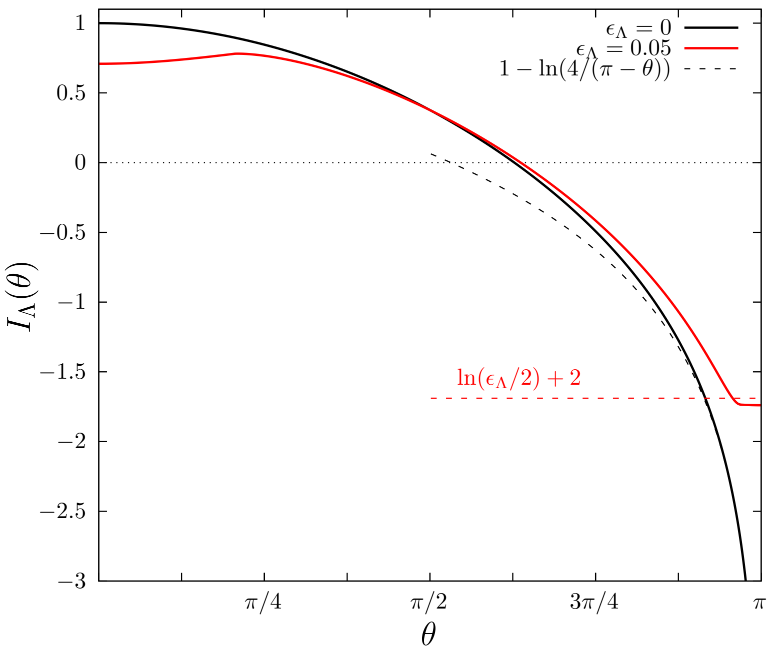

Figure 2: Angular dependence of the function I_Λ appearing in $\mathcal{A}_{\uparrow\downarrow}$ and $f_{\uparrow\downarrow}$. For $\epsilon_\Lambda = 0$ (black curve), the function displays a logarithmic divergence $\sim \ln(\pi-\theta) + 1 - \ln 4$ when $\theta \to \pi$ (black dashed curve). For $\epsilon_\Lambda \neq 0$ (red curve) the divergence is regularized, and the function saturates at $\ln(\epsilon_\Lambda/2) + 2 + O(\epsilon_\Lambda)$ in $\theta = \pi$ (red dashed curve).

When $\epsilon_\Lambda \to 0$, these functions converge pointwise in the open interval $(0,\pi)$ to the functions I and J usually found in this context [25,32]

$$I(\theta) \equiv \lim_{\epsilon_\Lambda \to 0} I_\Lambda(\theta) = 1 - \frac{s}{2}\ln\frac{1+s}{1-s}, \qquad s = \sin\frac{\theta}{2},\ c = \cos\frac{\theta}{2} \tag{88}$$

$$J(\theta) \equiv \lim_{\epsilon_\Lambda \to 0} J_\Lambda(\theta) = \frac{1}{2}\left(1 + \frac{c^2}{2s}\ln\frac{1+s}{1-s}\right) \tag{89}$$

While J is a smooth function in $[0,\pi]$, we note a logarithmic divergence in I when $\theta \to \pi$ (see Fig. 2).

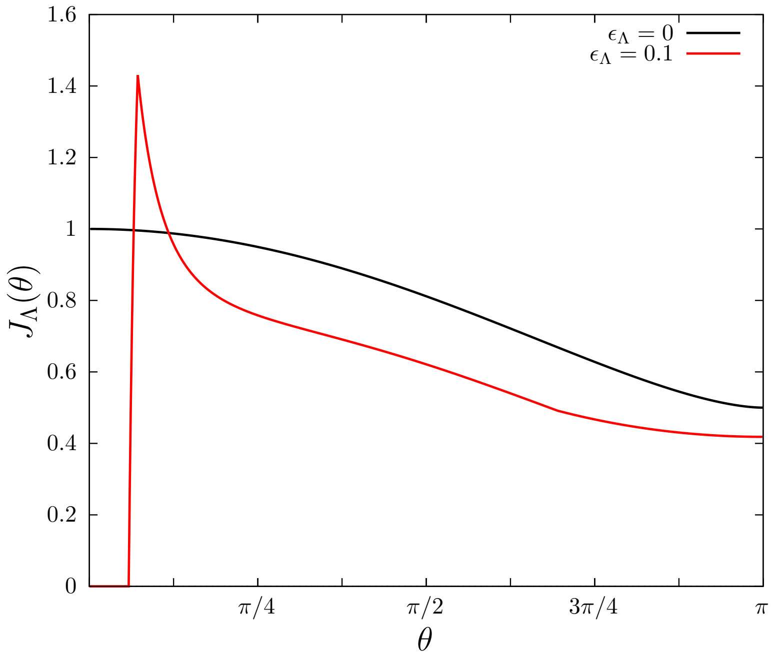

Figure 3: Angular dependence of the function J_Λ appearing in both $\mathcal{A}_{\uparrow\downarrow}$, $f_{\uparrow\downarrow}$ and $\mathcal{A}_{\sigma\sigma}$, $f_{\sigma\sigma}$. As $\epsilon_\Lambda \to 0$, the function converges pointwise to $J(\theta)$ (black curve) on $(0,\pi]$. It is however cancelled in an interval of width $\simeq 2\epsilon_\Lambda$ about $\theta = 0$ (red curve).

The convergence of I_Λ and J_Λ to I and J is however not uniform: ϵ_Λ regularises the divergence of I in $\theta = \pi$, and cancels J in a neighborhood of size $\approx \epsilon_\Lambda$ about $\theta = 0$. Taking the limit $\theta \to 0, \pi$ before $\epsilon_\Lambda \to 0$, we have:

$$\lim_{\theta\to\pi} I_\Lambda(\theta) = \ln\frac{\epsilon_\Lambda}{2} + 2 + O(\epsilon_\Lambda) \tag{90}$$

$$\lim_{\epsilon_\Lambda\to 0}\lim_{\theta\to 0} J_\Lambda(\theta) = 0 \tag{91}$$

We recover with these two points of non-uniform convergence the forward ($\theta = 0$) and BCS ($\theta = \pi$) collision channels. The singular behavior of $J_\Lambda(\theta \to 0)$ is reminiscent of the behavior of the 4-point vertex found in Ref. [11] (see Fig. 4 therein).

From the expression of $\mathcal{B}_{\sigma\sigma'}$, one obtains the Landau function f (Eqs. (50)–(54)) by taking $\mathbf{p} = \mathbf{p}_1 = \mathbf{p}_4$ and $\mathbf{p}' = \mathbf{p}_2 = \mathbf{p}_3$ (that is, $\theta_{12} = \theta_{13} = (\widehat{\mathbf{p},\mathbf{p}'}) \equiv \theta$):

$$\frac{f_{\uparrow\downarrow}(\mathbf{p},\mathbf{p}')}{g} = 1 + \frac{2k_\mathrm{F}a}{\pi}[I_\Lambda(\theta) + J_\Lambda(\theta)] + O(a^2) \tag{92}$$

$$\frac{f_{\sigma\sigma}(\mathbf{p},\mathbf{p}')}{g} = \frac{2k_\mathrm{F}a}{\pi} J_\Lambda(\theta) + O(a^2) \tag{93}$$

Similarly, one obtains the collision amplitudes (Eqs. (55)–(51)) as $\mathcal{A}_{\uparrow\downarrow} = \mathcal{B}_{\uparrow\downarrow}$ and $\mathcal{A}_{\sigma\sigma}(\mathbf{p}_1,\mathbf{p}_2|\mathbf{p}_3,\mathbf{p}_4) = \mathcal{B}_{\sigma\sigma}(\mathbf{p}_1,\mathbf{p}_2|\mathbf{p}_3,\mathbf{p}_4) - \mathcal{B}_{\sigma\sigma}(\mathbf{p}_1,\mathbf{p}_2|\mathbf{p}_4,\mathbf{p}_3)$:

$$\frac{\mathcal{A}'_{\uparrow\downarrow}(\mathbf{p}_1,\mathbf{p}_2|\mathbf{p}_3,\mathbf{p}_4)}{g} = 1 + \frac{2k_\mathrm{F}a}{\pi}[I_\Lambda(\theta_{12}) + J_\Lambda(\theta_{13})] + O(a^2) \tag{94}$$

$$\frac{\mathcal{A}'_{\uparrow\uparrow}(\mathbf{p}_1,\mathbf{p}_2|\mathbf{p}_3,\mathbf{p}_4)}{g} = \frac{2k_\mathrm{F}a}{\pi}\left[J_\Lambda(\theta_{13}) - J_\Lambda(\theta_{14})\right] + O(a^3) \tag{95}$$

With the Λ-dependence we may now reinterpret the mismatch between $f_{\uparrow\uparrow}$ and the forward-scattering limit of $\mathcal{A}_{\uparrow\uparrow}$. Both quantities follow from the limit $\mathbf{q} = \mathbf{p}_1 - \mathbf{p}_4 \to 0$ (that is $\theta_{14} \to 0$) in Eq. (95). However this limit does commute with the limit $\Lambda \to 0$: the Landau function f is obtained in the limit of energy transfer $\epsilon_{\mathbf{p}_1\sigma} - \epsilon_{\mathbf{p}_4\sigma} \approx v_{\mathrm{F}} q$ small compared to Λ (that is $\theta_{14} \ll \epsilon_\Lambda$), while the forward-scattering amplitude is for $v_{\mathrm{F}} q \gg \Lambda$ (that is $\theta_{14} \gg \epsilon_\Lambda$):

$$\mathcal{A}^{\text{forward}}_{\uparrow\uparrow}(\mathbf{p},\mathbf{p}') \equiv \lim_{\substack{q\to 0\\ v_{\mathrm{F}}q \gg \Lambda}} \mathcal{A}_{\uparrow\uparrow}\left(\mathbf{p}+\frac{\mathbf{q}}{2},\mathbf{p}'-\frac{\mathbf{q}}{2}\middle|\mathbf{p}'+\frac{\mathbf{q}}{2},\mathbf{p}-\frac{\mathbf{q}}{2}\right) = g\frac{2k_{\mathrm{F}}a}{\pi}\left[J(\theta)-1\right] + O(a^3) \tag{96}$$

$$f_{\uparrow\uparrow}(\mathbf{p},\mathbf{p}') \equiv \lim_{\substack{q\to 0\\ v_{\mathrm{F}}q \ll \Lambda}} \mathcal{A}_{\uparrow\uparrow}\left(\mathbf{p}+\frac{\mathbf{q}}{2},\mathbf{p}'-\frac{\mathbf{q}}{2}\middle|\mathbf{p}'+\frac{\mathbf{q}}{2},\mathbf{p}-\frac{\mathbf{q}}{2}\right) = g\frac{2k_{\mathrm{F}}a}{\pi}J(\theta) + O(a^3) \tag{97}$$

The Bethe-Salpeter relating $\mathcal{A}^{\text{forward}}_{\uparrow\uparrow}$ to $f_{\uparrow\uparrow}$ is then derived by renormalizing the effective action from $\Lambda_1 \gg v_{\mathrm{F}} q$ to $\Lambda_2 \ll v_{\mathrm{F}} q$, which involves the differential unitary operator $\exp\left(\hat{S}(\Lambda_2)\right)$ $\exp\left(-\hat{S}(\Lambda_1)\right)$. Finally, we note that $\mathcal{A}^{\text{forward}}_{\uparrow\downarrow}$ coincides with $f_{\uparrow\downarrow}$ to second-order in $k_{\mathrm{F}}a$; a mismatch between the two quantities will however appear at higher orders.

1.2.5 Residue and momentum distribution

We compute here the residue $Z_{\mathbf{p}\sigma}$ of the quasiparticles in powers of $k_{\mathrm{F}}a$. With $|\psi\rangle = |\mathrm{FS}\rangle$ our definition Eq. (36) can be reinterpreted[6] as the discontinuity of the momentum distribution at p_{F}:

$$\begin{aligned} Z_{\mathbf{p}\sigma} &= \langle \mathbf{p}\sigma, \mathrm{FS}|\hat{a}^\dagger_{\mathbf{p}\sigma}\hat{a}_{\mathbf{p}\sigma}|\mathbf{p}\sigma,\mathrm{FS}\rangle - \langle \overline{\mathbf{p}\sigma}, \mathrm{FS}|\hat{a}^\dagger_{\mathbf{p}\sigma}\hat{a}_{\mathbf{p}\sigma}|\overline{\mathbf{p}\sigma},\mathrm{FS}\rangle & (98)\\ &= \langle \mathrm{FS}|\hat{a}^\dagger_{\mathbf{p}_+\sigma}\hat{a}_{\mathbf{p}_+\sigma} - \hat{a}^\dagger_{\mathbf{p}_-\sigma}\hat{a}_{\mathbf{p}_-\sigma}|\mathrm{FS}\rangle & (99)\end{aligned}$$

where $p_\pm = p_{\mathrm{F}} \pm 0^+$. The (particle) momentum distribution in an arbitrary quasiparticle state $|\{n_{\mathbf{p}\sigma}\}\rangle$ is given to second order in g by

$$\begin{aligned} n_{\mathbf{p}\sigma}^{|\{n_{\mathbf{p}'\sigma'}\}\rangle} &\equiv \langle\{n_{\mathbf{p}'\sigma'}\}|\hat{a}^\dagger_{\mathbf{p}\sigma}\hat{a}_{\mathbf{p}\sigma}|\{n_{\mathbf{p}'\sigma'}\}\rangle = {}_0\langle\{n_{\mathbf{p}'\sigma'}\}|\hat{a}^\dagger_{\mathbf{p}\sigma}\hat{a}_{\mathbf{p}\sigma} + \frac{1}{2}\left[[\hat{a}^\dagger_{\mathbf{p}\sigma}\hat{a}_{\mathbf{p}\sigma},\hat{S}_1],\hat{S}_1\right]|\{n_{\mathbf{p}'\sigma'}\}\rangle_0 + O(g^3)\\ &= n_{\mathbf{p}\sigma} + \left(\frac{g}{V}\right)^2 \sum_{\mathbf{p}_2\mathbf{p}_3\mathbf{p}_4\in\mathcal{D}} \delta^{\mathbf{p}_3+\mathbf{p}_4}_{\mathbf{p}+\mathbf{p}_2} \frac{\bar{n}_{\mathbf{p},\sigma}\bar{n}_{\mathbf{p}_2,-\sigma}n_{\mathbf{p}_3,-\sigma}n_{\mathbf{p}_4,\sigma} - n_{\mathbf{p},\sigma}n_{\mathbf{p}_2,-\sigma}\bar{n}_{\mathbf{p}_3,-\sigma}\bar{n}_{\mathbf{p}_4,\sigma}}{(\omega_{\mathbf{p}}+\omega_{\mathbf{p}_2}-\omega_{\mathbf{p}_3}-\omega_{\mathbf{p}_4})^2}\\ &\qquad \times Q_\Lambda(\omega_{\mathbf{p}}+\omega_{\mathbf{p}_2}-\omega_{\mathbf{p}_3}-\omega_{\mathbf{p}_4}) + O(g^3) \qquad (100)\end{aligned}$$

with $Q_\Lambda(x) = 1 - \Pi_\Lambda(x)$. Applying (98), we obtain

$$\begin{aligned} Z_{\mathbf{p}\sigma} &= 1 - \left(\frac{g}{V}\right)^2 \sum_{\mathbf{p}_2\mathbf{p}_3\mathbf{p}_4\in\mathcal{D}} \delta^{\mathbf{p}_3+\mathbf{p}_4}_{\mathbf{p}+\mathbf{p}_2} \frac{\bar{n}^0_{\mathbf{p}_2,-\sigma}n^0_{\mathbf{p}_3,-\sigma}n^0_{\mathbf{p}_4,\sigma} + n^0_{\mathbf{p}_2,-\sigma}\bar{n}^0_{\mathbf{p}_3,-\sigma}\bar{n}^0_{\mathbf{p}_4,\sigma}}{(\omega_{\mathbf{p}}+\omega_{\mathbf{p}_2}-\omega_{\mathbf{p}_3}-\omega_{\mathbf{p}_4})^2}\\ &\qquad \times Q_\Lambda(\omega_{\mathbf{p}}+\omega_{\mathbf{p}_2}-\omega_{\mathbf{p}_3}-\omega_{\mathbf{p}_4}) + O(g^3) \qquad (101)\end{aligned}$$

In $p = p_{\mathrm{F}}$, the residue has a well-defined $\Lambda \to 0$ limit, which recovers the result of Belyakov [45]:

$$\begin{aligned} \langle \mathrm{FS}|\hat{n}_{\mathbf{p}\sigma}|\mathrm{FS}\rangle &= n^0_{\mathbf{p}\sigma}\left[1 - \frac{2\bar{a}^2}{\pi^2}\left(\ln 2 + \frac{1}{3}\right)\right] + \bar{n}^0_{\mathbf{p}\sigma}\frac{2\bar{a}^2}{\pi^2}\left(\ln 2 - \frac{1}{3}\right) + O(g^3) & (102)\\ Z_{p_{\mathrm{F}}} &= 1 - \frac{4\bar{a}^2}{\pi^2}\ln 2 + O(g^3) & (103)\end{aligned}$$

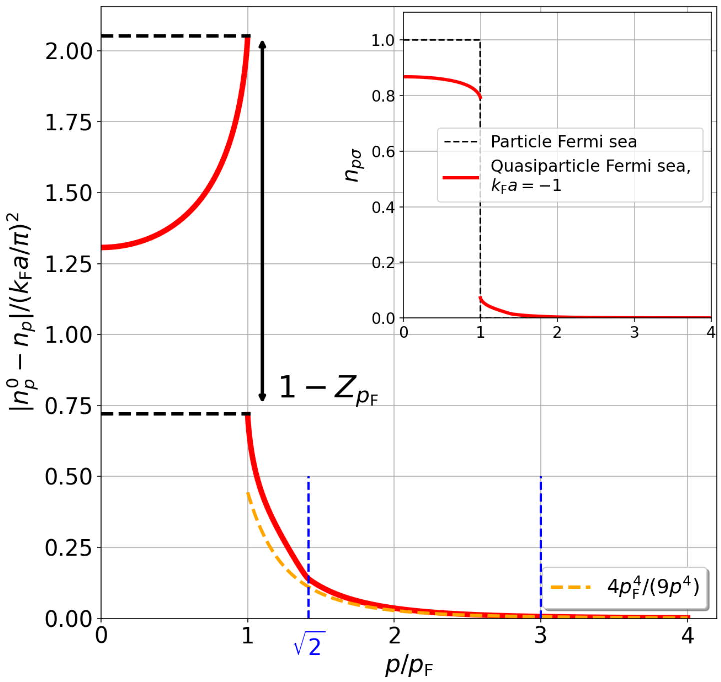

Figure 4: (Main pannel) Difference between the particle momentum distribution $n_p^{|\mathrm{FS}\rangle} = \langle \mathrm{FS}|\hat{a}^\dagger_{\mathbf{p}\sigma}\hat{a}_{\mathbf{p}\sigma}|\mathrm{FS}\rangle$ (see Eq. (100)) and the zero-temperature Fermi-Dirac distribution n_p^0 as a function of p/p_{F}. The difference is scaled to $(k_{\mathrm{F}}a/\pi)^2$ so as to be independent of a in the weak-coupling limit. The discontinuity across the Fermi surface, *i.e.* between the asymptotic values in $p_{\mathrm{F}} - 0^-$ and $p_{\mathrm{F}} + 0^+$ (black dashed lines), is given by $1 - Z_{p_{\mathrm{F}}}$. At large momenta, the distribution follows a $1/p^4$ behavior, from which the contact $C = 4\bar{a}^2/9\pi^2$ can be extracted (orange dashed curve). (Inset) The bare distribution $n_p^{|\mathrm{FS}\rangle}$ in function of p/p_{F}, evaluated in second-order perturbation theory at $k_{\mathrm{F}}a = -1$. The distribution displays the familiar shape of a depleted Fermi sea, with $n_p < 1$ down to $p = 0$.

Contrarily to Z, the momentum distribution $n_p^{|\mathrm{FS}\rangle}$ of the particles in the quasiparticle Fermi sea is well defined for all values of p/p_{F}. We depict it on Fig. 4 using the expressions given in [46], which correct the original calculation of Belyakov [45]. We first remark that the depletion of the particle Fermi sea is not limited to the vicinity of p_{F} but extends all the way to $p = 0$. Then, at large momenta, the distribution decays as $1/p^4$:

$$n_{\mathbf{p}\sigma} = \frac{C}{p^4} \tag{104}$$

This provides a way to identify the first perturbative contribution to Tan's contact [47]:

$$C = \frac{4}{9\pi^2}(k_{\mathrm{F}}a)^2 \tag{105}$$

Finally, besides the discontinuity in p_{F}, we note two corner points in $p/p_{\mathrm{F}} = \sqrt{2}$ and 3.

[6]We use the continuity of the residue at the Fermi level $Z_{\mathbf{p}_+\sigma} = Z_{\mathbf{p}_-\sigma}$, and the relations $\langle \mathbf{p}_+\sigma, \mathrm{FS}|\hat{a}^\dagger_{\mathbf{p}_+\sigma}\hat{a}_{\mathbf{p}_+\sigma}|\mathbf{p}_+\sigma, \mathrm{FS}\rangle = \langle \mathrm{FS}|\hat{a}^\dagger_{\mathbf{p}_-\sigma}\hat{a}_{\mathbf{p}_-\sigma}|\mathrm{FS}\rangle$, $\langle \overline{\mathbf{p}_-\sigma}, \mathrm{FS}|\hat{a}^\dagger_{\mathbf{p}_-\sigma}\hat{a}_{\mathbf{p}_-\sigma}|\overline{\mathbf{p}_-\sigma}, \mathrm{FS}\rangle = \langle \mathrm{FS}|\hat{a}^\dagger_{\mathbf{p}_+\sigma}\hat{a}_{\mathbf{p}_+\sigma}|\mathrm{FS}\rangle$

1.3 Derivation of the Fermi liquid kinetic equations

Knowing the energy and transition amplitudes of the quasiparticle fluid, we can now attempt to describe its dynamics by a kinetic equation. We recall that Fermi systems at intermediate temperatures $T \approx T_{\rm F}$ and strong interactions do not obey a kinetic equation, as there is no separation of timescales to break the BBGKY hierarchy. By introducing the long-lived states $|\psi\rangle = {\rm e}^{\hat{S}}|\psi\rangle_0$, the quasiparticle description manages to overcome this limitation in the low temperature limit $T \ll T_{\rm F}$, irrespectively of the interaction strength (as long as the quasiparticle picture holds).

This section uses the effective Hamiltonian Eq. (49) to rigorously derive the kinetic equation, and discuss its domain of validity. In Sec. 1.3.1, we consider the case of an homogeneous system with an out-of-equilibrium quasiparticle distribution. We show that if the cloud of excited quasiparticles is contained in a low-energy shell $\epsilon_0 \ll \epsilon_{\rm F}$, one can treat the evolution of the quasiparticle distribution in the Born-Markov approximation. This results in a nonlinear kinetic equation, from which we extract the thermal lifetime of the quasiparticles.

In Sec. 1.3.2 and 1.3.3, we study transport phenomena, where the quasiparticle gas is excited by a perturbation periodic in space and time, at frequency ω and wavenumber q. We assume that the corresponding energy scales are comparable and small compared to Λ:

$$v_{\rm F}q \ \approx \ \omega \ll \Lambda \tag{106}$$

In presence of the dynamical parameters q and ω, there exists several ways to take the low temperature limit. In Sec. 1.3.2, we derive the collisional transport equation in the limit

$$\frac{T}{T_{\rm F}} \to 0 \text{ at fixed } v_{\rm F}q\tau,\ \omega\tau \tag{107}$$

where the mean collision time τ scales, as we shall see, as $1/T^2$. In this regime, all the lower bounds on Λ in Eq. (6) are of order T^2:

$$v_{\rm F}q,\ \omega,\ \Gamma_{\rm typ} \approx T^2 \tag{108}$$

Varying the parameter $\omega\tau$ (after the limit $T \to 0$ is taken), this regime describes the crossover from hydrodynamic $\omega\tau \ll 1$ to collisionless transport $\omega\tau \gg 1$.

In Sec. 1.3.3 instead, we take the limit:

$$\frac{T}{T_{\rm F}} \to 0 \text{ at fixed } v_{\rm F}q,\ \omega \ll \epsilon_{\rm F} \tag{109}$$

In this regime, the excitation energy $v_{\rm F}q$ sets the high energy tail of the quasiparticle distribution and the lower bound on Λ. The collision integral vanishes as $(v_{\rm F}q/\epsilon_{\rm F})^2$, such that transport is collisionless to leading order in q.

1.3.1 Kinetic equation in a spatially homogeneous state

Equation of motion of the quasiparticle distribution We assume that the initial state $\hat{\varrho}$ of the system describes an uncorrelated distribution of quasiparticles

$$\hat{\varrho}(0) = \prod_{\alpha\sigma} \hat{\varrho}_{\alpha\sigma} \tag{110}$$

The reduced density matrix $\hat{\varrho}_{\alpha\sigma}$ is a function of $\hat{\gamma}_{\alpha\sigma}$ and $\hat{\gamma}^\dagger_{\alpha\sigma}$ only which defines the occupation of mode $\alpha\sigma$

$$\delta n_{\alpha\sigma} = {\rm Tr}(\hat{\varrho}_{\alpha\sigma}\delta\hat{n}_{\alpha\sigma}) \tag{111}$$

We assume that the excited quasiparticles are contained in a low-energy shell of width p_0

$$\delta n_{\mathbf{p}\sigma} = 0 \quad \text{for} \quad |p - p_{\rm F}| > p_0 \tag{112}$$

Note that this is more restrictive than just assuming a "low density of excitation" $\sum_{\alpha\sigma} \delta n_{\alpha\sigma} \ll N$. In fact, exciting even a low energy density in highly energetic modes would result in a breakdown of the quasiparticle picture.

We describe the evolution of $\delta n_{\alpha\sigma}$ in Heisenberg picture using the expansion Eq. (49) of the Hamiltonian, which we rewrite in the form

$$\hat{H} = E_0 + \hat{H}_2 + \hat{H}_4^{\rm d} + \hat{H}_4^{\rm x} + O\left(\delta(\hat{\gamma}^\dagger\hat{\gamma})^3\right) \tag{113}$$

where

$$\hat{H}_2 = \sum_{\mathbf{p}\in\mathcal{D},\sigma} \epsilon_{\mathbf{p}} \delta\hat{n}_{\mathbf{p}\sigma} \tag{114}$$

and we have splitted the terms quadratic in $\delta(\hat{\gamma}^\dagger\hat{\gamma})$ into diagonal and off-diagonal parts

$$\hat{H}_4^{\rm d} = \frac{1}{2L^3} \sum_{\substack{\mathbf{p}\mathbf{p}'\in\mathcal{D} \\ \sigma,\sigma'=\uparrow,\downarrow}} f_{\sigma\sigma'}(\mathbf{p},\mathbf{p}')\delta\hat{n}_{\mathbf{p}\sigma}\delta\hat{n}_{\mathbf{p}'\sigma'} \tag{115}$$

$$\hat{H}_4^{\rm x} = \frac{1}{2L^3} \sum_{\substack{(\mathbf{p}_\alpha,\mathbf{p}_\beta)\neq(\mathbf{p}_\delta,\mathbf{p}_\gamma) \\ \sigma,\sigma'=\uparrow,\downarrow}} \delta^{\mathbf{p}_\gamma+\mathbf{p}_\delta}_{\mathbf{p}_\alpha+\mathbf{p}_\beta} \mathcal{B}_{\sigma\sigma'}(\mathbf{p}_\alpha\mathbf{p}_\beta|\mathbf{p}_\gamma\mathbf{p}_\delta)\gamma^\dagger_{\mathbf{p}_\alpha\sigma}\gamma^\dagger_{\mathbf{p}_\beta\sigma'}\gamma_{\mathbf{p}_\gamma\sigma'}\gamma_{\mathbf{p}_\delta\sigma} \tag{116}$$

The equation of motion of $\delta n_{\alpha\sigma}$ is triggered only by $\hat{H}_4^{\rm x}$

$$\mathrm{i}\partial_t\delta n_{\mathbf{p}\sigma} = \frac{1}{2L^3}\sum_{\substack{\mathbf{p}_2,\mathbf{p}_3,\mathbf{p}_4 \\ \sigma'=\uparrow\downarrow}} \left[s_{\sigma\sigma'}\mathcal{A}_{\sigma\sigma'}\left(\mathbf{p},\mathbf{p}_2|\mathbf{p}_3,\mathbf{p}_4\right)\delta^{\mathbf{p}_3+\mathbf{p}_4}_{\mathbf{p}+\mathbf{p}_2}\langle\hat{\gamma}^\dagger_{\mathbf{p},\sigma}\hat{\gamma}^\dagger_{\mathbf{p}_2\sigma'}\hat{\gamma}_{\mathbf{p}_3\sigma'}\hat{\gamma}_{\mathbf{p}_4\sigma}\rangle - \text{c.c.}\right] + O(\delta(\hat{\gamma}^\dagger\hat{\gamma}))^3 \tag{117}$$

where $\langle\hat{O}\rangle \equiv \mathrm{Tr}(\hat{\varrho}\hat{O})$ and $s_{\uparrow\downarrow} = 1$ and $s_{\uparrow\uparrow} = 1/2$ is a counting factor. Notice that the bare $\mathcal{B}_{\sigma\sigma'}$ amplitudes have been replaced by the symmetrized ones $\mathcal{A}_{\sigma\sigma'}$.

Born-Markov approximation Eq. (117) is not a closed system, due to the presence of terms quartic in $\hat{\gamma}$. To perform a Born-Markov approximation on the dynamics of those quartic terms, similar to the classical "molecular chaos hypothesis", we introduce the quartic cumulants

$$Q^{\sigma\sigma'}_{\alpha\beta\gamma\delta} \equiv (\hat{\gamma}^\dagger_{\alpha\sigma}\hat{\gamma}^\dagger_{\beta\sigma'}\hat{\gamma}_{\gamma\sigma'}\hat{\gamma}_{\delta\sigma})_c \tag{118}$$

$$\begin{aligned}\left(\hat{a}^\dagger\hat{b}^\dagger\hat{c}\hat{d}\right)_c &\equiv \hat{a}^\dagger\hat{b}^\dagger\hat{c}\hat{d} - \hat{a}^\dagger\hat{d}\langle\hat{b}^\dagger\hat{c}\rangle - \hat{b}^\dagger\hat{c}\langle\hat{a}^\dagger\hat{d}\rangle + \hat{a}^\dagger\hat{c}\langle\hat{b}^\dagger\hat{d}\rangle + \hat{b}^\dagger\hat{d}\langle\hat{a}^\dagger\hat{c}\rangle \\ &+ \langle\hat{a}^\dagger\hat{d}\rangle\langle\hat{b}^\dagger\hat{c}\rangle - \langle\hat{a}^\dagger\hat{c}\rangle\langle\hat{b}^\dagger\hat{d}\rangle\end{aligned} \tag{119}$$

and we note that the contracted terms $\hat{\gamma}^\dagger_{\mathbf{p},\sigma}\hat{\gamma}^\dagger_{\mathbf{p}_2\sigma'}\hat{\gamma}_{\mathbf{p}_3\sigma'}\hat{\gamma}_{\mathbf{p}_4\sigma} - \hat{Q}^{\sigma\sigma'}_{\mathbf{p}\mathbf{p}_2\mathbf{p}_3\mathbf{p}_4}$ drop out from Eq. (117). The quartic cumulant is described by the equation of motion

$$\mathrm{i}\partial_t\hat{Q}^{\sigma\sigma'}_{\alpha\beta\gamma\delta} = \left(\hat{\epsilon}_{\delta\sigma} + \hat{\epsilon}_{\gamma\sigma'} - \hat{\epsilon}_{\beta\sigma'} - \hat{\epsilon}_{\alpha\sigma}\right)\hat{Q}^{\sigma\sigma'}_{\alpha\beta\gamma\delta} + \hat{S}^{\sigma\sigma'}_{\alpha\beta\gamma\delta}(t) \tag{120}$$

where

$$\hat{S}^{\sigma\sigma'}_{\alpha\beta\gamma\delta} \equiv [\hat{Q}^{\sigma\sigma'}_{\alpha\beta\gamma\delta}, \hat{H}_4^{\rm x}] = \frac{1}{2L^3}\sum_{abcd} \mathcal{B}_{\sigma_a\sigma_b}(dc|ba)\delta^{c+d}_{a+b}[(\hat{\gamma}^\dagger_{\alpha\sigma}\hat{\gamma}^\dagger_{\beta\sigma'}\hat{\gamma}_{\gamma\sigma'}\hat{\gamma}_{\delta\sigma})_c, (\hat{\gamma}^\dagger_{d\sigma_a}\hat{\gamma}^\dagger_{c\sigma_b}\hat{\gamma}_{b\sigma_b}\hat{\gamma}_{a\sigma_a})_c] \tag{121}$$

is the source term of the equation of motion. The "local energy" energy of the quasiparticle appears as an operator in our formalism:

$$\hat{\epsilon}_{\mathbf{p}\sigma} = \epsilon_{\mathbf{p}\sigma} + \frac{1}{L^3}\sum_{\mathbf{p}'\sigma'} f_{\sigma\sigma'}(\mathbf{p},\mathbf{p}')\delta\hat{n}_{\mathbf{p}'\sigma'} \tag{122}$$

The deviation $\delta\hat{\epsilon}_{\mathbf{p}\sigma} = \hat{\epsilon}_{\mathbf{p}\sigma} - \epsilon_{\mathbf{p}\sigma}$ from the Fermi sea eigenenergy originates from $\hat{H}_4^{\rm d}$: $[\hat{\gamma}_{\mathbf{p}\sigma}, \hat{H}_4^{\rm d}] = \delta\hat{\epsilon}_{\mathbf{p}\sigma}\hat{\gamma}_{\mathbf{p}\sigma}$; in the low-energy state $\hat{\varrho}$, it is negligible $\langle \delta\hat{\epsilon}_{\alpha\sigma} + \delta\hat{\epsilon}_{\beta\sigma'} - \delta\hat{\epsilon}_{\gamma\sigma'} - \delta\hat{\epsilon}_{\delta\sigma}\rangle = O(p_0/p_{\rm F})^2$.

In the Born approximation, we assume that the correlations among quasiparticle modes remain small at all times. We then replace $\langle\hat{S}\rangle$ by its Wick contraction

$$\langle \hat{S}^{\sigma\sigma'}_{\alpha\beta\gamma\delta}\rangle = \frac{\mathcal{A}_{\sigma\sigma'}(\alpha\beta|\gamma\delta)}{L^3}\left[n_{\alpha\sigma}n_{\beta\sigma'}\bar{n}_{\gamma\sigma'}\bar{n}_{\delta\sigma} - \bar{n}_{\alpha\sigma}\bar{n}_{\beta\sigma'}n_{\gamma\sigma'}n_{\delta\sigma}\right] + O(p_0/p_{\rm F})^2 \tag{123}$$

where $n_{\mathbf{p}\sigma}(t) \equiv \langle \hat{\gamma}^\dagger_{\mathbf{p}\sigma}\hat{\gamma}_{\mathbf{p}\sigma}(t)\rangle$, and we use the short-hand notations $\bar{n} = 1 - n$. The contractions have imposed imposed $(\sigma_a, \sigma_b) = (\sigma, \sigma')$ or $(\sigma_a, \sigma_b) = (\sigma', \sigma)$ and removed all the summations over momentum in Eq. (121). The correction of order $O(p_0/p_{\rm F})^2$ to this Born approximation is discuss in Appendix.

With the Born approximation, the source term $\hat{S}$ becomes independent of $\hat{Q}$, such that we can formally integrate Eq. (120)

$$\hat{Q}^{\sigma\sigma'}_{\alpha\beta\gamma\delta}(t) = -\mathrm{i}\int_{-\Delta t}^{0} \mathrm{d}t' \mathrm{e}^{-\mathrm{i}(\epsilon_\delta + \epsilon_\gamma - \epsilon_\beta - \epsilon_\alpha)t'} \hat{S}^{\sigma\sigma'}_{\alpha\beta\gamma\delta}(t + t') \tag{124}$$

Modelling the slow time-dependence of $\hat{S}$ as $\hat{S}^{\sigma\sigma'}_{\alpha\beta\gamma\delta}(t+t') = \hat{S}^{\sigma\sigma'}_{\alpha\beta\gamma\delta}(t)\mathrm{e}^{\eta t}$, we obtain the Markovian approximation of $\hat{Q}$:

$$\hat{Q}^{\sigma\sigma'}_{\alpha\beta\gamma\delta}(t) = -\frac{\hat{S}^{\sigma\sigma'}_{\alpha\beta\gamma\delta}(t)}{\epsilon_\delta + \epsilon_\gamma - \epsilon_\beta - \epsilon_\alpha + \mathrm{i}\eta} \tag{125}$$

Anticipating on Eq. (128) which gives the time scale at which $n_{\alpha\sigma}(t)$ and $\hat{S}(t)$ vary, one can estimate $\eta = O(p_0/p_{\rm F})^2$.

Nonlinear kinetic equation Replacing the expression of $\hat{Q}$ in the kinetic equation (117) and using the Plemelj formula $1/(x + \mathrm{i}0^+) = \mathcal{P} - \mathrm{i}\pi\delta(x)$, we obtain

$$\begin{aligned}\partial_t \delta n_{\mathbf{p}\sigma} = I_{\mathbf{p}\sigma}[\delta n] \equiv \frac{2\pi}{L^6}\sum_{\mathbf{p}_2,\mathbf{p}_3,\mathbf{p}_4\in\mathcal{D}} &\delta^{\mathbf{p}_3+\mathbf{p}_4}_{\mathbf{p}+\mathbf{p}_2}\delta(\epsilon_{\mathbf{p}} + \epsilon_{\mathbf{p}_2} - \epsilon_{\mathbf{p}_3} - \epsilon_{\mathbf{p}_4}) \\ &\Big(W_{\uparrow\downarrow}(\mathbf{p},\mathbf{p}_2|\mathbf{p}_3,\mathbf{p}_4)\left[n_{\mathbf{p}\uparrow}n_{\mathbf{p}_2\downarrow}\bar{n}_{\mathbf{p}_3\downarrow}\bar{n}_{\mathbf{p}_4\uparrow} - \bar{n}_{\mathbf{p}\uparrow}\bar{n}_{\mathbf{p}_2\downarrow}n_{\mathbf{p}_3\downarrow}n_{\mathbf{p}_4\uparrow}\right] \\ &+ \frac{1}{2}W_{\uparrow\uparrow}(\mathbf{p},\mathbf{p}_2|\mathbf{p}_3,\mathbf{p}_4)\left[n_{\mathbf{p}\uparrow}n_{\mathbf{p}_2\uparrow}\bar{n}_{\mathbf{p}_3\uparrow}\bar{n}_{\mathbf{p}_4\uparrow} - \bar{n}_{\mathbf{p}\uparrow}\bar{n}_{\mathbf{p}_2\uparrow}n_{\mathbf{p}_3\uparrow}n_{\mathbf{p}_4\uparrow}\right]\Big) + O(p_0/p_{\rm F})^3\end{aligned} \tag{126}$$

where

$$W_{\sigma\sigma'}(\mathbf{p}_1,\mathbf{p}_2|\mathbf{p}_3,\mathbf{p}_4) = \left[\mathcal{A}_{\sigma\sigma'}(\mathbf{p}_1,\mathbf{p}_2|\mathbf{p}_3,\mathbf{p}_4)\right]^2 \tag{127}$$

are the collision probabilities. Note that W inherits symmetry properties from Eqs. (43)–(42).

The collision integral $I_{\mathbf{p}\sigma}$ is a functional of the quasiparticle distribution δn. If $\mathbf{p}$ is inside the low-energy shell ($|p - p_{\rm F}| < p_0$), then, by the conservation of energy and the absence of highly-excited quasiparticles, so are all the collision momenta[7] $\mathbf{p}_2$, $\mathbf{p}_3$ and $\mathbf{p}_4$. In other words, the low-energy space is stable under collisions. The double summation over $\mathbf{p}_2$ and $\mathbf{p}_3$ (assuming that $\mathbf{p}_4$ is fixed by momentum conservation) is then restricted to a small interval $[p_\mathrm{F} - p_0, p_\mathrm{F} + p_0]$ about the Fermi momentum, which allows us to estimate

$$I_{\mathbf{p}\sigma} = O\left(\frac{p_0}{p_\mathrm{F}}\right)^2 \tag{128}$$

Subleading terms $O(p_0/p_\mathrm{F})^3$ in the collision integral then arise either from the Markov approximation $\eta \to 0^+$ in Eq. (125) or from the omission of the local energy $\hat{\epsilon}_{\mathbf{p}\sigma} = \epsilon_{\mathbf{p}\sigma} + O(p_0/p_\mathrm{F})$.

Thermal lifetime In its general form, the kinetic equation Eq. (126) is a nonlinear differential equation where we cannot single-out the lifetime of quasiparticles in mode $\mathbf{p}\sigma$.

To linearize the kinetic equation, we assume that the initial state is a thermal equilibrium state, which we approximate[8] by the matrix density

$$\hat{\varrho}_\mathrm{eq} = \frac{1}{\mathcal{Z}} \mathrm{e}^{-(\hat{H}_2 - \mu \hat{N})/T} \tag{129}$$

Here μ is the chemical potential, $\mathcal{Z} = \mathrm{Tr}(\mathrm{e}^{-(\hat{H}_2 - \mu\hat{N})/T})$ is a low-temperature approximation of the partition function, and $\hat{N}$ is the number of quasiparticles (see Eq. (29)). The state $\hat{\varrho}_\mathrm{eq}$ populates the quasiparticle modes according to the Fermi-Dirac distribution

$$n_\mathbf{p}^\mathrm{eq}(T) = \mathrm{Tr}(\hat{\varrho}_\mathrm{eq} \hat{n}_{\mathbf{p}\sigma}) = \frac{1}{1 + \mathrm{e}^{(\epsilon_\mathbf{p} - \mu)/T}} \tag{130}$$

It then fullfills the low-energy condition Eq. (112) with $p_\mathrm{F} \gg p_0 \gg T/v_\mathrm{F}$.

We excite the quasiparticle in mode $\mathbf{p}\sigma$, leaving the rest of the gas in the thermal state, which amounts to preparing the initial distribution

$$\langle \hat{n}_{\mathbf{p}'\sigma'} \rangle = \begin{cases} n_\mathbf{p}^\mathrm{eq}(T) + \delta n_{\mathbf{p}\sigma}^\mathrm{eq}, & \mathbf{p}'\sigma' = \mathbf{p}\sigma \\ n_{\mathbf{p}'}^\mathrm{eq}(T), & \mathbf{p}'\sigma' \neq \mathbf{p}\sigma \end{cases} \tag{131}$$

As long as it remains much below p_F, the excited quasiparticle does not need to be inside the thermal window.

The kinetic Eq. (126) then describes the thermal relaxation of $\delta n_{\mathbf{p}\sigma}^\mathrm{eq}$:

$$\partial_t \delta n_{\mathbf{p}\sigma}^\mathrm{eq} = -\Gamma_{\mathbf{p}\sigma} \delta n_{\mathbf{p}\sigma}^\mathrm{eq} \tag{132}$$

The thermal damping rate is given by Fermi's golden rule

$$\Gamma_{\mathbf{p}\sigma} = \frac{2\pi}{L^6} \sum_{\mathbf{p}_2\mathbf{p}_3\mathbf{p}_4 \in \mathcal{D}} W(\mathbf{p}, \mathbf{p}_2 | \mathbf{p}_3, \mathbf{p}_4) \delta_{\mathbf{p}+\mathbf{p}_2}^{\mathbf{p}_3+\mathbf{p}_4} \delta(\epsilon_\mathbf{p} + \epsilon_{\mathbf{p}_2} - \epsilon_{\mathbf{p}_3} - \epsilon_{\mathbf{p}_4}) \left[n_{\mathbf{p}_2}^\mathrm{eq} \bar{n}_{\mathbf{p}_3}^\mathrm{eq} \bar{n}_{\mathbf{p}_4}^\mathrm{eq} + \bar{n}_{\mathbf{p}_2}^\mathrm{eq} n_{\mathbf{p}_3}^\mathrm{eq} n_{\mathbf{p}_4}^\mathrm{eq} \right] \tag{133}$$

with the spin-averaged collision probability

$$W(\mathbf{p}_1, \mathbf{p}_2 | \mathbf{p}_3, \mathbf{p}_4) = W_{\uparrow\downarrow}(\mathbf{p}_1, \mathbf{p}_2 | \mathbf{p}_3, \mathbf{p}_4) + \frac{1}{2} W_{\sigma\sigma}(\mathbf{p}_1, \mathbf{p}_2 | \mathbf{p}_3, \mathbf{p}_4) \tag{134}$$

[7]Energy conservation guarantees that one of the outgoing wavevector is at low energy, say $|p_4 - p_\mathrm{F}| < p_0$. Then if the remaining wavevectors $\mathbf{p}_2$ and $\mathbf{p}_3$ are at high energy, they are necessarily on the same side of the Fermi level, $n_{p_2}^0 = n_{p_3}^0$. The collision in the state $\hat{\varrho}$ is then suppressed by the factor $n_{\mathbf{p}_2\sigma'} \bar{n}_{\mathbf{p}_3\sigma'} = n_{p_2}^0 \bar{n}_{p_3}^0$ in the square bracket of Eq. (126).

[8]At low temperatures, $n_\mathbf{p}^\mathrm{eq}$ differs from the zero-temperature Fermi-Dirac distribution $n_\mathbf{p}^0$ by a $O(T)$. In omitting $\hat{H}_4$ (and higher order terms) from $\hat{\varrho}_\mathrm{eq}$ we commit a small error, of order $O(T^2)$ on $n_\mathbf{p}^\mathrm{eq}$.

Integrating over energies and angles, as detailed in [32] (see the End Matter), we recover the standard result for $\Gamma_{\mathbf{p}\sigma}$:

$$\Gamma_{\mathbf{p}\sigma} = \left(\frac{m^*}{2\pi}\right)^3 \left\langle \frac{W}{\cos\frac{\theta}{2}} \right\rangle_{\theta,\phi} \left[\pi^2 T^2 + (\epsilon_{\mathbf{p}} - \mu)^2)\right] \tag{135}$$

We have reparametrized the probability W in terms of the two angles $\theta = (\widehat{\mathbf{p}_1, \mathbf{p}_2})$ and $\phi = (\mathbf{p}_1 - \widehat{\mathbf{p}_2, \mathbf{p}_3} - \mathbf{p}_4)$ that locate the four momenta $\mathbf{p}_1$, $\mathbf{p}_2$, $\mathbf{p}_3$, $\mathbf{p}_4$ of norm p_{F}: $W(\mathbf{p}_1, \mathbf{p}_2|\mathbf{p}_3, \mathbf{p}_4) = W(\theta, \phi)$. We have then introduced the average over solid angles

$$\langle f \rangle_{\theta,\phi} = \frac{1}{4\pi}\int_0^{\pi}\int_0^{2\pi} f(\theta,\phi)\sin\theta \,\mathrm{d}\theta\,\mathrm{d}\phi \tag{136}$$

Since $|\epsilon_{\mathbf{p}} - \mu|$ and T are both below $v_{\mathrm{F}}p_0$, Eq. (135) illustrates the $O(p_0/p_{\mathrm{F}})^2$ scaling of the collision integral.

1.3.2 Linearized transport equation at nonzero temperature

Linear response approximation We now imagine that the system is driven out-of-equilibrium by an external field U_σ coupled to quasiparticle density operators $\hat{\gamma}^\dagger\hat{\gamma}$

$$\hat{H}_{\mathrm{ext}} = \sum_{\mathbf{p}\in\mathcal{D},\sigma} U_\sigma(\mathbf{q},t)\hat{n}_{\mathbf{p}\sigma}^{-\mathbf{q}} \tag{137}$$

where we use Anderson's notations for the quasiparticle-quasihole excitation operator

$$\hat{n}_{\mathbf{p}\sigma}^{\mathbf{q}}(t) = \hat{\gamma}_{\mathbf{p}+\mathbf{q}/2,\sigma}^\dagger \hat{\gamma}_{\mathbf{p}-\mathbf{q}/2,\sigma} \tag{138}$$

One can also see $\hat{H}_{\mathrm{ext}}$ as driving the density of quasiparticles in real space:

$$\hat{H}_{\mathrm{ext}} = \int \mathrm{d}^3\mathbf{r} \sum_\sigma U_\sigma(\mathbf{r},t)\hat{\psi}_{\gamma,\sigma}^\dagger(\mathbf{r})\hat{\psi}_{\gamma,\sigma}(\mathbf{r}) \tag{139}$$

where[9] $\hat{\psi}_{\gamma,\sigma}(\mathbf{r}) = L^{-3/2}\sum_{\mathbf{p}\in\mathcal{D}} \mathrm{e}^{\mathrm{i}\mathbf{p}\cdot\mathbf{r}}\hat{\gamma}_{\mathbf{p}\sigma}$ is the field operator associated to the quasiparticles, and $U_\sigma(\mathbf{r}) = U_\sigma(\mathbf{q})\mathrm{e}^{\mathrm{i}\mathbf{q}\cdot\mathbf{r}}$. Placing ourselves in the linear response regime, we assume a weak driving compared to the temperature

$$|U_\sigma| \ll T \tag{140}$$

and we decompose the state of the system at time t as

$$\hat{\varrho}(t) = \hat{\varrho}_{\mathrm{eq}} + \delta\hat{\varrho}(t) \tag{141}$$

with $\delta\hat{\varrho} = O(U_\sigma/T)$. In the linear response regime, the fluctuations about the thermal state are small $\hat{n}_{\mathbf{p}\sigma} - n_{\mathbf{p}}^{\mathrm{eq}} = O(U)$, and we approximate the contribution of the drive to the Heisenberg equation of motion by

$$[\hat{n}_{\mathbf{p}\sigma}^{\mathbf{q}}, \hat{H}_{\mathrm{ext}}] = U_\sigma(\mathbf{q})\left(\hat{n}_{\mathbf{p}+\frac{\mathbf{q}}{2},\sigma} - \hat{n}_{\mathbf{p}-\frac{\mathbf{q}}{2},\sigma}\right) = U_\sigma(\mathbf{q})\left(n_{\mathbf{p}+\frac{\mathbf{q}}{2}}^{\mathrm{eq}} - n_{\mathbf{p}-\frac{\mathbf{q}}{2}}^{\mathrm{eq}}\right) + O(U^2) \tag{142}$$

[9] Note that taking the continuous limit $l \to 0$, we have converted the discreet sum $l^3\sum_{\mathbf{r}}$ over the sites $\mathbf{r}$ of the lattice model into the $\int \mathrm{d}^3 r$ integral.

Quantum Boltzmann equation We obtain the streaming term[10] of the Boltzmann equation as the contribution of $\hat{H}_2 + \hat{H}_4^{\mathrm{d}}$:

$$[\hat{n}^{\mathbf{q}}_{\mathbf{p}\sigma}, \hat{H}_2 + \hat{H}_4^{\mathrm{d}}] = \left(\hat{\epsilon}_{\mathbf{p}-\mathbf{q}/2,\sigma} - \hat{\epsilon}_{\mathbf{p}+\mathbf{q}/2,\sigma}\right)\hat{n}^{\mathbf{q}}_{\mathbf{p}\sigma} \tag{143}$$

The contribution of $\hat{H}_4^x$ is no longer antihermitian

$$\begin{aligned}[\hat{n}^{\mathbf{q}}_{\mathbf{p}\sigma}, \hat{H}_4^{\mathrm{x}}] = \frac{1}{2L^3} \sum_{\substack{\mathbf{p}_4,\mathbf{p}_2 \neq \mathbf{p}_3 \\ \sigma'=\uparrow\downarrow}} s_{\sigma\sigma'} \Bigg[& \mathcal{A}_{\sigma\sigma'}\left(\mathbf{p} - \frac{\mathbf{q}}{2}, \mathbf{p}_2 | \mathbf{p}_3, \mathbf{p}_4\right) \quad \delta^{\mathbf{p}_3+\mathbf{p}_4}_{\mathbf{p}-\frac{\mathbf{q}}{2}+\mathbf{p}_2} \quad \hat{\gamma}^{\dagger}_{\mathbf{p}+\frac{\mathbf{q}}{2},\sigma} \hat{\gamma}^{\dagger}_{\mathbf{p}_2\sigma'} \hat{\gamma}_{\mathbf{p}_3\sigma'} \hat{\gamma}_{\mathbf{p}_4\sigma} \\ & - \mathcal{A}_{\sigma\sigma'}\left(\mathbf{p} + \frac{\mathbf{q}}{2}, \mathbf{p}_2 | \mathbf{p}_3, \mathbf{p}_4\right) \quad \delta^{\mathbf{p}_3+\mathbf{p}_4}_{\mathbf{p}+\frac{\mathbf{q}}{2}+\mathbf{p}_2} \quad \hat{\gamma}^{\dagger}_{\mathbf{p}_4\sigma} \hat{\gamma}^{\dagger}_{\mathbf{p}_3\sigma'} \hat{\gamma}_{\mathbf{p}_2\sigma'} \hat{\gamma}_{\mathbf{p}-\frac{\mathbf{q}}{2}\sigma} \Bigg]\end{aligned} \tag{144}$$

where $s_{\uparrow\downarrow} = 1$ and $s_{\uparrow\uparrow} = 1/2$. We treat this contribution using the cumulant expansion (Eq. (119)) to obtain:

$$[\hat{n}^{\mathbf{q}}_{\mathbf{p}\sigma}, \hat{H}_4^{\mathrm{x}}] = (n^{\mathrm{eq}}_{\mathbf{p}+\frac{\mathbf{q}}{2}} - n^{\mathrm{eq}}_{\mathbf{p}-\frac{\mathbf{q}}{2}}) \frac{1}{L^3} \sum_{\mathbf{p}',\sigma'} \mathcal{A}_{\sigma\sigma'}\left(\mathbf{p} - \frac{\mathbf{q}}{2}, \mathbf{p}' + \frac{\mathbf{q}}{2} | \mathbf{p}' - \frac{\mathbf{q}}{2}, \mathbf{p} + \frac{\mathbf{q}}{2}\right) \hat{n}^{\mathbf{q}}_{\mathbf{p}',\sigma'} + \mathrm{i}\hat{I}_{\mathbf{p}\sigma} \tag{145}$$

where $\hat{I}_{\mathbf{p}\sigma}$ is the cumulant part of Eq. (144). Restricting to leading order in U, we have replaced the average values in the partially contracted terms by thermal averages:

$$\langle \hat{\gamma}^{\dagger}_{\mathbf{p}\sigma} \hat{\gamma}_{\mathbf{p}'\sigma'} \rangle = \delta_{\mathbf{p}\mathbf{p}'} \delta_{\sigma\sigma'} n^{\mathrm{eq}}_{\mathbf{p}} + O(U/T) \tag{146}$$

To recognize the Vlasov force in those terms, we use Eq. (60) and the condition $v_{\mathrm{F}} q \ll \Lambda$:

$$\mathcal{A}_{\sigma\sigma'}\left(\mathbf{p} - \frac{\mathbf{q}}{2}, \mathbf{p}' + \frac{\mathbf{q}}{2} | \mathbf{p}' - \frac{\mathbf{q}}{2}, \mathbf{p} + \frac{\mathbf{q}}{2}\right) = f_{\sigma\sigma'}(\mathbf{p}, \mathbf{p}') + O(v_{\mathrm{F}} q/\Lambda) \tag{147}$$

Note that the partial contractions also replace the local energies in Eq. (143) by their thermal value $\langle \hat{\epsilon}_{\mathbf{p}\sigma} \rangle = \langle \hat{\epsilon}_{\mathbf{p}\sigma} \rangle_{\mathrm{eq}} + O(U)$.

Collision integral Following the steps discussed in Sec. 1.3.1, we compute the collision integral $\hat{I}_{\mathbf{p}\sigma}$ in the Born-Markov approximation. Restricting to leading order in $v_{\mathrm{F}} q/T$, we obtain the transport equation

$$(\mathrm{i}\partial_t + v_{\mathrm{F}} q u) \hat{n}^{\mathbf{q}}_{\mathbf{p}\sigma} - v_{\mathrm{F}} q u \frac{\partial n_{\mathrm{eq}}}{\partial \epsilon}\Big|_{\epsilon=\epsilon_{\mathbf{p}}} \left(U_{\sigma}(\mathbf{q}) + \frac{1}{L^3} \sum_{\mathbf{p}'\sigma'} f_{\sigma\sigma'}(\mathbf{p}, \mathbf{p}') \hat{n}^{\mathbf{q}}_{\mathbf{p}'\sigma'} \right) = \mathrm{i}\hat{I}^{\mathrm{lin}}_{\mathbf{p}\sigma}(\hat{n}^{\mathbf{q}}) \tag{148}$$

where $u = \cos(\widehat{\mathbf{p}, \mathbf{q}})$, $n_{\mathrm{eq}}(\epsilon) = 1/(1 + \mathrm{e}^{(\epsilon-\mu)/T})$, and the collision integral linearized about the thermal state takes the form

$$\begin{aligned}\hat{I}^{\mathrm{lin}}_{\mathbf{p}\uparrow}[\hat{n}^{\mathbf{q}}] = \frac{2\pi}{L^6} & \sum_{\beta,\gamma,\delta \in \mathcal{D}} \delta^{\gamma+\delta}_{\mathbf{p}+\beta} \delta(\epsilon_{\mathbf{p}} + \epsilon_{\beta} - \epsilon_{\gamma} - \epsilon_{\delta}) \\ & \times \Bigg\{ \left[n^{\mathrm{eq}}_{\beta} \bar{n}^{\mathrm{eq}}_{\gamma} \bar{n}^{\mathrm{eq}}_{\delta} + \bar{n}^{\mathrm{eq}}_{\beta} n^{\mathrm{eq}}_{\gamma} n^{\mathrm{eq}}_{\delta} \right] \left(W_{\uparrow\downarrow}(\mathbf{p}, \beta | \gamma, \delta) + \frac{1}{2} W_{\sigma\sigma}(\mathbf{p}, \beta | \gamma, \delta) \right) \hat{n}^{\mathbf{q}}_{\mathbf{p}\uparrow} \\ & + \left[n^{\mathrm{eq}}_{\mathbf{p}} \bar{n}^{\mathrm{eq}}_{\gamma} \bar{n}^{\mathrm{eq}}_{\delta} + \bar{n}^{\mathrm{eq}}_{\mathbf{p}} n^{\mathrm{eq}}_{\gamma} n^{\mathrm{eq}}_{\delta} \right] \left(W_{\uparrow\downarrow}(\mathbf{p}, \beta | \gamma, \delta) \hat{n}^{\mathbf{q}}_{\beta,\downarrow} + \frac{1}{2} W_{\sigma\sigma}(\mathbf{p}, \beta | \gamma, \delta) \hat{n}^{\mathbf{q}}_{\beta\uparrow} \right) \\ & - \left[n^{\mathrm{eq}}_{\delta} \bar{n}^{\mathrm{eq}}_{\mathbf{p}} \bar{n}^{\mathrm{eq}}_{\beta} + \bar{n}^{\mathrm{eq}}_{\delta} n^{\mathrm{eq}}_{\mathbf{p}} n^{\mathrm{eq}}_{\beta} \right] \left(W_{\uparrow\downarrow}(\mathbf{p}, \beta | \gamma, \delta) \hat{n}^{\mathbf{q}}_{\gamma,\downarrow} + \frac{1}{2} W_{\sigma\sigma}(\mathbf{p}, \beta | \gamma, \delta) \hat{n}^{\mathbf{q}}_{\gamma\uparrow} \right) \\ & - \left[n^{\mathrm{eq}}_{\gamma} \bar{n}^{\mathrm{eq}}_{\mathbf{p}} \bar{n}^{\mathrm{eq}}_{\beta} + \bar{n}^{\mathrm{eq}}_{\gamma} n^{\mathrm{eq}}_{\mathbf{p}} n^{\mathrm{eq}}_{\beta} \right] \left(W_{\uparrow\downarrow}(\mathbf{p}, \beta | \gamma, \delta) + \frac{1}{2} W_{\sigma\sigma}(\mathbf{p}, \beta | \gamma, \delta) \right) \hat{n}^{\mathbf{q}}_{\delta\uparrow} \Bigg\}\end{aligned} \tag{149}$$

[10]We have used the property $f_{\sigma\sigma}(\mathbf{p}+\mathbf{q}/2, \mathbf{p}-\mathbf{q}/2) = 0$, valid for $v_{\mathrm{F}} q \ll \Lambda$, which guarantees that $\hat{n}^{\mathbf{q}}_{\mathbf{p}\sigma}$ commutes with $\delta\hat{\epsilon}_{\mathbf{p}\pm\mathbf{q}/2,\sigma}$

We may interpret the linearized transport equation in real space by performing an inverse Wigner transform

$$n_\sigma(\mathbf{p},\mathbf{q}) \equiv \langle \hat{n}^{-\mathbf{q}}_{\mathbf{p}\sigma}\rangle = \frac{1}{\sqrt{L^3}}\int \mathrm{d}^3 r \mathrm{e}^{-\mathrm{i}\mathbf{q}\cdot\mathbf{r}}\delta n_\sigma(\mathbf{p},\mathbf{r}) \tag{150}$$

The Wigner transform of $\langle \hat{I}^{\mathrm{lin}}_{\mathbf{p}\sigma}\rangle$ is then interpreted as a collision integral linearized for small spatial fluctuations:

$$I_{\mathbf{p}\sigma}[n^{\mathrm{eq}}+\delta n(\mathbf{r})] = \langle \hat{I}^{\mathrm{lin}}_{\mathbf{p}\sigma}(\mathbf{r})\rangle + O(\delta n)^2 \tag{151}$$

where $I_{\mathbf{p}\sigma}[n]$ is defined by Eq. (126). The transport equation may now be written in real space

$$\partial_t n_\sigma + \frac{\partial \epsilon_{\mathbf{p}\sigma}}{\partial \mathbf{p}}\cdot\frac{\partial n_\sigma}{\partial \mathbf{r}} - \frac{\partial n^{\mathrm{eq}}_{\mathbf{p}\sigma}}{\partial \mathbf{p}}\cdot\left(\frac{1}{L^3}\sum_{\mathbf{p}'\sigma'} f_{\sigma\sigma'}(\mathbf{p},\mathbf{p}')\frac{\partial n_{\sigma'}}{\partial \mathbf{r}} + U_\sigma(\mathbf{r})\right) = I_{\mathbf{p}\sigma}[n^{\mathrm{eq}}+\delta n(\mathbf{r})] \tag{152}$$

We stress that this transport equation in real space is linearized. Obtaining a nonlinear equation in real space appears far from obvious in our formalism; in particular it is not clear, when looking at Eq. (62), if the Vlasov force (the first term between bracket in Eq. (152)) still depends only on $f_{\sigma\sigma'}(\mathbf{p},\mathbf{p}')$ or also on $\mathcal{A}_{\sigma\sigma'}(\mathbf{p},\mathbf{p}_2|\mathbf{p}_3,\mathbf{p}_4)$ at $v_{\mathrm{F}}|\mathbf{p}-\mathbf{p}_4|\gg\Lambda$.

1.3.3 Transport equation at $T=0$

We now let $T\to 0$ at fixed q and ω. We describe the state of the system in presence of $\hat{H}_{\mathrm{ext}}$ by

$$\hat{\varrho}(t) = |\mathrm{FS}\rangle\langle\mathrm{FS}| + \delta\hat{\varrho}(t) \tag{153}$$

The linear response regime (*i.e.* the absence of second harmonic generation) ensures that only the momenta that differs from p_{F} by q are excited. The fluctuations of the quasiparticle distribution thus remain zero for $|p-p_{\mathrm{F}}|\gg q$, and the wavenumber q acts as the small parameter p_0 of the low-energy expansion. The linearized transport equation is then

$$\left(i\partial_t + \epsilon_{\mathbf{p}+\mathbf{q}/2} - \epsilon_{\mathbf{p}-\mathbf{q}/2}\right)\hat{n}^{\mathbf{q}}_{\mathbf{p}\sigma} - \left(n^0_{\mathbf{p}+\frac{\mathbf{q}}{2}} - n^0_{\mathbf{p}-\frac{\mathbf{q}}{2}}\right)\left(U_\sigma(\mathbf{q}) + \frac{1}{L^3}\sum_{\mathbf{p}'\sigma'} f_{\sigma\sigma'}(\mathbf{p},\mathbf{p}')\hat{n}^{\mathbf{q}}_{\mathbf{p}'\sigma'}\right)$$
$$= \mathrm{i}\hat{I}^{\mathrm{lin}}_{\mathbf{p}\sigma}(\hat{n}^{\mathbf{q}}, T=0) \tag{154}$$

The zero-temperature collision integral $\hat{I}^{\mathrm{lin}}_{\mathbf{p}\sigma}(\hat{n}^{\mathbf{q}}, T=0)$ is obtained by replacing $n^{\mathrm{eq}}_{\mathbf{p}\sigma}\to n^0_{\mathbf{p}}$ in the nonzero temperature expression (149); it is of order $O(q/p_{\mathrm{F}})^2$ to leading order, with non-Markovian corrections of order $O(q/p_{\mathrm{F}})^3$ (see Eqs. (125) and (128)). To leading order in q/p_{F} the transport equation (154) then reduces to its collisionless left-hand side.

2 Transport dynamics in Fermi liquids

2.1 The transport equation as a linear integral equation

In this section, we study the linear integral kernel contained in the collision integral Eq. (149) at nonzero temperature.

2.1.1 Collision kernel

We express the collision collision integral in terms of the collision kernel

$$\mathcal{N}_{\sigma\sigma'}(\mathbf{p},\mathbf{p}') = -\Gamma(\mathbf{p})L^3\delta_{\sigma\sigma'}\delta_{\mathbf{p}\mathbf{p}'} - E_{\sigma\sigma'}(\mathbf{p},\mathbf{p}') + S_{\sigma\sigma'}(\mathbf{p},\mathbf{p}') \tag{155}$$

$$I^{\mathrm{lin}}_\sigma(\mathbf{p},n) = \frac{1}{L^3}\sum_{\mathbf{p}'\sigma'}\mathcal{N}_{\sigma'\sigma}(\mathbf{p}',\mathbf{p})n_{\sigma'}(\mathbf{p}') \tag{156}$$

Note the transposed order of $\mathbf{p}'\sigma'$ and $\mathbf{p}\sigma$ in Eq. (156). The diagonal part of $\mathcal{N}$ is given by the quasiparticles damping rate Eq. (133) and the off-diagonal part involves the four subkernels:

$$E_{\sigma\sigma}(\mathbf{p},\mathbf{p}') = \frac{2\pi}{L^3}\sum_{\mathbf{p}_3,\mathbf{p}_4\in\mathcal{D}} \frac{W_{\sigma\sigma}(\mathbf{p}',\mathbf{p}|\mathbf{p}_3,\mathbf{p}_4)}{2}\delta_{\mathbf{p}+\mathbf{p}'}^{\mathbf{p}_3+\mathbf{p}_4}\delta(\epsilon_{\mathbf{p}}+\epsilon_{\mathbf{p}'}-\epsilon_{\mathbf{p}_3}-\epsilon_{\mathbf{p}_4})N_{\mathbf{p}_3\mathbf{p}_4}^{\mathbf{p}'} \tag{157}$$

$$E_{\uparrow\downarrow}(\mathbf{p},\mathbf{p}') = \frac{2\pi}{L^3}\sum_{\mathbf{p}_3,\mathbf{p}_4\in\mathcal{D}} W_{\uparrow\downarrow}(\mathbf{p}',\mathbf{p}|\mathbf{p}_3,\mathbf{p}_4)\delta_{\mathbf{p}+\mathbf{p}'}^{\mathbf{p}_3+\mathbf{p}_4}\delta(\epsilon_{\mathbf{p}}+\epsilon_{\mathbf{p}'}-\epsilon_{\mathbf{p}_3}-\epsilon_{\mathbf{p}_4})N_{\mathbf{p}_3\mathbf{p}_4}^{\mathbf{p}'} \tag{158}$$

$$S_{\sigma\sigma}(\mathbf{p},\mathbf{p}') = \frac{2\pi}{L^3}\sum_{\mathbf{p}_2,\mathbf{p}_4\in\mathcal{D}} \left[W_{\sigma\sigma}(\mathbf{p}',\mathbf{p}_2|\mathbf{p}_4,\mathbf{p})+W_{\uparrow\downarrow}(\mathbf{p}',\mathbf{p}_2|\mathbf{p}_4,\mathbf{p})\right]\delta_{\mathbf{p}+\mathbf{p}_4}^{\mathbf{p}_2+\mathbf{p}'}\delta(\epsilon_{\mathbf{p}}+\epsilon_{\mathbf{p}_4}-\epsilon_{\mathbf{p}'}-\epsilon_{\mathbf{p}_2})N_{\mathbf{p}'\mathbf{p}_2}^{\mathbf{p}_4}$$

$$S_{\uparrow\downarrow}(\mathbf{p},\mathbf{p}') = \frac{2\pi}{L^3}\sum_{\mathbf{p}_2,\mathbf{p}_4\in\mathcal{D}} W_{\uparrow\downarrow}(\mathbf{p}',\mathbf{p}_2|\mathbf{p},\mathbf{p}_4)\delta_{\mathbf{p}+\mathbf{p}_4}^{\mathbf{p}'+\mathbf{p}_2}\delta(\epsilon_{\mathbf{p}}+\epsilon_{\mathbf{p}_4}-\epsilon_{\mathbf{p}'}-\epsilon_{\mathbf{p}_2})N_{\mathbf{p}'\mathbf{p}_2}^{\mathbf{p}_4} \tag{159}$$

where $N_{\mathbf{p}_1\mathbf{p}_2}^{\mathbf{p}_3} = n_{\mathbf{p}_1}^{\rm eq}n_{\mathbf{p}_2}^{\rm eq}\overline{n}_{\mathbf{p}_3}^{\rm eq}+\overline{n}_{\mathbf{p}_1}^{\rm eq}\overline{n}_{\mathbf{p}_2}^{\rm eq}n_{\mathbf{p}_3}^{\rm eq}$. The collisions kernels $E_{\sigma\sigma'}$ describe the coupling between quasiparticles in mode $\mathbf{p}\sigma$ and $\mathbf{p}'\sigma'$ through collisions where $\mathbf{p}$ and $\mathbf{p}'$ are on the same side of the collision (either incoming or outgoing). Conversely, $S_{\sigma\sigma'}$ describes the couplings where $\mathbf{p}$ and $\mathbf{p}'$ are on opposite sides.

2.1.2 Conservation laws

Collisions obey a few conservation laws which play a prominent role in transport phenomena: the numbers of spin ↑ and ↓ particles, the momentum and the energy are the same before and after any collision. In mathematical terms, this means that the collision kernel $\mathcal{N}$ has 6 zero eigenfunctions (counting the 3 components of the momentum). Since the kernel is not symmetric, it has distinct left and right eigenfunctions.

To recognize the conservation laws on our collision kernel, let us contract it with some arbitrary functions $n_\sigma(\mathbf{p})$ to the left and $\nu_\sigma(\mathbf{p})$ to the right:

$$\begin{aligned}\sum_{\mathbf{p}\mathbf{p}'\in\mathcal{D},\sigma\sigma'=\uparrow\downarrow} n_\sigma(\mathbf{p})\mathcal{N}_{\sigma\sigma'}(\mathbf{p},\mathbf{p}')\nu_{\sigma'}(\mathbf{p}') = \frac{2\pi}{L^6}&\sum_{\mathbf{p}_1\mathbf{p}_2\mathbf{p}_3\mathbf{p}_4\in\mathcal{D},\sigma=\uparrow\downarrow}\delta_{\mathbf{p}_1+\mathbf{p}_2}^{\mathbf{p}_3+\mathbf{p}_4}\delta(\epsilon_{\mathbf{p}_1}+\epsilon_{\mathbf{p}_2}-\epsilon_{\mathbf{p}_3}-\epsilon_{\mathbf{p}_4})N_{\mathbf{p}_3\mathbf{p}_4}^{\mathbf{p}_2}\\ \times\Bigg[&\frac{1}{2}W_{\uparrow\uparrow}(\mathbf{p}_1,\mathbf{p}_2|\mathbf{p}_3,\mathbf{p}_4)\big(\nu_\sigma(\mathbf{p}_1)+\nu_\sigma(\mathbf{p}_2)-\nu_\sigma(\mathbf{p}_3)-\nu_\sigma(\mathbf{p}_4)\big)\\ &+W_{\uparrow\downarrow}(\mathbf{p}_1,\mathbf{p}_2|\mathbf{p}_3,\mathbf{p}_4)(\nu_\sigma(\mathbf{p}_1)+\nu_{-\sigma}(\mathbf{p}_2)-\nu_{-\sigma}(\mathbf{p}_3)-\nu_\sigma(\mathbf{p}_4))\Bigg]n_\sigma(\mathbf{p}_1)\end{aligned} \tag{160}$$

The 6 functions ν_σ which cancel this expression for all n_σ, *i.e.* the right zero-energy eigenfunctions, are $\nu_\sigma(\mathbf{p}) = \delta_{\sigma,\uparrow}$, $\delta_{\sigma,\downarrow}$, p_x, p_y, p_z and $\epsilon_{\mathbf{p}}$. The corresponding conserved physical quantities are the density fluctuations $\delta\rho_\sigma$, the macroscopic velocity $\mathbf{v}$ and the energy density δe:

$$\delta\rho_\sigma = \frac{1}{L^3}\sum_{\mathbf{p}\in\mathcal{D}} n_\sigma(\mathbf{p}) \tag{161}$$

$$m\mathbf{v} = \frac{1}{N}\sum_{\mathbf{p}\in\mathcal{D}} \mathbf{p}n_\sigma(\mathbf{p}) \tag{162}$$

$$\delta e = \frac{1}{L^3}\sum_{\mathbf{p}\in\mathcal{D}} \epsilon_{\mathbf{p}}n_\sigma(\mathbf{p}) \tag{163}$$

Unsurprisingly, opposite spin collisions (with probability $W_{\uparrow\downarrow}$) are responsible for the absence of conservation of the velocity imbalance $\mathbf{v}_\uparrow - \mathbf{v}_\downarrow$ and energy imbalance $e_\uparrow - e_\downarrow$.

2.1.3 Total density and polarization

In our unpolarized Fermi liquid, fluctuations of the density $n_+ = n_\uparrow + n_\downarrow$ and polarisation $n_- = n_\uparrow - n_\downarrow$ are decoupled, by the transport equation in general, and by the collision integral in particular. The corresponding collision kernel are:

$$\mathcal{N}_\pm(\mathbf{p},\mathbf{p}') = -\Gamma(\mathbf{p})L^3\delta_{\sigma\sigma'}\delta_{\mathbf{p}\mathbf{p}'} - E_\pm(\mathbf{p},\mathbf{p}') + 2S_\pm(\mathbf{p},\mathbf{p}'), \qquad I_\pm(\mathbf{p}) = I_\uparrow^{\text{lin}}(\mathbf{p}) \pm I_\downarrow^{\text{lin}}(\mathbf{p}) \tag{164}$$

with

$$E_\pm(\mathbf{p},\mathbf{p}') = \frac{1}{L^3}\sum_{\mathbf{p}_3\mathbf{p}_4} W_{E\pm}(\mathbf{p},\mathbf{p}'|\mathbf{p}_3,\mathbf{p}_4)\ \delta_{\mathbf{p}+\mathbf{p}'}^{\mathbf{p}_3+\mathbf{p}_4}\delta(\epsilon_\mathbf{p}+\epsilon_{\mathbf{p}'}-\epsilon_{\mathbf{p}_3}-\epsilon_{\mathbf{p}_4})N_{\mathbf{p}_3\mathbf{p}_4}^{\mathbf{p}'} \tag{165}$$

$$S_\pm(\mathbf{p},\mathbf{p}') = \frac{1}{L^3}\sum_{\mathbf{p}_2\mathbf{p}_4} W_{S\pm}(\mathbf{p},\mathbf{p}_2|\mathbf{p}',\mathbf{p}_4)\ \delta_{\mathbf{p}+\mathbf{p}_2}^{\mathbf{p}'+\mathbf{p}_4}\delta(\epsilon_\mathbf{p}+\epsilon_{\mathbf{p}_2}-\epsilon_{\mathbf{p}'}-\epsilon_{\mathbf{p}_4})N_{\mathbf{p}'\mathbf{p}_4}^{\mathbf{p}_2} \tag{166}$$

We have defined the (anti)-symmetrized probabilities $W_{E\pm}$ and $W_{S\pm}$:

$$W_{E\pm}(\mathbf{p}_1,\mathbf{p}_2|\mathbf{p}_3,\mathbf{p}_4) = \frac{1}{2}W_{\uparrow\uparrow}(\mathbf{p}_1,\mathbf{p}_2|\mathbf{p}_3,\mathbf{p}_4) \pm \frac{1}{2}\left(W_{\uparrow\downarrow}(\mathbf{p}_1,\mathbf{p}_2|\mathbf{p}_3,\mathbf{p}_4) + W_{\uparrow\downarrow}(\mathbf{p}_1,\mathbf{p}_2|\mathbf{p}_4,\mathbf{p}_3)\right) \tag{167}$$

$$W_{S\pm}(\mathbf{p}_1,\mathbf{p}_2|\mathbf{p}_3,\mathbf{p}_4) = \frac{1}{2}W_{\uparrow\uparrow}(\mathbf{p}_1,\mathbf{p}_2|\mathbf{p}_3,\mathbf{p}_4) \pm \frac{1}{2}\left(W_{\uparrow\downarrow}(\mathbf{p}_1,\mathbf{p}_2|\mathbf{p}_3,\mathbf{p}_4) \pm W_{\uparrow\downarrow}(\mathbf{p}_1,\mathbf{p}_2|\mathbf{p}_4,\mathbf{p}_3)\right) \tag{168}$$

Remark that $W_{E+} = W_{S+}$. We have used the symmetry properties (inherited from Eqs. (41)–(43)):

$$W(\mathbf{p}_4,\mathbf{p}_3|\mathbf{p}_2,\mathbf{p}_1) = W(\mathbf{p}_2,\mathbf{p}_1|\mathbf{p}_4,\mathbf{p}_3) = W(\mathbf{p}_1,\mathbf{p}_2|\mathbf{p}_3,\mathbf{p}_4) \tag{169}$$

Among the conserved quantities Eqs. (161)–(163), $\mathcal{N}_+$ inherits $\delta\rho_\uparrow + \delta\rho_\downarrow$, $\mathbf{v}$ and δe, while $\mathcal{N}_-$ inherits only $\delta\rho_\uparrow - \delta\rho_\downarrow$.

2.1.4 Quasiparticle distribution in the thermal window

To focus on the thermal energy window, to which the fluctuations of $n(\mathbf{p})$ are limited, we reparametrized the quasiparticle distributions as

$$n_\pm(\mathbf{p}) = -\frac{U_\pm(\mathbf{q})}{T}g(y)\ \nu_\pm(y,\theta), \qquad \text{with} \qquad g(y) = \frac{1}{4\text{ch}^2(y/2)} \tag{170}$$

We have parametrized the 3D momentum $\mathbf{p}$ with $y = (\epsilon_{\mathbf{p}\sigma}-\mu)/T$, $\theta = (\widehat{\mathbf{p},\mathbf{q}})$ and an azimuthal angle ϕ, of which ν is independent due to the rotational invariance about $\mathbf{q}$. In the spirit of linear response theory, we have scale the distribution ν to the intensity $U_\pm = U_\uparrow \pm U_\downarrow$ of the drive. By taking out the thermal broadening function $\partial n_{\text{eq}}/\partial\epsilon = -1/(Tg(y))$, the change of variable Eq. (170) smoothens the dependence of $\nu_\pm$ on y. It also transposes[11] the collision kernels

$$\mathcal{N}(\mathbf{p}',\mathbf{p})\frac{g(y')}{g(y)} = \mathcal{N}(\mathbf{p},\mathbf{p}') \tag{171}$$

and similarly for $E_\pm$ and $S_\pm$. In term of ν, the collision integral becomes (compare with Eq. (156))

$$I_\pm^{\text{lin}}(\mathbf{p},n) = \frac{\bar{n}_\mathbf{p}^{\text{eq}}n_\mathbf{p}^{\text{eq}}}{L^3}\sum_{\mathbf{p}'}\mathcal{N}_\pm(\mathbf{p},\mathbf{p}')\nu_\pm(\mathbf{p}') \tag{172}$$

[11]This can be seen by writing $\frac{g(y')}{g(y)} = \frac{\bar{n}_{\mathbf{p}'}^{\text{eq}}n_{\mathbf{p}'}^{\text{eq}}}{\bar{n}_\mathbf{p}^{\text{eq}}n_\mathbf{p}^{\text{eq}}}$ and using $\bar{n}_\mathbf{p}^{\text{eq}}n_\mathbf{p}^{\text{eq}}N_{\mathbf{p}_3\mathbf{p}_4}^{\mathbf{p}'} = \bar{n}_{\mathbf{p}'}^{\text{eq}}n_{\mathbf{p}'}^{\text{eq}}N_{\mathbf{p}_3\mathbf{p}_4}^{\mathbf{p}}$ for 4 wavectors $\mathbf{p}$, $\mathbf{p}'$, $\mathbf{p}_3$ and $\mathbf{p}_4$ constrained by energy-momentum conservation.

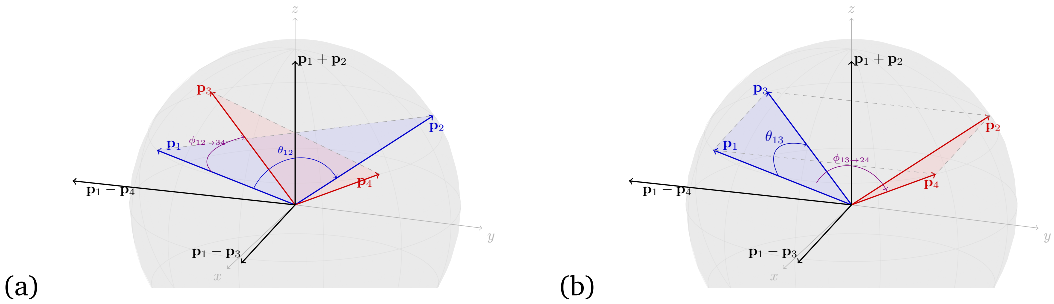

Figure 5: (a) The angular parametrization where $\mathbf{p}_1+\mathbf{p}_2$ is chosen as the polar axis of the spherical frame. This parametrization is used for W_E in Eq. (173). (b) The angular parametrization where $\mathbf{p}_1-\mathbf{p}_3$ is chosen as the polar axis of the spherical frame. This parametrization is used for W_S in Eq. (174) . The last parametrization where $\mathbf{p}_1-\mathbf{p}_4$ is chosen as the polar axis is not shown here.

2.1.5 Angular parametrization of 4 momentum-conserving wavevectors of the Fermi surface

To leading order in temperature, collisions of wavenumbers within the thermal window depend solely on the angles between these wavevectors. Four wavevectors of the Fermi surface constrained by momentum conservation $\mathbf{p}_1+\mathbf{p}_2=\mathbf{p}_3+\mathbf{p}_4$ are advantageously expressed in the orthogonal frame made of $(\mathbf{p}_1+\mathbf{p}_2,\mathbf{p}_1-\mathbf{p}_3,\mathbf{p}_1-\mathbf{p}_4)$. Depending on which vector is chosen as the z axis frame, this leaves three different ways of parametrizing the angles, depicted on Fig. 5. Since $\mathbf{p}$ and $\mathbf{p}'$ play the role of $\mathbf{p}_1$ and $\mathbf{p}_2$ in E, we use the parametrization of Fig. 5a for this kernel:

$$w_{E\pm}(\theta_{12},\phi_{12\to34})\equiv W_{E\pm}(\mathbf{p}_1,\mathbf{p}_2|\mathbf{p}_3,\mathbf{p}_4)\text{ with }\begin{cases}\theta_{12}\equiv(\widehat{\mathbf{p}_1,\mathbf{p}_2})\\ \phi_{12\to34}\equiv(\mathbf{p}_1-\widehat{\mathbf{p}_2,\mathbf{p}_3}-\mathbf{p}_4)\\ \cos\theta_3=\cos\theta_4=\cos\frac{\theta_{12}}{2},\theta_i=(\widehat{\mathbf{p}_1+\mathbf{p}_2,\mathbf{p}_i})\end{cases}\tag{173}$$

where the third line is the angular version of the momentum conservation constraint. For S in which $\mathbf{p}$ and $\mathbf{p}'$ play the role of $\mathbf{p}_1$ and $\mathbf{p}_3$ we use the parametrization of Fig. 5b:

$$w_{S\pm}(\theta_{13},\phi_{13\to24})\equiv W_{S\pm}(\mathbf{p}_1,\mathbf{p}_2|\mathbf{p}_3,\mathbf{p}_4)\text{ with }\begin{cases}\theta_{13}\equiv(\widehat{\mathbf{p}_1,\mathbf{p}_3})\\ \phi_{13\to24}\equiv(\mathbf{p}_1+\widehat{\mathbf{p}_3,\mathbf{p}_2}+\mathbf{p}_4)\\ \cos\theta_2=-\cos\theta_4=\sin\frac{\theta_{13}}{2},\theta_i=(\widehat{\mathbf{p}_1-\mathbf{p}_3,\mathbf{p}_i})\end{cases}\tag{174}$$

Since the collision amplitudes $A_{\sigma\sigma'}$ are more readily expressed, as in Eqs. (94)–(95) in terms of the angles θ_{ij} between $\mathbf{p}_i$ and $\mathbf{p}_j$, we use geometrical relations to express the angles of a given parametrization. For example for the parametrization of Fig. 5a:

$$\sin^2\frac{\theta_{13}}{2}=\sin^2\frac{\theta_{12}}{2}\sin^2\frac{\phi_{12\to34}}{2}\tag{175}$$

$$\sin^2\frac{\theta_{14}}{2}=\sin^2\frac{\theta_{12}}{2}\cos^2\frac{\phi_{12\to34}}{2}\tag{176}$$

The angular integration in different parametrizations are related by the change of variable

$$\int\frac{\sin\theta_{13}\mathrm{d}\theta_{13}\mathrm{d}\phi_{13\to24}}{2\sin\frac{\theta_{13}}{2}}\tilde{W}(\theta_{13},\phi_{13\to24})=\int\frac{\sin\theta_{12}\mathrm{d}\theta_{12}\mathrm{d}\phi_{12\to34}}{2\cos\frac{\theta_{12}}{2}}W(\theta_{12},\phi_{12\to34})\tag{177}$$

for any function $\tilde{W}(\theta_{13},\phi_{13\to24})=W(\theta_{12},\phi_{12\to34})$.

2.1.6 Low temperature factorization of the kernel

Among the fluids described by a Boltzmann equation, Fermi liquid have a remarkable property: their collision kernel $\mathcal{N}(\mathbf{p},\mathbf{p}')$ can be factorized into a radial (or energy) dependance and an angular dependence on

$$\alpha = (\widehat{\mathbf{p},\mathbf{p}'}), \quad \cos\alpha = \cos\theta\cos\theta' + \sin\theta\sin\theta'\cos\phi \tag{178}$$

This a consequence of the restriction of both the collision probabilities and energy-conservation constraint to the Fermi surface, such that the only remaining energy dependence in the kernel stems from the thermal populations $n^{\rm eq}$.

We illustrate this decoupling in the calculation of $S_\pm$:

$$S_\pm(\mathbf{p},\mathbf{p}') = \frac{(m^*)^2 T}{4\pi p_{\rm F}|\sin\frac{\alpha}{2}|}\int_{-\infty}^{+\infty} N^{y_2}_{y',y+y_2-y'}\mathrm{d}y_2 \int \frac{\mathrm{d}\Omega_2}{2\pi} W_{S\pm}(\mathbf{p},\mathbf{p}_2|\mathbf{p}',\mathbf{p}-\mathbf{p}'+\mathbf{p}_2)\delta\left(\cos\theta_2+\sin\frac{\alpha}{2}\right) + O(T^2) \tag{179}$$

with $N^{y_3}_{y_1 y_2} = n(y_1)n(y_2)\bar{n}(y_3)+\bar{n}(y_1)\bar{n}(y_2)n(y_3)$ and $n(y)=1/(1+\mathrm{e}^y)$. From the original expression (166), we have eliminated $\mathbf{p}_4$ using momentum conservation, and switched the radial integration from p_2 to y_2 using the relation, valid for a function $h(\mathbf{p}_2)$ peaked about $p_{\rm F}$:

$$\int \frac{\mathrm{d}^3\mathbf{p}_2}{(2\pi)^3} h(\mathbf{p}_2) = \frac{m^* p_{\rm F} T}{(2\pi)^2}\int_{-\infty}^{+\infty}\mathrm{d}y_2 \int\frac{\mathrm{d}\Omega_2}{2\pi} h(y_2,\theta_2,\phi_2) + O(T) \tag{180}$$

where the solid angle $\mathrm{d}\Omega_2 = \sin\theta_2\mathrm{d}\theta_2\mathrm{d}\phi_2$ locates $\mathbf{p}_2$ on the spherical frame of axis $\mathbf{p}-\mathbf{p}'$, as depicted by Fig. 5b (with $\mathbf{p}=\mathbf{p}_1$, $\mathbf{p}'=\mathbf{p}_3$). To leading order in T, the resonance condition is

$$\epsilon_{\mathbf{p}} + \epsilon_{\mathbf{p}_2} - \epsilon_{\mathbf{p}'} - \epsilon_{\mathbf{p}+\mathbf{p}_2-\mathbf{p}'} = \frac{2p_{\rm F}^2\sin(\alpha/2)}{m^*}\left(\sin\frac{\alpha}{2}+\cos\theta_2\right) + O(T) \tag{181}$$

and allows us to integrate over θ_2 in Eq. (179). Recognizing the angles of Eq. (174), we replace $W_{S\pm}(\mathbf{p},\mathbf{p}_2|\mathbf{p}',\mathbf{p}-\mathbf{p}'+\mathbf{p}_2)$ by $w_{S\pm}(\alpha,\phi_2)$, and there remains to integrate separately over the energy coordinate y_2 and the angle ϕ_2. The same calculation for E leads to an expression similar to Eq. (179) with $\mathbf{p}_3$ playing to role of $\mathbf{p}_2$.

We thus obtain the factorized kernels

$$E_\pm(y,y',\alpha) = \frac{(m^*)^2 T}{2\pi p_{\rm F}}\mathcal{S}(y,-y')\Omega_{E\pm}(\alpha) + O(T^2) \tag{182}$$

$$S_\pm(y,y',\alpha) = \frac{(m^*)^2 T}{2\pi p_{\rm F}}\mathcal{S}(y,y')\Omega_{S\pm}(\alpha) + O(T^2) \tag{183}$$

Here, $\mathcal{S}$ is an energy kernel independent of the collision probabilities and thus universal to all Fermi liquids:

$$\mathcal{S}(y,y') = \frac{y-y'}{2}\frac{1}{\sinh\frac{y-y'}{2}}\frac{\cosh\frac{y}{2}}{\cosh\frac{y'}{2}} \tag{184}$$

The angular kernel $\Omega(\alpha)$ follows from an azimuthal integration over ϕ in the appropriate spherical frame

$$\Omega_{E\pm}(\alpha) = \int_0^{2\pi}\frac{\mathrm{d}\phi}{2\pi}\frac{w_{E\pm}(\alpha,\phi)}{2|\cos\frac{\alpha}{2}|} \tag{185}$$

$$\Omega_{S\pm}(\alpha) = \int_0^{2\pi}\frac{\mathrm{d}\phi}{2\pi}\frac{w_{S\pm}(\alpha,\phi)}{2|\sin\frac{\alpha}{2}|} \tag{186}$$

Changing the summation over $\mathbf{p}'$ into integrals over y' and θ', we express the collision integral in Eq. (172) as

$$I_\pm(y,\theta) = \frac{\mathrm{i}}{\tau} g(y) \Big\{ \overline{\Gamma}(y) \nu_\pm(y,\theta) + \int \mathrm{d}y' \frac{\mathrm{d}\Omega'}{2\pi} \left(\mathcal{S}(y,-y') \frac{\Omega_{\mathrm{E}\pm}(\alpha)}{\Omega_\Gamma} - 2\mathcal{S}(y,y') \frac{\Omega_{\mathrm{S}\pm}(\alpha)}{\Omega_\Gamma} \right) \nu_\pm(y',\theta') \Big\} \tag{187}$$

We have extracted a typical collision time τ which gives the order of magnitude of the collision integral:

$$\frac{1}{\tau} = \frac{(m^*)^3 T^2}{(2\pi)^3} \left\langle \frac{W_{E+}(\theta,\phi)}{2\cos\theta/2} \right\rangle_{\theta,\phi} \tag{188}$$

where $\langle \ldots \rangle_{\theta\phi}$ is the average over solid angles, see Eq. (136). The damping rate Eq. (135) also scales with $1/\tau$:

$$\Gamma(\mathbf{p}) = \frac{1}{\tau} \overline{\Gamma}(y), \qquad \overline{\Gamma}(y) \equiv \pi^2 + y^2 \tag{189}$$

Note that this can also be deduced from the number conservation law $\Gamma(\mathbf{p}) = (1/L^3) \sum_{\mathbf{p}'} S_+(\mathbf{p},\mathbf{p}') = (1/\tau) \int_{-\infty}^{+\infty} \mathcal{S}($

2.1.7 Transport equation in the thermal window

We conclude this subsection by giving a dimensionless form of the transport equation (148) in the thermal window. Assuming a periodic driving $U_\sigma(\mathbf{q},t) = U_\sigma(\mathbf{q})\mathrm{e}^{-\mathrm{i}\omega t}$ and taking the average of (148) in $\hat{\varrho} = \hat{\varrho}_{\mathrm{eq}}(T) + \delta\hat{\varrho}(t)$, we get:

$$(\omega - v_\mathrm{F} q u) n_\sigma(\mathbf{p}) + v_\mathrm{F} q u \frac{\partial n_{\mathrm{eq}}}{\partial \epsilon}\Big|_{\epsilon=\epsilon_\mathbf{p}} \left(U_\sigma(\mathbf{q}) + \frac{1}{L^3} \sum_{\mathbf{p}'\sigma'} f_{\sigma\sigma'}(\mathbf{p},\mathbf{p}') n_{\sigma'}(\mathbf{p}') \right) = \mathrm{i} I_\sigma^{\mathrm{lin}}(\mathbf{p},n) \tag{190}$$

where the quasiparticle distribution $n(\mathbf{p},\mathbf{q},t) = n(\mathbf{p},\mathbf{q})\mathrm{e}^{\mathrm{i}\omega t}$ is defined by Eq. (150) and $I_\sigma^{\mathrm{lin}}(\mathbf{p},n) = \langle \hat{I}_{\mathbf{p}\sigma}^{\mathrm{lin}}(\hat{n}^{-\mathbf{q}}) \rangle$.

Inserting the change of variable Eq. (170) we obtain:

$$\left(\frac{\omega}{\omega_0} - \cos\theta \right) \nu_\pm(y,\theta) + \cos\theta \left(1 - \frac{1}{2} \int \mathrm{d}y' \frac{\mathrm{d}\Omega'}{2\pi} F^\pm(\alpha) g(y') \nu_\pm(y',\theta') \right) = \\ -\frac{\mathrm{i}}{\omega_0 \tau} \left\{ \overline{\Gamma}(y) \nu_\pm(y,\theta) + \int \mathrm{d}y' \frac{\mathrm{d}\Omega'}{2\pi} \left(\mathcal{S}(y,-y') \frac{\Omega_{\mathrm{E}\pm}(\alpha)}{\Omega_\Gamma} - 2\mathcal{S}(y,y') \frac{\Omega_{\mathrm{S}\pm}(\alpha)}{\Omega_\Gamma} \right) \nu_\pm(y',\theta') \right\} \tag{191}$$

where

$$\omega_0 = v_\mathrm{F} q \tag{192}$$

is the typical excitation frequency, and

$$F^\pm(\alpha) = \frac{m^* p_\mathrm{F}}{\pi^2} \frac{f_{\uparrow\uparrow}(\alpha) \pm f_{\uparrow\downarrow}(\alpha)}{2} \tag{193}$$

are the dimensionless symmetric and anti-symmetric Landau functions. The $f_{\sigma\sigma'}$ are expressed here as in Eqs. (92)–(93) in terms of the angle α between the two wavevectors $\mathbf{p}$ and $\mathbf{p}'$ of norm p_F.

2.2 Zero sound in the collisionless regime

Since the regime of hydrodynamic transport is covered by Ref. [32], we concentrate here on the collisionless regime $\omega_0\tau \to +\infty$, where the collision integral can be treated as a perturbation of the transport equation. We will perform an expansion of the quasiparticle distribution $\nu_\pm$ in powers of $1/\omega_0\tau$:

$$\nu_\pm = \nu_\pm^{\rm cl} + \frac{\delta\nu_\pm}{\omega_0\tau} + O(\omega_0\tau)^{-2}. \tag{194}$$

2.2.1 Dispersion equation in the perfect collisionless regime ($\omega_0\tau = +\infty$)

Let us first compute the leading term $\nu_\pm^{\rm cl}$ in the perfect collisionless regime limit $1/\omega_0\tau = 0$. The low-temperature transport equation (191) in this regime is

$$(c-\cos\theta)\ \nu_\pm(y,\theta) = -\cos\theta\left(1-\frac{1}{2}\int \mathrm{d}y'\frac{\mathrm{d}\Omega'}{2\pi}F^\pm(\alpha)g(y')\ \nu_\pm(y',\theta')\right) \tag{195}$$

where $c = \omega/\omega_0$. Since there is no explicit dependence on the energy variable y on the right-hand side, the collisionless distribution is energy-independent, $\nu_\pm^{\rm cl} = \nu_\pm^{\rm cl}(\theta)$. To solve the remaining 1D integral equation, we project $\nu_\pm$ and the interactions functions $F^\pm(\alpha)$ onto the basis of Legendre polynomials

$$\nu_\pm(\theta) = \sum_{l=0}^{+\infty}\nu_l^\pm P_l(\cos\theta) \tag{196}$$

$$F^\pm(\alpha) = \sum_{l=0}^{+\infty}F_l^\pm P_l(\cos\alpha) \tag{197}$$

To lighten the notations, the subscript "cl" is implicit here and until Sec. 2.2.4. The integral equation folds onto a matrix equation whose l-th component is given by

$$\nu_l^\pm(c) - \sum_{l'}A_{ll'}^\pm(c)\nu_{l'}^\pm(c) + B_{l0}(c) = 0 \tag{198}$$

where we have introduced the matrices

$$B_{ll'}(c) = \int_{-1}^{1}\frac{\mathrm{d}u}{2}P_l(u)\frac{u}{c-u}P_{l'}(u) \tag{199}$$

$$A_{ll'}^\pm(c) = F_{l'}^\pm B_{ll'}(c) \tag{200}$$

This infinite-dimension linear system is solved by formally inverting the matrix $1-A$:

$$\vec{\nu}^\pm(c) = -\frac{1}{1-A^\pm(c)}\vec{B}_0(c) \tag{201}$$

where the source vector $\vec{B}_0 = (B_{l0})_{l\in\mathbb{N}}$ is the consequence of the external drive (recall that ν is scaled to the drive intensity U). A phononic collective modes occur when some component of the quasiparticle distribution ν diverges in response to the drive, *i.e.* when the matrix $1-A^\pm(c)$ has a zero-energy eigenvector. The dispersion equation on the reduced velocity $c_0 = \omega_{\mathbf{q}}/v_{\rm F}q$ of the collective modes is then

$$\det\left(1-A^\pm(c_0)\right) = 0, \tag{202}$$

This dispersion equation can have several solutions, both real and complex. However, when F_0 is much larger than the other F_l's, as in the case of weakly-interacting Fermi gases and ^{3}He, there is a dominant real solution, traditionally called zero sound. Physically, this solution describes a longitudinal collisionless phononic branch.

2.2.2 Log-perturbative expansion of the zero-sound velocity

We are now calcutating the zero-sound reduced frequency c_0 in powers of $\overline{a}$ in a weakly-interacting Fermi gas. In equation (198) for $l > 0$, the summation over l' is dominated by the term $l' = 0$ (which contains the dominant coefficient F_0) so that:

$$\nu_l^{\pm} = -B_{l0}(c) + F_0^{\pm} B_{l0}(c)\ \nu_0^{\pm} + O(\overline{a}), \quad \text{for } l \geq 1 \tag{203}$$

Anticipating on the followings, we have estimated $B_{ll'} = O(1/\overline{a})$. Reinjecting in (198) for $l = 0$, we eventually obtain $\bar{\chi}_{\pm} \equiv \nu_0^{\pm}$, which represents either the dimensionless density $\bar{\chi}_\rho$ or polarization $\bar{\chi}_{\rm p}$ response, depending on the $\pm$ index:

$$\overline{\chi}_{\pm}(c) = -\frac{B_{00}(c) + \sum_{l'>0} F_{l'}^{\pm} B_{0,l'}(c) B_{l',0}}{1 - F_0^{\pm} B_{0,0}(c) - \sum_{l'} F_0^{\pm} F_{l'}^{\pm} B_{0,l'}(c) B_{l',0}(c)} \tag{204}$$

The dispersion relation $1/\overline{\chi}(c_0) = 0$ now reduces to:

$$1 - F_0^{\pm} B_{0,0}(c_0) - \sum_{l'} F_0^{\pm} F_{l'}^{\pm} B_{0,l'}(c_0) B_{l',0}(c_0) = 0 \tag{205}$$

Since we expect that $c_0 - 1$ tends to zero exponentially as $|\overline{a}| \to 0$, we introduce the variable $\gamma = \ln[(c_0 - 1)/2]$. Contrarily to c_0, γ can be expanded in power of $\overline{a}$:

$$\gamma^{\pm} = \frac{\gamma_0^{\pm}}{\overline{a}} + \gamma_1^{\pm} + O(\overline{a}) \tag{206}$$

The log-perturbative corrections to γ convert into a prefactor correction in $c_0 - 1$, reminiscent of the Gork'ov Melik-Barkhudarov prefactor in the calculation of the superfluid critical temperature [37]. When c_0 tends to 1 exponentially, the functions $B_{ll'}$ have the following expansion

$$B_{00}(c_0) = -1 - \frac{1}{2}\gamma^{\pm} + O(\overline{a}) \ \text{ and } \ B_{l0}(c_0) = B_{0l}(c_0) = \frac{\gamma^{\pm}}{2} + O(1) \tag{207}$$

By substituting the expansions of γ, of the Landau parameters $F_l^{\pm}$ and of the functions $B_{ll'}$ into (205), and by restricting to terms of order $O(\overline{a})$, we obtain the following expressions of $\gamma_0^{\pm}$ and $\gamma_1^{\pm}$:

$$\gamma_0^{\pm} = \mp\pi \ \text{ and } \ \gamma_1^{\pm} = -2 + \frac{\pi^2}{2\overline{a}^2}\left(\sum_{l>0} F_l^{\pm} + \delta F_0^{\pm}\right) = \pm 4 \tag{208}$$

where we have expanded $F_0^{\pm}$ as:

$$F_0^{\pm} = \pm\frac{2\overline{a}}{\pi} + \delta F_0^{\pm}, \quad \delta F_0^{\pm} = O(\bar{a}^2) \tag{209}$$

We eventually recognize in $\gamma^{\pm}$ the sum of the $F_l^{\pm}$ that is the forward value ($\alpha = 0$) of $F^{\pm}$.

$$\gamma^{\pm} = -\frac{2}{F^{\pm}(\alpha = 0)} - 2 + O(\overline{a}) \tag{210}$$

This shows that the Landau function $F(\alpha)$ in the integral equation (195) can be replaced (to leading and subleading order in $\overline{a}$) by its value in $\alpha = 0$, that is for quasiparticles with colinear momenta $\mathbf{p} \parallel \mathbf{p}'$. This is a consequence of the longitudinal nature of zero sound at weak-coupling: the quasiparticle distribution $\nu_{\pm}(\theta) \propto \cos\theta/(c_0 - \cos\theta)$ is peaked about $\theta = 0$, such that the quasiparticle momenta $\mathbf{p}$ are all nearly colinear to $\mathbf{q}$.

In short, the zero sound velocity (in units of v_F) for the density mode is given by

$$c_0^+ = 1 + 2e^4\, e^{-\pi/\overline{a}}, \qquad \overline{a} > 0 \tag{211}$$

and the velocity for the zero polarization mode is:

$$c_0^- = 1 + 2e^{-4}\, e^{\pi/\overline{a}}, \qquad \overline{a} < 0 \tag{212}$$

Second order corrections thus shift the density zero sound peak to higher velocities in the density-density response, increasing $c_0^+ - 1$ by a factor $\exp(6) \simeq 403$. We then expect the resonance to be more easily observable than predicted by first-order approximations. Since it exists only for $\overline{a} > 0$, the density zero sound is observable in a Fermi gas only on the metastable branch. Experimental exploration of this metastable branch are restricted to $|\overline{a}| \lesssim 0.1$, where zero sound is visible only at very low temperatures.

Conversely, the polarisation sound mode, which is observable on the ground branch at $\overline{a} < 0$, is shifted closer to the continuum edge, with $c_0^- - 1$ reduced by a factor $\exp(-2) \simeq 0.14$. This reduces the temperature range in which this zero sound mode is observable.

We have benchmarked these analytical results using a numerical solution of Eq. (198). More details for the numerical evaluation are given in Appendix B.

2.2.3 Response function in the collisionless regime

Our discussion of zero sound so far has focused on reduced frequencies $c \approx c_0 \approx 1$. We now discuss numerically the rest of the spectrum in the density-density response $\mathrm{Im}[\overline{\chi}_\rho] = \mathrm{Im}[\nu_+^0]$ and polarisation-polarisation response. Figs. 6 and 7 show the reduced spectral density $\mathrm{Im}[\overline{\chi}_{\rho,\mathrm{p}}(c+i0^+)]$. In the attractive case $\overline{a} < 0$ (red curves), second-order corrections tend to decrease the deviations of $\mathrm{Im}[\overline{\chi}_\rho]$ and $\mathrm{Im}[\overline{\chi}_\mathrm{p}]$ from the Lindhard response of an ideal gas (black curve). Since a stable Fermi liquid regime exists in ultracold Fermi gases only for $\overline{a} < 0$, this behavior should be the easiest to observe in cold atom experiments. Conversely, in the repulsive case $\overline{a} > 0$ (blue curves), the deviations are increased to second-order. This can be understood by comparing the first- and second-order approximation of the Landau parameters. For the leading coefficient, $F_0^\pm$, we have:

$$\frac{F_0^{+(2)}}{F_0^{+(1)}} \simeq 1 + 1.143\, \overline{a} \tag{213}$$

$$\frac{F_0^{-(2)}}{F_0^{-(1)}} \simeq 1 + 0.130\ \overline{a} \tag{214}$$

Thus, for negative (resp. positive) $\overline{a}$, the second-order $F_0^\pm$ is smaller (resp. larger) than its first-order counterpart both. As a result, the effective interaction between quasiparticles is reduced (resp. increase), tending to restore (resp. remove) the behavior of an ideal gas. Even though this is true both in the density and polarisation channel, the effect is ≈ 10 times larger in the density channel.

In the density response (Fig. 6), a zero sound resonance appears, in the repulsive case, as a Dirac peak at $c_0 > 1$; there remains also a secondary peak near the edge of the quasiparticle-quasihole continuum for $c \lesssim 1$ (see inset). This secondary peak visibly shrinks as second-order corrections push the zero sound resonance away from the continuum. In the attractive case, interactions tend to smoothen the sharp behavior at the continuum edge, and the density response becomes a broad, featureless spectral function.

Conversely, in the polarisation response (Fig. 7), the resonance appears in the attractive case, and the broad structure in the repulsive case, which indicates a repulsive/attractive,

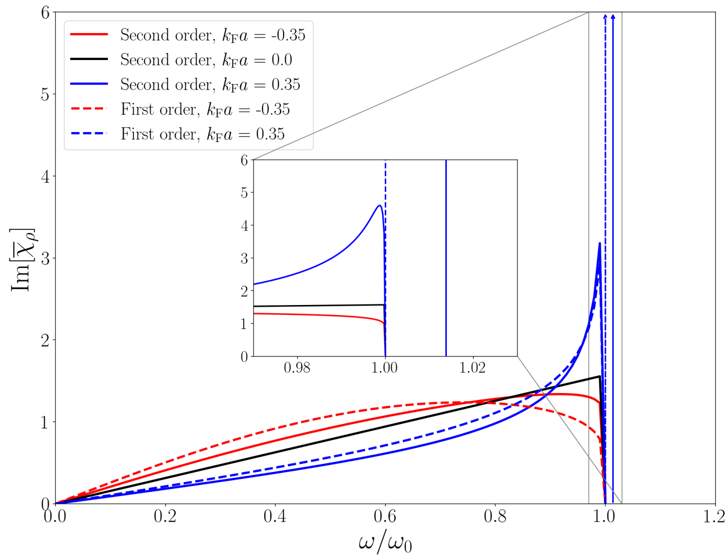

Figure 6: The reduced spectral density $\mathrm{Im}[\overline{\chi}_\rho(c+\mathrm{i}0^+)] = \mathrm{Im}[\nu_0^+(c+\mathrm{i}0^+)]$ as a function of $c = \omega/\omega_0$, for different values of $\overline{a} = k_\mathrm{F}a$, blue curves for $\overline{a} > 0$ and red curves for $\overline{a} < 0$. The dashed lines correspond to the first order calculation [48]. The black line is the non-interacting case. The solid curves include second-order effects; they are obtained by numerically solving (198) truncated to $l_\mathrm{max} = 100$.

density/polarisation duality. This time, the resonance is brought closer to the continuum edge by second-order corrections, and the secondary peak near the continuum edge grows. In presence of a small spectral broadening (either due to collisional damping, Landau damping or experimental resolution) the two peaks would become indistinguishable.

2.2.4 Collisional damping of zero sound

We now aim to include the collisional correction $\delta\nu_\pm$ (see Eq. (194)) in the distribution $\nu_\pm$. In the regime where c is exponentially close to 1 ($\gamma = \ln([c-1]/2) \to -\infty$), the leading-order solution $\nu_\pm^\mathrm{cl}$ can be written more simply by discarding the Legendre decomposition and returning to the angular variable θ:

$$\nu_\pm^\mathrm{cl}(\theta) = \frac{\cos\theta}{c-\cos\theta} \cdot \frac{\rho_\pm^\mathrm{cl}}{2B_{00}(c)} \tag{215}$$

This solution was obtained by replacing $F^\pm(\alpha)$ with $F^\pm(0)$ in Eq. (195), as shown in Section 2.2.2. To simplify the notation, we denote by $\delta\rho^{\mathrm{cl}}\pm$ the $l=0$ component of $\nu\pm^{\mathrm{cl}}$, that is:

$$\rho_\pm^\mathrm{cl} = \nu_\pm^{0,\mathrm{cl}} = \int_0^\pi \sin\theta \mathrm{d}\theta \;\; \nu_\pm^\mathrm{cl}(\theta) \tag{216}$$

We define $\rho_\pm$ in the same way. We then substitute the expansion of $\nu_\pm$ given in Eq. (194) into (191), keeping terms up to order $1/\omega_0\tau$. Thus, in the collision integral, $\nu_\pm$ is replaced by its leading-order expression $\nu_\pm^\mathrm{cl}$. Since $\nu_\pm^\mathrm{cl}$ does not depend on energy, we perform an averaging to eliminate the dependence of the collision integral on y and y':

$$\int_{-\infty}^{+\infty} \mathrm{d}y' \; \mathcal{S}(y, \pm y') = \overline{\Gamma}(y), \qquad \int_{-\infty}^{+\infty} \mathrm{d}y \; g(y)\overline{\Gamma}(y) = \frac{4\pi^2}{3} \tag{217}$$

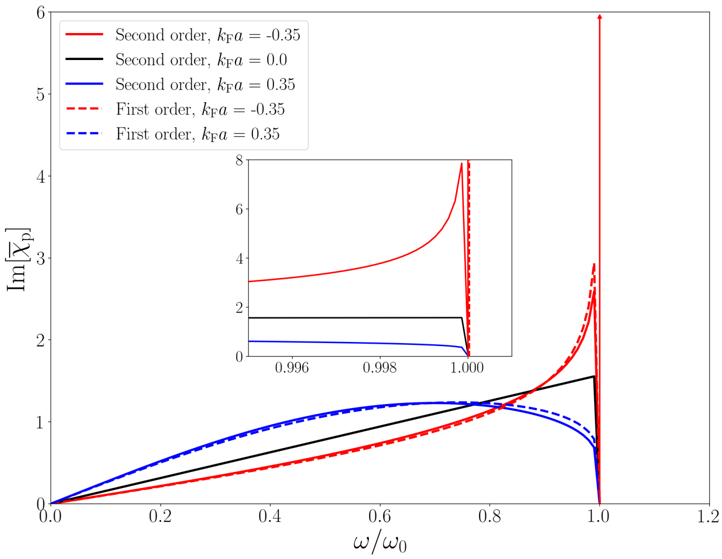

Figure 7: The reduced spectral density for the polarisation $\mathrm{Im}[\overline{\chi}_{\mathrm{p}}(c+\mathrm{i}0^+)] = \mathrm{Im}[\nu_0^-(c+\mathrm{i}0^+)]$ for the same parameters as Fig. 6.

We then obtain the following equation for $\nu_\pm$:

$$\nu_\pm(\theta) = -\frac{\cos\theta}{c-\cos\theta}\left(1-\frac{F^\pm(0)}{2}\rho_\pm\right) - \frac{4\pi^2}{3}\frac{\mathrm{i}}{\omega_0\tau}\frac{1}{c-\cos\theta}\left(\nu_\pm^{\mathrm{cl}}(\theta) + \int\frac{\mathrm{d}\Omega'}{2\pi}\,\mathcal{N}_\pm(\alpha)\,\nu_\pm^{\mathrm{cl}}(\theta')\right) \tag{218}$$

where the angular collision kernel $\mathcal{N}_\pm(\alpha)$ and its expansion in Legendre polynomials are given in Appendix C.

We then integrate over θ so as to obtain $\rho_\pm$ on the left-hand side. In the collision integral, $\rho_\pm^{\mathrm{cl}}$ can be replaced by the total density $\rho_\pm$, neglecting terms of order $1/(\omega_0\tau)^2$. We thus obtain the following solution:

$$\rho_\pm(c) = \frac{-2B_{00}(c)}{1-F^\pm(0)B_{00}(c) + \frac{\mathrm{i}}{\omega_0\tau}\frac{2\pi^2}{3}\frac{C_\pm(c)}{B_{00}(c)}} \tag{219}$$

where the collisional contribution $C_\pm$ is given by:

$$C_\pm(c) = \int_0^\pi \mathrm{d}\theta\,\frac{\sin\theta\cos\theta}{(c-\cos\theta)^2} + \int\frac{\mathrm{d}\Omega'}{2\pi}\mathrm{d}\theta\,\frac{\sin\theta\cos\theta'}{(c-\cos\theta)(c-\cos\theta')}\mathcal{N}_\pm(\alpha) \tag{220}$$

Since these integrals are dominated by the vicinity of $\theta=0$ and $\theta'=0$, the collision kernel $\mathcal{N}_\pm(\alpha)$ can be replaced by its value at $\alpha=0$. This can again be interpreted as a consequence of the quasi-longitudinal nature of zero sound in the weak-interaction regime. We thus arrive at

$$C_\pm(c) \simeq -B'_{00}(c)\big(1+2(c-1)\gamma^2(c)\,\mathcal{N}_\pm(0)\big) \tag{221}$$

with $\gamma(c) = \ln\frac{c-1}{2}$. A more general calculation of the function $C_\pm$ is given in Appendix C.

To obtain the collisional correction to the zero-sound velocity, we now solve the equation

$$\frac{1}{\rho_\pm(z_0^\pm)} = 0, \quad \text{with } z_0^\pm = c_0^\pm + \delta c_0^\pm. \tag{222}$$

Expanding the denominator of $\rho_\pm$ in powers of $O(1/\omega_0\tau)$, we finally extract the collisional correction to zero sound, which is purely imaginary:

$$\delta c_0^\pm = \frac{2\pi^2}{3}\frac{\mathrm{i}}{\omega_0\tau}\frac{C_\pm(c_0^\pm)}{B'_{00}(c_0^\pm)} = -\frac{2\pi^2}{3}\frac{\mathrm{i}}{\omega_0\tau} + O(c_0 - 1). \tag{223}$$

This result describes the broadening of the zero-sound resonance in the response functions $\chi_\rho(c)$ and $\chi_p(c)$, or equivalently, its exponential damping in the time domain. It is worth noting that $\mathrm{Im}(c_0)$ depends on the collision probability W only through the mean collision time τ, which makes the product $\omega_0\tau, \mathrm{Im}(c_0)$ universal in weakly interacting Fermi liquids.

In this sense, the damping of zero sound differs from that of hydrodynamic sound (first sound), which is sensitive—via the shear viscosity η—to the angular dependence of W, and therefore varies with $k_\mathrm{F}a$ in a way that differs significantly from τ.

2.3 Numerical solution in the collisionless to hydrodynamic crossover

Between the weakly collisional regime studied in Section 2.2 and the hydrodynamic regime treated in Ref. [32], there exists a smooth transition as a function of $\omega_0\tau$ [31, 49]. In the following, we develop a numerical method that allows us to solve the transport equation (191) in this intermediate regime.

2.3.1 Numerical method

In order to solve the transport equation (191), we project $\nu_\pm$ onto basis of orthogonal polynomials:

$$\nu_\pm(y,\theta) = \sum_{n,l\in\mathbb{N}} \nu^l_{n\pm} P_l(\cos\theta) Q_n(y) \tag{224}$$

where the P_l are the Legendre polynomials. The orthogonal polynomials Q_n for the energy dependence [50] are defined by $Q_0 = 1$, $Q_1 = y$ and

$$\int_{-\infty}^{\infty} \frac{\mathrm{d}y}{4\cosh^2\frac{y}{2}} Q_n(y) Q_m(y) = \delta_{n,m}||Q_n||^2 \tag{225}$$

$$yQ_n = Q_{n+1} + \xi_n Q_{n-1} \quad \text{with} \quad \xi_n = \frac{||Q_n||^2}{||Q_{n-1}||^2} \tag{226}$$

The decomposition over the Q_n allows for an exact treatment of the energy dependance, beyond the relaxation time approximations, which limit the quasiparticle distribution to its $n = 0$ component. The decomposed transport equation reads

$$\left(\frac{\omega}{\omega_0} + \frac{\mathrm{i}}{\omega_0\tau}\mathcal{M}^l_\pm\right)\vec{\nu}^l_\pm - \frac{l}{2l-1}\overline{F}^\pm_{l-1}\vec{\nu}^{l-1}_\pm - \frac{l+1}{2l+3}\overline{F}^\pm_{l+1}\vec{\nu}^{l+1}_\pm = -\delta_{l,1}\vec{u}_0 \tag{227}$$

where we have introduced a set of vectors and matrices

$$\vec{\nu}^l_\pm = \begin{pmatrix} \nu^l_{0\pm} \\ \nu^l_{1\pm} \\ \vdots \end{pmatrix}, \qquad \vec{u}_0 = \begin{pmatrix} 1 \\ 0 \\ \vdots \end{pmatrix}, \qquad \mathcal{U}_0 = \begin{pmatrix} 1 & 0 & 0 & \cdots \\ 0 & 0 & 0 & \cdots \\ \vdots & & & \end{pmatrix} \tag{228}$$

$$\overline{F}^\pm_l = \left(1 + \frac{F^\pm_l}{2l+1}\mathcal{U}_0\right) = \begin{pmatrix} 1 + \frac{F^\pm_l}{2l+1} & 0 & 0 & \cdots \\ 0 & 1 & 0 & \cdots \\ \vdots & & \ddots & \\ 0 & \cdots & \cdots & 1 \end{pmatrix} \tag{229}$$

The collision time τ has been defined (188). The infinite matrix $\left(\mathcal{M}^l_\pm\right)_{nn'}$ follows from the decomposition of the collision kernel $\mathcal{N}(\mathbf{p},\mathbf{p}')$ (see Eq. (164)) over the orthogonal basis; its expression in terms of W is given in Ref. [32].

We now present a numerical scheme to solve the transport equation (227) based on a backward recurrence on l. Assuming that at rank $l+1$, the component $\vec{\nu}^{l+1}$ has been linearly expressed in terms of $\vec{\nu}^l$, we can propagate the linear relation backward in l:

$$\vec{\nu}^l = \mathcal{H}^l \vec{\nu}^{l-1} \tag{230}$$

where we omited the $\pm$ index for convenience. Numerically, we introduce a truncation parameter $n_{\max}$ and represent the infinite matrix $\mathcal{H}^l$ by a complex $n_{\max}\times n_{\max}$ matrix. Substituting this relation into equation (227) for $l>1$, we derive the following backward recurrence relation on $\mathcal{H}^l$.

$$\mathcal{H}^l = \frac{l}{2l-1}\left(\left(\frac{\omega}{\omega_0}+\frac{\mathrm{i}}{\omega_0\tau}\mathcal{M}^l\right)-\frac{l+1}{2l+3}\overline{F}_{l+1}\mathcal{H}^{l+1}\right)^{-1}\overline{F}_{l-1} \tag{231}$$

To initialize the recurrence, we introduce a cutoff $l_{\max}$ and we assume $\mathcal{H}^{l_{\max}+1}=0$. At the end of the backward recurrence, we solve the remaining $2n_{\max}\times 2n_{\max}$ coupled system on $\vec{\nu}^0$ and $\vec{\nu}^1$

$$\begin{cases}\left(\frac{\omega}{\omega_0}+\frac{\mathrm{i}}{\omega_0\tau}\mathcal{M}^0_+\right)\vec{\nu}^0_+ = \frac{1}{3}\overline{F}^+_1\vec{\nu}^1_+\\ \left(\frac{\omega}{\omega_0}+\frac{\mathrm{i}}{\omega_0\tau}\mathcal{M}^1_+\right)\vec{\nu}^1_+ - \overline{F}^+_0\vec{\nu}^0_+ - \frac{2}{5}\overline{F}^+_2\mathcal{H}^2_+\vec{\nu}^1_+ = -\vec{u}_0\end{cases} \tag{232}$$

Here, $\mathcal{H}^2_+$ is computed recursively, starting from $l=l_{\max}$. We choose the values of $l_{\max}$ and $n_{\max}$ based on a convergence analysis. Selecting cutoffs that are too low may lead to non-physical oscillations in the response functions. We note that $l_{\max}$ and $n_{\max}$ depend on the regime of $\omega_0\tau$ under study. In the collisionless regime, we can restrict ourselves to small values of $n_{\max}$. This confirms the observation made in the previous section: the energy dependence of $\rho_\pm$ is contained in the collision term, which is subdominant. Conversely, in the hydrodynamic regime, small values of $l_{\max}$ suffice. The conserved quantities are at $l=0$ or 1 and the non-conserved quantities at $l\geq 2$ decay as $(\omega_0\tau)^l$ [50].

2.3.2 Anisotropic driving potential for the polarisation

The polarisation response to the isotropic drive introduced in Eq. (137) vanishes as $\omega_0\tau$ in the hydrodynamic regime. This is because such a drive couples to a dissipative component (ν^1_{0-}). To make the diffusive mode of polarisation observable, one should rather couple the drive directly to the conserved quantity $n_\uparrow - n_\downarrow$, in the $l=0$ channel. To do so, we assume that the driving potential can be varied independently with $\mathbf{q}$ and $\mathbf{p}$:

$$\hat{H}_{\text{ext}} = \sum_{\mathbf{p}\in\mathcal{D}} U_-(\mathbf{p},\mathbf{q})\left(\hat{\gamma}^\dagger_{\mathbf{p}+\mathbf{q}/2,\uparrow}\hat{\gamma}_{\mathbf{p}-\mathbf{q}/2,\uparrow}-\hat{\gamma}^\dagger_{\mathbf{p}+\mathbf{q}/2,\downarrow}\hat{\gamma}_{\mathbf{p}-\mathbf{q}/2,\downarrow}\right) \tag{233}$$

The dependence of the driving potential on p is irrelevant, so that we can write:

$$U_-(\mathbf{p},\mathbf{q}) = U_-(\mathbf{q})u(\theta) \tag{234}$$

This change of $\hat{H}_{\text{ext}}$ modifies the source term in the polarisation transport equation:

$$\left(\frac{\omega}{\omega_0}-\cos\theta\right)\nu_-(y,\theta)+\cos\theta\left[u(\theta)-\frac{1}{2}\int \mathrm{d}y'\frac{\mathrm{d}\Omega'}{2\pi}F^-(\alpha)g(y')\nu_-(y',\theta')\right] = -\mathrm{i}I(y,\theta) \tag{235}$$

To couple the drive directly to the polarisation fluctuations, the product $u(\theta)\cos\theta$ should have a non-vanishing $l=0$ component, which can be achieved with $u(\theta)=\cos\theta$ for example.

For simplicity, we omit here the components $l \geq 1$ whose contribution is negligible in the hydrodynamic limit, *i.e.* we assume $u(\theta)\cos\theta = 1$. The set of equations to be solved at the end of the backward recurrence is then:

$$\begin{cases} \left(\frac{\omega}{\omega_0}+\frac{\mathrm{i}}{\omega_0\tau}\mathcal{M}^0_-\right)\vec{v}^0_- = \frac{1}{3}\overline{F_1}\,\vec{v}^1_- - \vec{u}_0 \\ \left(\frac{\omega}{\omega_0}+\frac{\mathrm{i}}{\omega_0\tau}\mathcal{M}^1_-\right)\vec{v}^1_- - \overline{F_0}\,\vec{v}^0_- - \frac{2}{5}\overline{F_2}\,\mathcal{H}^2_-\vec{v}^1_- = 0 \end{cases} \tag{236}$$

2.3.3 Response functions in the collisionless-to-hydrodynamic crossover

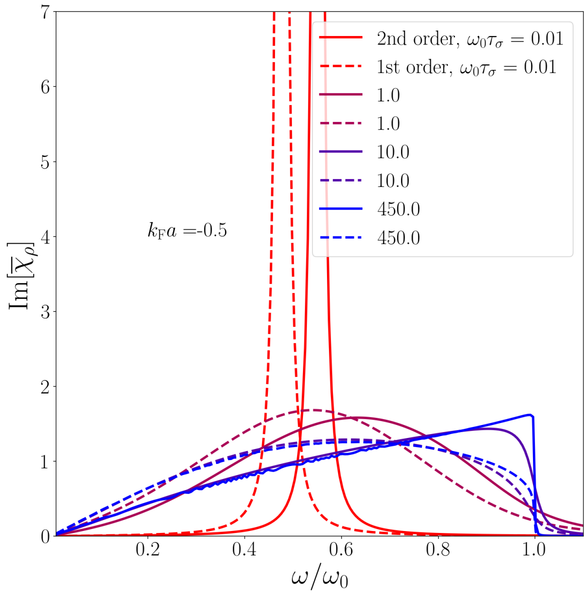

Figure 8: The crossover between the hydrodynamic (red curves) and collisionless (blue curves) regimes in the reduced spectral density, $\mathrm{Im}[\bar{\chi}_\rho] = \mathrm{Im}[\nu^0_{0+}]$, at interaction strength $k_{\mathrm{F}}a = -0.5$. The collision parameter $\omega_0\tau_\sigma$ is given in [32]. Dashed lines indicate the first-order analytical solution, while solid lines correspond to the second-order correction. Here and in Figs. 9 and 10, the summation over n is truncated from $n_{\max} = 50$ in the hydrodynamic regime to $n_{\max} = 5$ in the collisionless regime. Similarly, the truncation in l is set to $l_{\max} = 5$ in the hydrodynamic regime and to $l_{\max} = \omega_0\tau_0$ outside of it.

We illustrate the collisionless-to-hydrodynamic crossover for the density (Figs. 8 and 9 for the attractive and repulsive case respectively) and for the polarization response functions (Figs. 10, for the attractive case). We compare the first-order prediction (dashed curves) to the second-order prediction derived in this work (solid curves).

In the density response function, we observe a shift of the first sound peak toward higher velocities when comparing the first-order and second-order calculations. Recall that the first sound velocity (in units of v_{F}) is given by

$$c_1 = \sqrt{\frac{(1+F_0^+)(1+F_1^+/3)}{3}}. \tag{237}$$

Since the second-order terms in F_0^+ and F_1^+ are positive (irrespectively of the sign of $k_{\mathrm{F}}a$), they increase the value of c_1 compared to the first-order result.

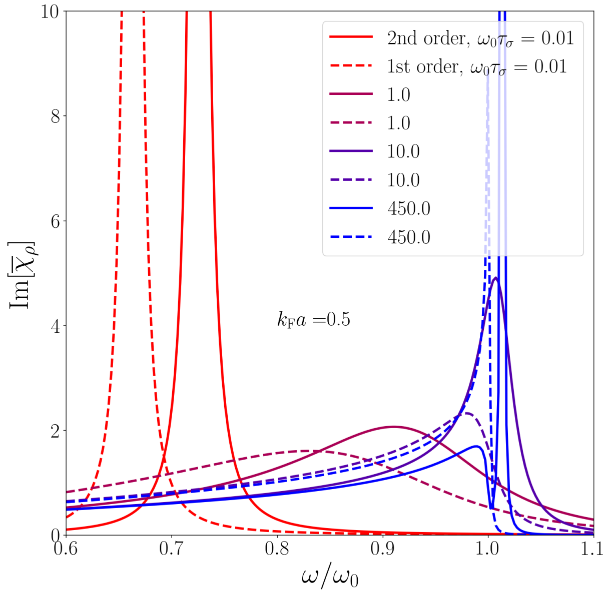

Figure 9: The crossover between the hydrodynamic (red curves) and collisionless (blue curves) regimes in the reduced spectral density, $\mathrm{Im}[\bar{\chi}_\rho] = \mathrm{Im}[\nu^0_{0+}]$, at interaction strength $k_{\rm F}a = 0.5$. Dashed lines indicate the first-order analytical solution, while solid lines correspond to the second-order correction. The summation over n is truncated from $n_{\rm max} = 50$ in the hydrodynamic regime to $n_{\rm max} = 5$ in the collisionless regime. Similarly, the truncation in l is set to $l_{\rm max} = 5$ in the hydrodynamic regime and to $l_{\rm max} = \omega_0\tau_\sigma$ outside of it.

In the collisionless regime, a zero-sound mode is present in the repulsive case (Fig. 9), possibly with a secondary peak near the edge the continuum. The resolution of those two peaks allows us to further divide the collisionless regime into two sub-regimes according to the value of $\omega_0\tau$. For $1/(c_0-1) \gg \omega_0\tau \gg 1$ ($\omega_0\tau \approx 100$ in Fig. 9) the zero-sound mode is not separated from the quasiparticle-hole continuum, which gives rise to a single peak with an important left skewness. A deeper collisionless regime, or true zero sound regime, is reached for $\omega_0\tau \gg 1/(c_0-1)$ ($\omega_0\tau \approx 4500$ in Fig. 9). In this regime, zero sound separates from the continuum, which however retains a significant spectral weight. This deep regime is more easily reached when second order terms are included (compare the blue solid and blue dashed curves in Fig. 9); this is because $c_0 - 1$ is much larger in the second- than in the first-order approximation. In between the hydrodynamic and collisionless regimes, the density response function retains a shallow maximum whose location smoothly evolves from c_1 to c_0. This peak is however too broad to be identified as a collective mode: its width Δc is comparable to 1 in units of $v_{\rm F}$.

We now turn to the polarisation response (Fig 10). In the collisionless regime (blue curves), we observe a skewed peaked at the continuum edge, but no zero sound resonance yet for $\omega_0\tau = 4500$ (blue curve). Again, this can be understood by comparing $\omega_0\tau$ to $1/(c_0-1)$: the log-perturbative corrections from the second-order approximation reduce the deep collisionless regime to $\omega_0\tau \gtrsim 10^5$ for $k_{\rm F}a = -0.5$. In the hydrodynamic regime (red curves), there appears a diffusive mode centered in $\omega = 0$, as predicted by the Navier-Stokes equations of the Fermi liquid [32]. Note that the large spectral weight of this peak is a consequence of our choice of an anisotropic drive Eq. (233). In between the collisionless and hydrodynamic

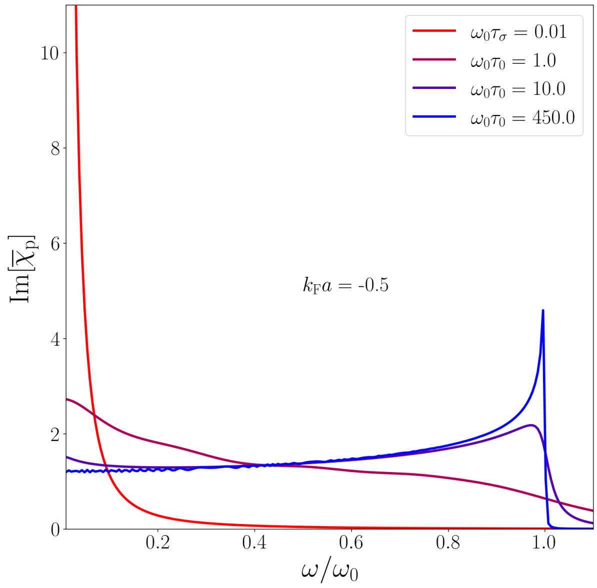

Figure 10: The crossover between the hydrodynamic (red curves) and collisionless (blue curves) regimes in the reduced spectral density for the polarisation, $\mathrm{Im}[\bar{\chi}_{\mathrm{p}}] = \mathrm{Im}[\nu^0_{0-}]$, at interaction strength $k_{\mathrm{F}}a = -0.5$.

limits, the polarisation response displays a very flat profile between two local minima in $c = 0$ and $c \approx 1$.

3 Superfluid pairing of Landau quasiparticles

In this section, we use the Landau quasiparticles, and their effective Hamiltonian Eq. (49), to describe (in principle exactly) the superfluid phase from the superfluid instability down to $T = 0$. Our description is valid provided superfluidity remains a weak phenomenon in the sense that

$$\Delta,\ T_c \ll \epsilon_{\mathrm{F}} \tag{238}$$

where Δ is the superfluid order parameter and T_c is the critical temperature. Weak fermionic superfluids should then be viewed as condensates of quasiparticle pairs [34], schematically depicted by Fig. 11; this is a substantial improvement from the pairs of bare particles interacting via the bare interaction (as described by BCS theory), or even from the frequent picture of bare particles interacting via a screened interaction. The head-on collisions $\mathbf{p}, -\mathbf{p} \to \mathbf{p}', -\mathbf{p}'$ among quasiparticles, described by the amplitude $\mathcal{A}$, favor the pairing instability and the appearance of a nonzero pairing field. We shall see that the pairing collision amplitude $\mathcal{A}(\mathbf{p}, -\mathbf{p}|\mathbf{p}', -\mathbf{p}')$ must exhibit a logarithmic divergence as $\Lambda/\epsilon_{\mathrm{F}} \to 0$ to ensure the existence of a superfluid phase.

In our approach, the compatibility of the quasiparticle picture with the existence of a superfluid ground state is tied to the cutoff Λ. Exciting a few pairs at the Fermi level (from *e.g.* the Fermi sea or the superfluid ground state) will change the energy of the interacting system by $\approx \Delta$. The corresponding transition in the noninteracting fluid is conversely quasi-resonant. Thus the weak crossing condition on the spectrum of the Fermi liquid (Eq. (4)) is compatible

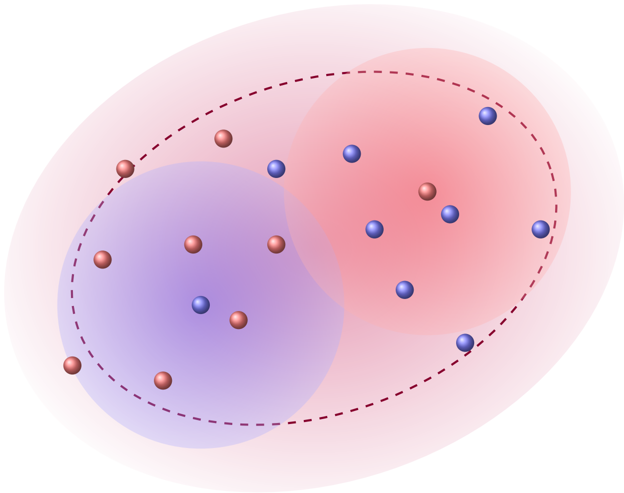

Figure 11: Cooper pairs (dashed ellipse) in a Fermi superfluid are pairs of ↑ and ↓ Landau quasiparticles (red and blue clouds). To first order, the spin-↑ quasiparticle can be seen as a cloud of spin-↓ particles (blue dots) surrounding the original spin-↑ particle (red dot).

with the existence of a pair binding energy as long as

$$\Delta,\ T_c \ll \Lambda \tag{239}$$

3.1 Pairing equation

We formulate an evolution equation that captures the onset of quasiparticle pairing in the normal phase [17], as the system approaches the critical temperature $T \to T_c^+$. This equation is to the quasiparticle pairing field $\hat{\gamma}_\sigma \hat{\gamma}_{\sigma'}$ what the transport equation is to the density field $\hat{\gamma}_\sigma^\dagger \hat{\gamma}_\sigma$. Although pairing is in principle not restricted to the singlet spin wavefunction (as in *e.g.* the A-phase of ^{3}He), we have in mind here the case of ultracold fermions, where the interactions among opposite spin quasiparticles $\mathcal{A}_{\uparrow\downarrow}$ dominateand favor the formation of ↑↓ pairs. We thus restrict to spin-singlet pairs; the corresponding quantum pairing field in momentum space is

$$\hat{d}_{\mathbf{p}}^{\mathbf{q}} = \hat{\gamma}_{-\mathbf{p}-\mathbf{q}/2,\downarrow}\hat{\gamma}_{\mathbf{p}-\mathbf{q}/2,\uparrow} \tag{240}$$

This operator effectively annihilates a pair of $\mathbf{p}\uparrow, -\mathbf{p}\downarrow$ quasiparticles with a center-of-mass momentum $\mathbf{q}$. By definition, its expectation value vanishes in an equilibrium state of the normal phase $\langle \hat{d}_{\mathbf{p}}^{\mathbf{q}} \rangle_{\text{eq}} = 0$ for $T > T_c$. However, fluctuations of $\hat{d}$ are possible for example under the influence of an external potential. The pair susceptibility, or pair response function, then quantifies the magnitude of these fluctuations with respect to the drive intensity. We are looking for a divergence of the pair susceptibility, that would signal that the normal phase becomes unstable, and the system undergoes a phase transition.

To compute the pair susceptibility, we introduce an external perturbation $\hat{H}_{\text{ext}}$ that couples directly to the pair field:

$$\hat{H}_{\text{ext}} = \phi(-\mathbf{q}, t)\sum_{\mathbf{p}} \left(\hat{d}_{\mathbf{p}}^{-\mathbf{q}}\right)^\dagger + \text{h.c.} \tag{241}$$

where the external pairing source oscillates at frequency ω, $\phi(\mathbf{q}, t) = \phi(\mathbf{q})\mathrm{e}^{-\mathrm{i}\omega t}$, causing $\hat{d}_{\mathbf{p}}^{\mathbf{q}}$ to oscillate at frequency $\omega - 2\mu$. We expand the state of the system about a thermal quasiparticle state $\hat{\varrho} = \hat{\varrho}_{\rm eq}(T) + \delta\hat{\varrho}$ (see Eq. (129) for the definition of $\hat{\varrho}_{\rm eq}(T)$). Within linear response, the deviation from equilibrium is controlled by the drive intensity $\delta\hat{\varrho} = O(\phi/\epsilon_{\rm F})$. We then evolve $\hat{d}_{\mathbf{p}}^{\mathbf{q}}$ according to the Heisenberg equation of motion

$$i\partial_t \hat{d}_{\mathbf{p}}^{\mathbf{q}} = [\hat{d}_{\mathbf{p}}^{\mathbf{q}}, \hat{H} + \hat{H}_{\rm ext}] \tag{242}$$

The derivation proceeds analogously to the derivation of the transport equation in Sec. 1.3. The streaming term arises from the diagonal part of the Hamiltonian:

$$[\hat{d}_{\mathbf{p}}^{\mathbf{q}}, \hat{H}_2 + \hat{H}_4^{\rm d} + \hat{H}_{\rm ext}] = \left(\hat{\epsilon}_{\mathbf{p}-\mathbf{q}/2,\uparrow} + \hat{\epsilon}_{-\mathbf{p}-\mathbf{q}/2,\downarrow}\right)\hat{d}_{\mathbf{p}}^{\mathbf{q}} + (1 - n_{\mathbf{p}+\mathbf{q}/2}^{\rm eq} - n_{\mathbf{p}-\mathbf{q}/2}^{\rm eq})\phi(\mathbf{q}) + O(\phi)^2 \tag{243}$$

with $\hat{\epsilon}_{\mathbf{p},\sigma} = \epsilon_{\mathbf{p}}$ to leading order in $T/T_{\rm F}$. In the quartic terms stemming from $\hat{H}_4^{\rm x}$, we inject the cumulant expansion Eq. (119) :

$$[\hat{d}_{\mathbf{p}}^{\mathbf{q}}, \hat{H}_4^{\rm x}] = (1 - n_{\mathbf{p}+\mathbf{q}/2}^{\rm eq} - n_{\mathbf{p}-\mathbf{q}/2}^{\rm eq})\frac{1}{L^3}\sum_{\mathbf{p}'}\mathcal{A}_{\uparrow\downarrow}\left(\mathbf{p}-\frac{\mathbf{q}}{2}, -\mathbf{p}-\frac{\mathbf{q}}{2}\middle| -\mathbf{p}'-\frac{\mathbf{q}}{2}, \mathbf{p}'-\frac{\mathbf{q}}{2}\right)\hat{d}_{\mathbf{p}'}^{\mathbf{q}} + \hat{J}_{\mathbf{p}} \tag{244}$$

We have regrouped the quartic cumulants $(\hat{a}\hat{b}\hat{c}\hat{d})_c$ in a collision integral $\hat{J}_{\mathbf{p}}$ which is negligible for the calculation of T_c. Note that the interaction between same-spin quasiparticles $\mathcal{A}_{\sigma\sigma}$ contributes to $\hat{J}_{\mathbf{p}}$ but not to the partially contracted terms in Eq. (244). This is specific to the normal phase where the anomalous averages $\langle\hat{\gamma}_\downarrow\hat{\gamma}_\uparrow\rangle_{\rm eq}$ vanish. The pair transport equation of a Fermi liquid is then:

$$\begin{aligned}(\omega - \epsilon_{\mathbf{p}-\mathbf{q}/2} - \epsilon_{\mathbf{p}+\mathbf{q}/2} + 2\mu)\hat{d}_{\mathbf{p}}^{\mathbf{q}} &= (\overline{n}_{\mathbf{p}+\mathbf{q}/2}^{\rm eq} - n_{\mathbf{p}-\mathbf{q}/2}^{\rm eq}) \\ &\times\left\{\frac{1}{L^3}\sum_{\mathbf{p}'}\mathcal{A}_{\uparrow\downarrow}\left(\mathbf{p}-\frac{\mathbf{q}}{2}, -\mathbf{p}-\frac{\mathbf{q}}{2}\middle| -\mathbf{p}'-\frac{\mathbf{q}}{2}, \mathbf{p}'-\frac{\mathbf{q}}{2}\right)\hat{d}_{\mathbf{p}'}^{\mathbf{q}} + \phi(\mathbf{q})\right\}\end{aligned} \tag{245}$$

3.2 Uniform pair susceptibility

The Thouless criterion defines T_c as the temperature at which the pair susceptibility acquires a singularity for static and uniform perturbations, that is for $\omega = 0$ and $q = 0$. Restricting our pairing equation Eq. (245) first to $q = 0$, we obtain:

$$\left(\omega - 2(\epsilon_{\mathbf{p}} - \mu)\right)d(\mathbf{p}) = (1 - 2n_{\mathbf{p}}^{\rm eq})\left\{\frac{1}{L^3}\sum_{\mathbf{p}'}\mathcal{A}_{\uparrow\downarrow}(\mathbf{p}, -\mathbf{p}|\mathbf{p}', -\mathbf{p}')\, d(\mathbf{p}') + \phi\right\} \tag{246}$$

When superfluidity occurs in a high partial wave, d has a non trivial dependence on the angle between $\mathbf{p}$ and a reference direction; we focus here on s-wave pairing, for which the pairing function is isotropic $d(\mathbf{p}) = d(p)$. The angular part of the integral equations is then a mere angular average of the pairing amplitude

$$\overline{\mathcal{A}_{\uparrow\downarrow}}(p, p', \Lambda) \equiv \frac{1}{2}\int_0^\pi {\rm d}\alpha\, \sin\alpha\, \mathcal{A}_{\uparrow\downarrow}(\mathbf{p}, -\mathbf{p}|\mathbf{p}', -\mathbf{p}') \tag{247}$$

where $\alpha = \widehat{(\mathbf{p}, \mathbf{p}')}$. For the radial dependence, we introduce the following change of variable:

$$d(p) = \frac{1 - 2n_{\mathbf{p}}^{\rm eq}}{\beta\left(\omega - 2(\epsilon_{\mathbf{p}} - \mu)\right)}D(y) = \frac{\tanh(y/2)}{\beta\omega - 2y}\, D(y), \qquad y = \beta\left(\epsilon_{\mathbf{p}} - \mu\right) \tag{248}$$

with $\beta = 1/T$. This reparametrization may seem analogous to the change of variable $\delta n \to \nu$ (see Eq. (170)) performed on the density field to focus on the low-energy region. It extracts a prefactor that depends rapidly on energy from the unknown function d, and we may expect D to be a smooth function of y. However, the prefactor $\tanh(y/2)/(\beta\omega - 2y)$ here does not vanish at large y. In consequence, what restricts us to low energies is rather the finite energy width of the amplitude $\mathcal{A}$. As in Eq. (77), we must then separate the unconstrained amplitude $\mathcal{A}'$ from the low-energy projector Π_Λ:

$$\mathcal{A}_{\uparrow\downarrow}(\mathbf{p},-\mathbf{p}|\mathbf{p}',-\mathbf{p}') = \mathcal{A}'_{\uparrow\downarrow}(\mathbf{p},-\mathbf{p}|\mathbf{p}',-\mathbf{p}')\,\Pi_\Lambda(2(\epsilon_{\mathbf{p}'}-\epsilon_{\mathbf{p}})) \tag{249}$$

In presence of Π_Λ, we can now restrict the energy integrals to the low-energy region:

$$\frac{1}{L^3}\sum_{\mathbf{p}'}\Pi_\Lambda(2(\epsilon_{\mathbf{p}'}-\epsilon_{\mathbf{p}})) \to \frac{m^* T p_{\mathrm{F}}}{(2\pi)^3}\int_{-\infty}^{\infty}\Pi_\Lambda\left(2T(y-y')\right)\mathrm{d}y'\int_0^\pi\int_0^{2\pi}\sin\alpha\,\mathrm{d}\alpha\,\mathrm{d}\phi \tag{250}$$

where ϕ is an azimuthal angle locating $\mathbf{p}'$ in a spherical frame of axis $\mathbf{p}$. Up to corrections in $O(T/T_{\mathrm{F}})$, we can approximate the pairing amplitude $\mathcal{A}_{\uparrow\downarrow}$ by its value for $p = p' = p_{\mathrm{F}}$. The integral equation focused on the low-energy region becomes

$$D(y) = \frac{m^* p_{\mathrm{F}}}{2\pi^2}\overline{\mathcal{A}_{\uparrow\downarrow}}(\Lambda)\int_{-\frac{\beta\Lambda}{2}+y}^{\frac{\beta\Lambda}{2}+y}\frac{\mathrm{d}y'}{\beta\omega - 2y'}D(y')\tanh\frac{y'}{2} + \phi + O\left(\frac{T}{T_{\mathrm{F}}}\right) \tag{251}$$

where $\overline{\mathcal{A}_{\uparrow\downarrow}}(\Lambda) = \overline{\mathcal{A}_{\uparrow\downarrow}}(p_{\mathrm{F}}, p_{\mathrm{F}}, \Lambda)$. The only remaining energy dependence on the right-hand side is the integration interval $[-\frac{\beta\Lambda}{2}+y, \frac{\beta\Lambda}{2}+y]$ whose centre is shifted from 0 by y. To leading order in $1/\beta\Lambda$, we can then approximate the pair field D by a constant

$$D(y) = D_0 + O\left(\frac{y}{\beta\Lambda}\right) \tag{252}$$

The integral equation is now trivial, and yields the pair susceptibility

$$\chi_{\mathrm{pair}}(\omega) \equiv \frac{D_0(\omega)}{\phi} = \frac{1/\overline{\mathcal{A}_{\uparrow\downarrow}}(\Lambda)}{1/\overline{\mathcal{A}_{\uparrow\downarrow}}(\Lambda) + \frac{m^* p_{\mathrm{F}}}{2\pi^2}\mathcal{N}_\Lambda(\omega)} \tag{253}$$

with $\mathcal{N}_\Lambda(\omega)$ defined as:

$$\mathcal{N}_\Lambda(\omega) = \int_{-\beta\Lambda/2}^{\beta\Lambda/2}\frac{\mathrm{d}y'}{2y' - \beta\omega}\tanh\frac{y'}{2} \tag{254}$$

The critical temperature can finally be determined by applying Thouless' criterion to the pair susceptibility:

$$\chi^{-1}_{\mathrm{pair}}(\omega = 0, T = T_c) = 0 \iff \frac{1}{\overline{\mathcal{A}_{\uparrow\downarrow}}(\Lambda)} + \frac{m^* p_{\mathrm{F}}}{2\pi^2}\mathcal{N}_\Lambda(0, T_c) = 0 \tag{255}$$

In the limit where $\beta\Lambda \gg 1$, the integral $\mathcal{N}_\Lambda(0)$ diverges logarithmically

$$\mathcal{N}_\Lambda(0, T) = \ln\left(\frac{\Lambda}{\pi T}\right) + \gamma + O\left(\frac{T}{\Lambda}\right) \tag{256}$$

where $\gamma \approx 0.577$ is the Euler-Mascheroni constant. This divergence is compensated by a divergence of the s-wave pairing amplitude, which we write generically as

$$\frac{1}{\overline{\mathcal{A}_{\uparrow\downarrow}}(\Lambda)} = -\frac{m^* p_{\mathrm{F}}}{2\pi^2}\left(\ln\frac{\Lambda}{\epsilon_{\mathrm{F}}} + \alpha_{\uparrow\downarrow}\right) + O\left(\frac{\Lambda}{\epsilon_{\mathrm{F}}}\right) \tag{257}$$

This expression of $1/\overline{\mathcal{A}_{\uparrow\downarrow}}(\Lambda)$ in the s-wave channel was postulated by Popov [51] and demonstrated (in 2D and for all Fourier component m of $\mathcal{A}_{\uparrow\downarrow}(\theta)$) by Chitov and Sénéchal [10] using the renormalisation group flow. We introduced here an effective parameter $\alpha_{\uparrow\downarrow}$ of the low-energy theory, which we interpreted as the background value of $1/\overline{\mathcal{A}_{\uparrow\downarrow}}$, over which the logarithmic divergence develops. This parameter sets the critical temperature to

$$\frac{T_{\rm c}}{T_{\rm F}} = \frac{{\rm e}^{\gamma}}{\pi}\,{\rm e}^{-\alpha_{\uparrow\downarrow}} \tag{258}$$

This relation is valid generically in Fermi liquids subject to a weak superfluid instability. It is non-perturbative and exact if the effective parameter $\alpha_{\uparrow\downarrow}$ is known exactly rather than expanded in powers of the interaction strength; $\alpha_{\uparrow\downarrow}$ must however remain large and positive to maintain the validity of the quasiparticle picture, through the inequality $T_c \ll T_{\rm F}$.

Remark that the pairing amplitude must be attractive, $\overline{\mathcal{A}_{\uparrow\downarrow}} < 0$, to trigger the superfluid transition. It must also display a logarithmic divergence with Λ, which does not seem guaranteed, for example if the bare potential vanishes for head-on collisions: $V(\mathbf{p},-\mathbf{p}|\mathbf{p}',-\mathbf{p}') = 0$. In this case, there is no divergence in the pair susceptibility (on the contrary, it is logarithmically suppressed with Λ), i.e. there is no superfluid phase.

Extending our low-energy effective theory further into the superfluid phase, we now calculate the order parameter at $T = 0$, through the gap equation:

$$\Delta(\mathbf{p}) = -\sum_{\mathbf{p}'} \mathcal{A}_{\uparrow\downarrow}(\mathbf{p},-\mathbf{p}|\mathbf{p}',-\mathbf{p}') \frac{\Delta(\mathbf{p}')}{2\sqrt{(\epsilon_{\mathbf{p}'}-\mu)^2 + \Delta^2(\mathbf{p}')}} \tag{259}$$

Computing the integral restricted to the low-energy region, and assuming the logarithmically divergent expression (257) of $\overline{\mathcal{A}_{\uparrow\downarrow}}$ we obtain

$$\frac{\Delta}{\epsilon_{\rm F}} = {\rm e}^{-\alpha_{\uparrow\downarrow}} \tag{260}$$

The ratio $\Delta/T_c = \pi/{\rm e}^{\gamma} \simeq 1.764$ found by BCS theory is thus universal to all superfluids made of Landau quasiparticles [52]; it is well verified in superfluid ^{3}He [53], even though the fluid is strongly interacting ($F_0^+ > 10$). Deviations from the BCS ratio (as *e.g.* in a unitary Fermi gas [54, 55]) may then be interpreted as evidences of a non-Fermi liquid behavior.

3.3 Application to the contact Fermi gas: the Gor'kov-Melik-Barkhudarov correction to T_c

We return to the Fermi gas with contact interactions. BCS theory describes pairing of particles under the effect of the bare interactions, which provides a first approximation of the critical temperature:

$$\frac{T_{\rm c}^{\rm BCS}}{T_{\rm F}} = \frac{8{\rm e}^{\gamma-2}}{\pi}\,{\rm e}^{\pi/2k_{\rm F}a} \tag{261}$$

This perturbative expression is valid to leading order in $k_{\rm F}a$ for $\ln(T_c/T_{\rm F})$. Therefore, it makes an uncontrolled error on $T_c/T_{\rm F}$. To go beyond BCS approximation, Gor'kov and Melik-Barkhudarov [37] performed a second-order diagrammatic calculation, in which they introduce in particular a dressed Green's function and an effective interaction.

The GMB correction is often understood [56–58] as the result of the screening of the pairing interactions among particles. Our low-energy effective theory provides a simple and more general interpretation of the corrections to the BCS gap and critical temperature as the result of the renormalisation of the particles into Landau quasiparticles. In this picture, the GMB correction follows from a second order calculation of the effective parameters of the theory, in particular of $\mathcal{A}_{\uparrow\downarrow}$.

Averaging expression (94) of $\mathcal{A}_{\uparrow\downarrow}$ over $\theta_{13} = \alpha$ and for $\theta_{12} = \pi$ yields

$$\overline{\mathcal{A}_{\uparrow\downarrow}}(\Lambda) = g + g^2 \frac{m^* p_{\rm F}}{2\pi^2} \left[\ln \frac{\Lambda}{E_{\rm F}} + \frac{7}{3}(1 - 2\ln 2) \right] + O(g^3) \tag{262}$$

We may now identify the parameter $\alpha_{\uparrow\downarrow}$ in the expansion of $1/\overline{\mathcal{A}_{\uparrow\downarrow}}(\Lambda)$:

$$\alpha_{\uparrow\downarrow} = -\frac{\pi}{2k_{\rm F}a} - \frac{7}{3}(\ln 2 - 1) + O(k_{\rm F}a) \tag{263}$$

This pairing parameter is large and positive to leading order in $k_{\rm F}a < 0$, which guarantees the existence of a (weak) superfluid phase. It is however reduced by the second-order correction which weakens superfluidity, and reduces the critical temperature:

$$T_{\rm c}^{\rm GMB} = \frac{{\rm e}^{\gamma}}{\pi} \left(\frac{2}{\rm e} \right)^{7/3} {\rm e}^{\pi/2k_{\rm F}a}\, T_{\rm F} = \frac{T_c^{\rm BCS}}{(4{\rm e})^{1/3}} \tag{264}$$

with $(4{\rm e})^{1/3} \approx 2.2$. Corrections beyond GMB stemming from the third-order calculation of $\alpha_{\uparrow\downarrow}$ are small, *i.e* of order $O(k_{\rm F}a)$, in both $T_c/T_{\rm F}$ and $\ln(T_c/T_{\rm F})$.

Whereas the corrections to second order in $k_{\rm F}a$ coming from the renormalisation of particles into quasiparticles involve only the $\mathcal{A}_{\uparrow\downarrow}$ collision amplitude, and can therefore be understood as a "screening" effect, we note that this picture is not general and would fail to capture corrections to e.g. the effective mass to higher order in $k_{\rm F}a$ or in more complex fermionic fluids.

Conclusion

Using a new renormalisation scheme, we have formulated an intuitive and controlled construction of the Landau quasiparticles and the effective Hamiltonian governing their dynamics. Instead of the usual momentum cutoff, we introduce an energy cutoff Λ that separates resonant from off-resonant couplings. In this framework, we interpret the quasiparticle annihilation operator $\hat{\gamma}$ as the bare operator $\hat{a}$ dressed only by the off-resonant couplings. This dressing is implemented through a unitary transformation, which becomes a Continuous Unitary Transformation (CUT) in the limit of infinitesimal variations of Λ.

To truncate the infinite series generated when expressing the Hamiltonian in terms of $\hat{\gamma}$ and $\hat{\gamma}^\dagger$, we introduced the fluctuations of the density field $\delta(\hat{\gamma}_\alpha^\dagger \hat{\gamma}_\beta)$ around its Fermi-sea expectation value. Truncated to terms quadratic in these fluctuations, our effective Hamiltonian contains the functional of Fermi liquid theory via the diagonal terms ($\alpha = \beta$). Crucially, the same truncation also retains the full collision amplitude $\mathcal{A}_{\sigma\sigma'}(\mathbf{p}_1, \mathbf{p}_2 | \mathbf{p}_3, \mathbf{p}_4)$ encoded in the off-diagonal terms $\alpha \neq \beta$. This provides a single Hamiltonian describing both the interactions and the collisions of Landau quasiparticles, unifying ingredients that are usually treated separately. The interaction function f, the forward scattering amplitude and the BCS pairing amplitude appear as different limits of a general amplitude $\mathcal{A}$ regularized by Λ.

Armed with this effective Hamiltonian, we proposed a demonstration of the quasiparticle Boltzmann equation exploiting the validity of the Born-Markov approximation in the quasiparticle picture. We solved this Boltzmann equation exactly from the collisionless to the hydrodynamic regime by decomposing the quasiparticle distribution on a basis of orthogonal functions. Applying the effective picture to an atomic Fermi gas with contact interactions, we showed how the use of Landau quasiparticles systematically improves the weak-coupling approximations, in particular the RPA approximation on the speed of zero sound c_0, and the BCS approximation on the superfluid gap and critical temperature. In particular the celebrated Gork'ov-Melik Barkhudarov log-perturbative correction to T_c and Δ emerges here as a direct manifestation of the quasiparticle dressing.

Extensions of this work could address the hydrodynamic regime where a normal quasiparticle fluid and a quasiparticle condensate coexist. The Boltzmann and pairing equations derived here in the normal phase are a natural starting point for a microscopic derivation of the two-fluid hydrodynamics of Fermi systems [34, 59]. More generally, the concept of Landau quasiparticles is not restricted to unbalanced spin-1/2 Fermi systems, and applies more generally to quasiparticles whose low-energy spectrum ressemble that of the free particle, as *e.g.* the Bose [60] and Fermi polarons [61]. Our renormalization scheme could serve to derive an effective Hamiltonian for such quasiparticles, including static interactions and collision amplitudes.

Acknowledgements

Fruitful discussions with Nicolas Dupuis are gratefully acknowledged.

Funding information H.K. acknowledges support from the French Agence Nationale de la Recherche (ANR), under grant ANR-23-ERCS-0005 (project DYFERCO).

A Λ dependence of the collision amplitudes

In this appendix, we detail the calculation of the functions I_Λ and J_Λ introduced in Sec. 1.2.4 (see also Figs. 2 and 3) to characterize the angular dependence of $\mathcal{B}_{\sigma\sigma'}$. Comparing Eqs. (81)–(82) and Eqs. (86)–(87), we identify the dimensionless coefficients of the $O(k_\mathrm{F}a)^2$ terms in $\mathcal{B}_{\sigma\sigma'}$:

$$I_\Lambda(\mathbf{p},\mathbf{p}') = \frac{(2\pi)^2\epsilon_\mathrm{F}}{(p_\mathrm{F}L)^3}\sum_{\mathbf{p}_1\mathbf{p}_2\in\mathcal{D}}\left[n^0_{\mathbf{p}_1}+n^0_{\mathbf{p}_2}\right]\delta^{\mathbf{p}_1+\mathbf{p}_2}_{\mathbf{p}+\mathbf{p}'}\mathcal{P}_\Lambda\left(\frac{1}{\omega_{\mathbf{p}_1}+\omega_{\mathbf{p}_2}-2\epsilon_\mathrm{F}}\right) \tag{265}$$

$$J_\Lambda(\mathbf{p},\mathbf{p}') = -\frac{(2\pi)^2\epsilon_\mathrm{F}}{(p_\mathrm{F}L)^3}\sum_{\mathbf{p}_1\mathbf{p}_2\in\mathcal{D}}\left[n^0_{\mathbf{p}_1}-n^0_{\mathbf{p}_2}\right]\delta^{\mathbf{p}_2+\mathbf{p}}_{\mathbf{p}_1+\mathbf{p}'}\mathcal{P}_\Lambda\left(\frac{1}{\omega_{\mathbf{p}_1}-\omega_{\mathbf{p}_2}}\right) \tag{266}$$

With $p=p'=p_\mathrm{F}$, the functions depend on $\mathbf{p}$ and $\mathbf{p}'$ only through the angle $\alpha=\widehat{(\mathbf{p},\mathbf{p}')}$. We eliminate $\mathbf{p}_2$ through momentum conservation and locate $\mathbf{p}_1$ in a spherical frame with $\mathbf{p}+\mathbf{p}'$ or $\mathbf{p}-\mathbf{p}'$ as the z-axis respectively in I_Λ and J_Λ. Exploiting the invariance on the azimuthal angle, parameterizing the polar angle by $u=\cos\theta_1$, and introducing the dimensionless momentum $x=p_1/p_\mathrm{F}$, we write

$$I_\Lambda(\theta) = -2\int_0^1 x^2\mathrm{d}x\int_{-1}^1 \mathrm{d}u\mathcal{P}_\epsilon\left(\frac{1}{2(2cxu-x^2-2c^2+1)}\right) \tag{267}$$

$$J_\Lambda(\theta) = -2\int_0^1 x^2\mathrm{d}x\int_{-1}^1 \mathrm{d}u\mathcal{P}_\epsilon\left(\frac{1}{4(xsu-s^2)}\right) \tag{268}$$

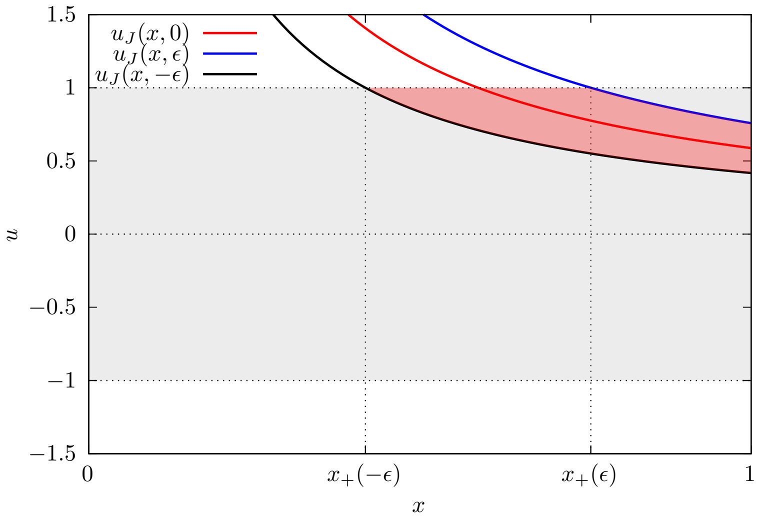

Figure 12: The resonance angle $u_J(x,\epsilon=0)$ (red curve) and the forbidden band $x\mapsto[u_J(x,-\epsilon),u_J(x,\epsilon)]$ (red area) inside the integration domain $[0,1]\times[-1,1]$ (grey area) for J_Λ at $\alpha=0.4\pi$ and $\epsilon=0.1$.

where $\mathcal{P}_\epsilon(1/f)=\Theta(|f|-\epsilon)/f$ is the ϵ–regularized principal part. We parametrize the small parameter associated to Λ using

$$\epsilon=\frac{\Lambda}{4\epsilon_\mathrm{F}},\qquad \epsilon'=2\epsilon \tag{269}$$

where ϵ coincides with the ϵ_Λ used in the main text. We have also parametrized the α-dependence through

$$c \;=\; \cos\frac{\alpha}{2}=\frac{||\mathbf{p}+\mathbf{p}'||}{2p_\mathrm{F}} \tag{270}$$

$$s \;=\; \sin\frac{\alpha}{2}=\frac{||\mathbf{p}-\mathbf{p}'||}{2p_\mathrm{F}} \tag{271}$$

The ϵ-principal part excludes a region of the integration domain $[0,1]\times[-1,1]$, and this forbidden band varies with α and ϵ. To identify the excluded region in the integration interval $[-1,1]$ over u, we introduce the resonance angles

$$u_I(x,\epsilon') \;=\; \frac{x^2+2c^2-1+\epsilon'}{2cx} \tag{272}$$

$$u_J(x,\epsilon) \;=\; \frac{s^2+\epsilon}{sx} \tag{273}$$

The ϵ-resonance conditions then read $u_I(x,-\epsilon')\le u\le u_I(x,\epsilon')$ and $u_J(x,-\epsilon)\le u\le u_J(x,\epsilon)$, which allows to rewrite I and J as:

$$I_\Lambda(\theta) \;=\; -\int_0^1\frac{x\mathrm{d}x}{2c}\int_{-1}^1\frac{\mathrm{d}u}{u-u_I(x,0)}\Big(1-\Theta\big[u_I(x,\epsilon')-u\big]\Theta\big[u-u_I(x,-\epsilon')\big]\Big) \tag{274}$$

$$J_\Lambda(\theta) \;=\; -\int_0^1\frac{x\mathrm{d}x}{2s}\int_{-1}^1\frac{\mathrm{d}u}{u-u_J(x,0)}\left(1-\Theta[u_J(x,\epsilon)-u]\Theta[u-u_J(x,-\epsilon)]\right) \tag{275}$$

Fig. 12 shows an example of the forbidden band in the calculation of J_Λ at $\alpha=0.4\pi$ and $\epsilon=0.1$.

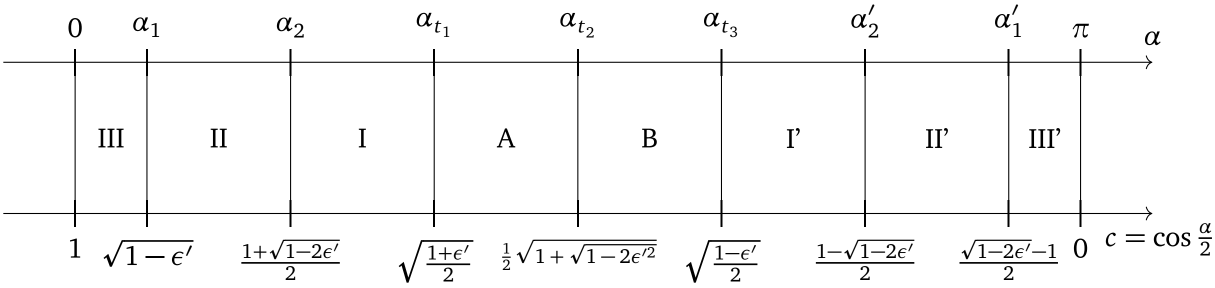

Figure 13: As α varies from 0 to π, I_Λ assumes 8 different expressions (Eqs. (280)–(287)). The corner points α_n that separate these expressions are given by $\cos\frac{\alpha_n}{2} = i_n(\epsilon')$, where $i_n(\epsilon')$ is given on the lower axis.

Expression of I_Λ Depending on the comparison of $u_I(x,\pm\epsilon')$ with ± 1, the excluded band may be $\emptyset$, the interval $[u_I(x,-\epsilon'), u_I(x,\epsilon')]$, $[u_I(x,-\epsilon'),1]$, $[-1,u_I(x,\epsilon'),1]$ or $[-1,1]$. Upon integration over u, this generates 3 different integrands of x:

$$f(x) = -\frac{x}{2c}\int_{-1}^{1}\frac{\mathrm{d}u}{u-u_I(x,0)} = \frac{x}{2c}\ln\left|\frac{(c+s+x)(c-s+x)}{(c+s-x)(c-s-x)}\right| \tag{276}$$

$$f_{+\epsilon'}(x) = -\frac{x}{2c}\int_{u_I(x,\epsilon')}^{1}\frac{\mathrm{d}u}{u-u_I(x,0)} = \frac{x}{2c}\ln\left|\frac{\epsilon'}{(c+s-x)(c-s-x)}\right| \tag{277}$$

$$f_{-\epsilon'}(x) = -\frac{x}{2c}\int_{-1}^{u_I(x,-\epsilon')}\frac{\mathrm{d}u}{u-u_I(x,0)} = \frac{x}{2c}\ln\left|\frac{(c+s+x)(c-s+x)}{\epsilon'}\right| \tag{278}$$

Note that f also describes the integral for $u \in [-1,u_I(x,-\epsilon')] \cup [u_I(x,\epsilon'),1]$. The remaining integral over x is divided in up to 4 intervals, where either one of the functions f, $f_{+\epsilon'}$ or $f_{-\epsilon'}$ is used. The bounds delimiting these intervals (see Fig. 12) are

$$x_\pm(\epsilon') = c \pm \sqrt{s^2-\epsilon'} \tag{279}$$

Again, depending on α, the boundaries $x_\pm(\pm\epsilon')$ maybe inside or outside the integration interval $[0,1]$ over x. This generates 8 different slicing configurations of $[0,1]$, listed in function of α on Fig. 13. The corresponding expression of I_Λ is given in Eqs. (280)–(287). We stitch together these expressions over the domain of variation $[0,\pi]$ of α to produce the red curve in Fig. 2 of the main text.

$$I_\Lambda^{\mathrm{III}} = \int_0^{x_-(-\epsilon')} \mathrm{d}x f(x) + \int_{x_-(-\epsilon')}^{1} \mathrm{d}x f_{-\epsilon'}(x) \tag{280}$$

$$I_\Lambda^{\mathrm{II}} = \int_0^{x_-(-\epsilon')} \mathrm{d}x f(x) + \int_{x_-(-\epsilon')}^{x_-(\epsilon')} \mathrm{d}x f_{-\epsilon'}(x) + \int_{x_-(\epsilon')}^{x_+(\epsilon')} \mathrm{d}x f(x) + \int_{x_+(\epsilon')}^{1} \mathrm{d}x f_{-\epsilon'}(x) \tag{281}$$

$$I_\Lambda^{\mathrm{I}} = \int_0^{x_-(-\epsilon')} \mathrm{d}x f(x) + \int_{x_-(-\epsilon')}^{x_-(\epsilon')} \mathrm{d}x f_{-\epsilon'}(x) + \int_{x_-(\epsilon')}^{1} \mathrm{d}x f(x) \tag{282}$$

$$I_\Lambda^{\mathrm{A}} = \int_{|x_-(-\epsilon')|}^{x_-(\epsilon')} \mathrm{d}x f_{-\epsilon'}(x) + \int_{x_-(\epsilon')}^{1} \mathrm{d}x f(x) \tag{283}$$

$$I_\Lambda^{\mathrm{B}} = \int_{x_-(\epsilon')}^{|x_-(-\epsilon')|} \mathrm{d}x f_{+\epsilon'}(x) + \int_{|x_-(-\epsilon')|}^{1} \mathrm{d}x f(x) \tag{284}$$

$$I_\Lambda^{\mathrm{I}'} = \int_0^{|x_-(\epsilon')|} \mathrm{d}x f(x) + \int_{|x_-(\epsilon')|}^{|x_-(-\epsilon')|} \mathrm{d}x f_{+\epsilon'}(x) + \int_{|x_-(-\epsilon')|}^{1} \mathrm{d}x f(x) \tag{285}$$

$$I_\Lambda^{\mathrm{II}'} = \int_0^{|x_-(\epsilon')|} \mathrm{d}x f(x) + \int_{|x_-(\epsilon')|}^{|x_-(-\epsilon')|} \mathrm{d}x f_{+\epsilon'}(x) + \int_{|x_-(-\epsilon')|}^{x_+(\epsilon')} \mathrm{d}x f(x) + \int_{x_+(\epsilon')}^{1} \mathrm{d}x f_{-\epsilon'}(x) \tag{286}$$

$$I_\Lambda^{\mathrm{III}'} = \int_0^{|x_-(\epsilon')|} \mathrm{d}x f(x) + \int_{|x_-(\epsilon')|}^{x_+(-\epsilon')} \mathrm{d}x f_{+\epsilon'}(x) \tag{287}$$

Expression of J_Λ Similarly, for J_Λ, the excluded band in u is either $\emptyset$, $[u_J(x,-\epsilon), u_J(x,\epsilon)]$, $[u_J(x,-\epsilon), 1]$ or $[-1,1]$, and the corresponding integrands are

$$g(x) = -\frac{x}{2s}\int_{-1}^{1} \frac{\mathrm{d}u}{u-u_J(x,0)} = \frac{x}{2s}\ln\left|\frac{x+s}{x-s}\right| \tag{288}$$

$$g_{-\epsilon}(x) = -\frac{x}{2s}\int_{-1}^{u_J(x,-\epsilon)} \frac{\mathrm{d}u}{u-u_J(x,0)} = \frac{x}{2s}\ln\left|\frac{x+s}{2\epsilon}\right| \tag{289}$$

The interval [0,1] of integration over x is divided by the boundaries

$$x_\pm(\epsilon) = \pm\left(s + \frac{\epsilon}{s}\right) \tag{290}$$

into 5 possible configurations listed in Fig. 14. The corresponding expressions of J_Λ are

$$J_\Lambda^{\mathrm{I}} = 0 \tag{291}$$

$$J_\Lambda^{\mathrm{II}} = \int_{x_-(-\epsilon)}^{1} \mathrm{d}x\, g_{-\epsilon}(x) \tag{292}$$

$$J_\Lambda^{\mathrm{III}} = \int_{x_-(-\epsilon)}^{x_+(\epsilon)} \mathrm{d}x\, g_{-\epsilon}(x) + \int_{x_+(\epsilon)}^{1} \mathrm{d}x\, g(x) \tag{293}$$

$$J_\Lambda^{\mathrm{IV}} = \int_0^{x_+(-\epsilon)} \mathrm{d}x\, g(x) + \int_{x_+(-\epsilon)}^{x_+(\epsilon)} \mathrm{d}x\, g_{-\epsilon}(x) + \int_{x_+(\epsilon)}^{1} \mathrm{d}x\, g(x) \tag{294}$$

$$J_\Lambda^{\mathrm{V}} = \int_0^{x_+(-\epsilon)} \mathrm{d}x\, g(x) + \int_{x_+(-\epsilon)}^{1} \mathrm{d}x\, g_{-\epsilon}(x) \tag{295}$$

$$\tag{296}$$

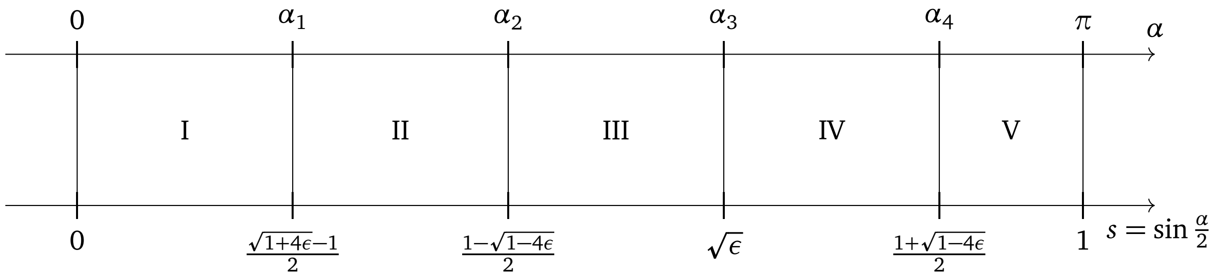

Figure 14: As α varies from 0 to π, J_Λ assumes 5 different expressions (Eqs. (291)–(295)). The corner points α_n that separate these expressions are given by $\sin\frac{\alpha_n}{2} = j_n(\epsilon)$, where $j_n(\epsilon)$ is given on the lower axis.

Combined as prescribed by Fig. 13, these expressions produce the red curve in Fig. 3 of the main text. Note that the $\epsilon = 0$ expressions of I and J (Eqs. (88)–(89)) are given by

$$I(\alpha) = \int_0^1 \mathrm{d}x f(x) \tag{297}$$

$$J(\alpha) = \int_0^1 \mathrm{d}x g(x) \tag{298}$$

B Numerical evaluation of the zero sound velocity

We present in this appendix the numerical method used to solve (198), and benchmark the analytic solution (208) of the prefactor $\exp(\gamma_1^\pm)$ in $c_0^\pm$

Recall that the transport equation for $\nu_\pm$ in the collisionless limit projects as:

$$\nu_\pm^l(c) - \sum_{l'} A_{ll'}^\pm(c)\nu_\pm^{l'}(c) + B_{l0}(c) = 0 \tag{299}$$

As mentioned in the main text, to compute c_0, we look for the zeros of the following determinant:

$$\mathrm{Det}\left(1 - \mathcal{A}_\pm(c_0^\pm)\right) = 0 \tag{300}$$

To do so, we truncate the matrix $\mathcal{A}_\pm$ at some l_{max}, and we check the convergence with respect to this parameter. Typically, $l_{\mathrm{max}} \approx 50$ is sufficient. To overcome the numerical limitation to $|k_\mathrm{F}a| > 0.1$, we perform a second-order polynomial extrapolation $\gamma^\pm + 2 - \pi/\bar{a} = A + B\bar{a} + C\bar{a}^2$.

We find that $\gamma_1^\pm = \pm 4$ within the numerical accuracy of our extrapolation. The coefficient B obtain from the extrapolation of $\gamma_1^\pm$ is larger than one, which restrict the observability of $\gamma_1^\pm$ to $|\bar{a}| < 0.1$.

We present in Figs. 15 and 16 these numerical interpolations.

C Collision effects in the collisionless regime

In this appendix we present the calculation of the function $C_\pm$ introduced (220):

$$C_\pm(c) = \int_0^\pi \mathrm{d}\theta \, \frac{\sin\theta\cos\theta}{(c-\cos\theta)^2} + \int_0^{2\pi}\frac{\mathrm{d}\phi'}{2\pi}\int_0^\pi \mathrm{d}\theta\mathrm{d}\theta' \, \frac{\sin\theta\sin\theta'\cos\theta'}{(c-\cos\theta)(c-\cos\theta')}\mathcal{N}_\pm(\alpha) \tag{301}$$

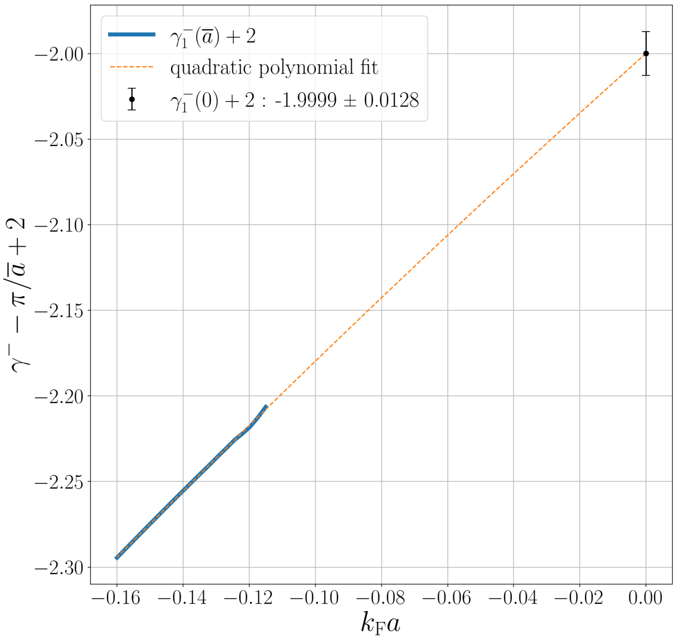

Figure 15: The reduced speed of the collisionless polarisation sound $\gamma^- + 2 - \pi/\bar{a}$ with $\gamma^- = \log((c_0^- - 1)/2)$. The blue curve is obtained by numerically solving (300) in the range $k_F a = -0.16, -0.125$. A quadratic polynomial fit (orange curve) provides the value extrapolated to $k_F a = 0$: $\gamma_1^- + 2 = -1.9999 \pm 0.0128$.

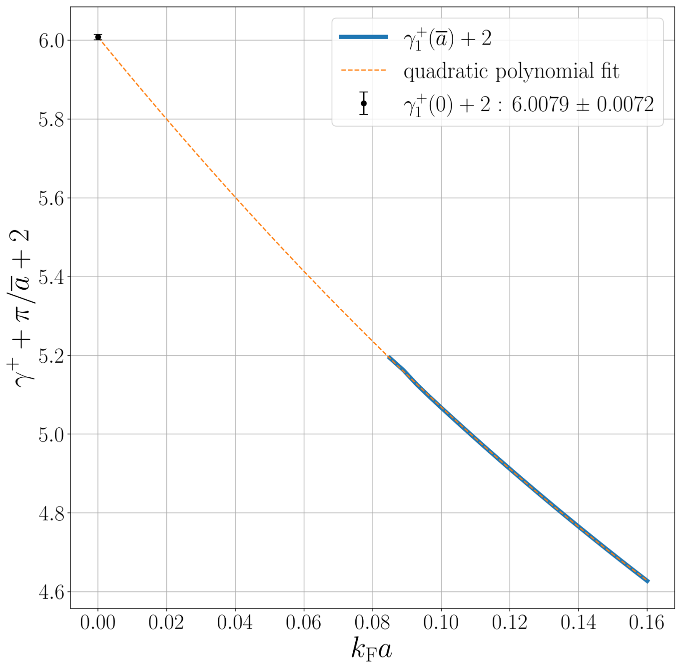

Figure 16: The reduced speed of the collisionless density sound $\gamma^+ + 2 + \pi/\bar{a}$ with $\gamma^+ = \log((c_0^+ - 1)/2)$. The blue curve is obtained by numerically solving (300) in the range $k_F a = 0.16, 0.085$. A quadratic polynomial fit (orange curve) provides the value extrapolated to $k_F a = 0$: $\gamma_1^+ + 2 = 6.0079 \pm 0.0072$.

with the angular collision kernel and its projection on Legendre polynomials given by:

$$\mathcal{N}_\pm(\alpha) = \frac{\Omega_{E\pm}(\alpha) - 2\Omega_{S\pm}(\alpha)}{\Omega_\Gamma} = \sum_l \mathcal{N}_\pm^l(\alpha) P_l(\cos\alpha) \tag{302}$$

We use the addition theorem:

$$\int_0^{2\pi} \frac{\mathrm{d}\phi'}{2\pi} P_l(\cos(\alpha)) = P_l(\cos\theta) P_l(\cos\theta') \tag{303}$$

This allows us to factorize the integrals over $u = \cos\theta$ and $u' = \cos\theta'$ in $C_\pm$:

$$C_\pm(c) = \int_{-1}^{1} \mathrm{d}u \, \frac{u}{(c-u)^2} + \sum_l \mathcal{N}_\pm^l \int_{-1}^{1} \mathrm{d}u \, \frac{P_l(u)}{c-u} \int_{-1}^{1} \mathrm{d}u' \, \frac{u' P_l(u')}{c-u'} \tag{304}$$

The different integrals are given by:

$$\int_{-1}^{1} \mathrm{d}u \, \frac{u}{(c-u)^2} = -B'_{00}(c) \tag{305}$$

$$\int_{-1}^{1} \mathrm{d}u \, \frac{P_l(u)}{c-u} = 2R_l(c) \tag{306}$$

$$\int_{-1}^{1} \mathrm{d}u' \, \frac{u' P_l(u')}{c-u'} = 2cR_l(c) - 2\delta_{l,0} \tag{307}$$

where we have introduced the Legendre functions of the second kind [62]. The contribution of collisions is therefore finally contained in the following formula:

$$C_\pm(c) = -B'_{00}(c) + 4\sum_l \mathcal{N}_\pm^l R_l(c)(cR_l(c) - \delta_{l,0}) \tag{308}$$

In fact, this last formula is quite general, as the characteristics of the interactions are contained in the collision parameter $\mathcal{N}_\pm^l$. We can now focus on the asymptotic behavior when c tends exponentially to 1. Note that:

$$\frac{R_0(c)(cR_0(c) - 1)}{B'_{00}(c)} \underset{\gamma\to-\infty}{\sim} -\gamma^2 \mathrm{e}^\gamma \tag{309}$$

Similarly, for $l > 0$:

$$\frac{R_l^2(c)}{B'_{00}(c)} \underset{\gamma\to-\infty}{\sim} -\gamma^2 \mathrm{e}^\gamma \tag{310}$$

In all cases, we can rewrite the function $C_\pm$ in the limit where c tends exponentially to 1 as:

$$C_\pm(c) \simeq -B'_{00}(c)\left(1 + 4\gamma^2(c)\mathrm{e}^\gamma \, \mathcal{N}_\pm(0)\right) \tag{311}$$

where we have recognized that $\sum_l \mathcal{N}_\pm^l = \mathcal{N}_\pm(0)$.

References

[1] L. Landau, *The theory of the Fermi Liquid*, Zh. Eksp. Teor. Fiz. **30**, 1058 (1956), [Sov. Phys. JETP, Vol. 3, No. 6, p. 920 (1956)].

[2] P. Nozières and D. Pines, *The theory of quantum liquids*, W.A. Benjamin, New York (1966).

[3] M. Pfitzner and P. Wölfle, *Quasiparticle scattering amplitude for normal liquid ^{3}He*, Journal of Low Temperature Physics **51**(5), 535 (1983), doi:10.1007/BF00683227.

[4] L. Landau, *On the theory of the Fermi liquid*, Zh. Eksp. Teor. Fiz. **35**, 97 (1959), [Sov. Phys. JETP, Vol. 8, No. 1, p. 70 (1959)].

[5] P. Nozières and J. M. Luttinger, *Derivation of the Landau Theory of Fermi Liquids. I. Formal Preliminaries*, Phys. Rev. **127**, 1423 (1962), doi:10.1103/PhysRev.127.1423.

[6] J. M. Luttinger and P. Nozières, *Derivation of the Landau Theory of Fermi Liquids. II. Equilibrium Properties and Transport Equation*, Phys. Rev. **127**, 1431 (1962), doi:10.1103/PhysRev.127.1431.

[7] V. N. Popov, *Functional Integral and Collective Excitations*, Cambridge University Press, Cambridge (1987).

[8] R. Shankar, *Renormalization-group approach to interacting fermions*, Rev. Mod. Phys. **66**, 129 (1994), doi:10.1103/RevModPhys.66.129.

[9] J. Polchinski, *Effective field theory and the Fermi surface*, In J. Harvey and J. Polchinski, eds., *Theoretical Advanced Study Institute (TASI 92): From Black Holes and Strings to Particles*, p. 0235–276. World Scientific, Singapore (1993).

[10] G. Y. Chitov and D. Sénéchal, *Renormalization-group study of interacting electrons*, Phys. Rev. B **52**, 13487 (1995), doi:10.1103/PhysRevB.52.13487.

[11] G. Y. Chitov and D. Sénéchal, *Fermi liquid as a renormalization-group fixed point: The role of interference in the Landau channel*, Phys. Rev. B **57**, 1444 (1998), doi:10.1103/PhysRevB.57.1444.

[12] N. Dupuis, *Fermi liquid theory: a renormalization group approach*, The European Physical Journal B - Condensed Matter and Complex Systems **3**(3), 315 (1998), doi:10.1007/s100510050318.

[13] L. V. Delacrétaz, Y.-H. Du, U. Mehta and D. T. Son, *Nonlinear bosonization of Fermi surfaces: The method of coadjoint orbits*, Phys. Rev. Res. **4**, 033131 (2022), doi:10.1103/PhysRevResearch.4.033131.

[14] H. Ma and S.-S. Lee, *Fermi liquids beyond the forward-scattering limit: The role of nonforward scattering for scale invariance and instabilities*, Phys. Rev. B **109**, 045143 (2024), doi:10.1103/PhysRevB.109.045143.

[15] U. Gran, E. Nilsson and J. Hofmann, *Shear viscosity in interacting two-dimensional Fermi liquids*, arXiv:2312.09977 (2023).

[16] J. Maki, U. Gran and J. Hofmann, *Odd-parity effect and scale-dependent viscosity in atomic quantum gases*, Communications Physics **8**(1), 319 (2025), doi:10.1038/s42005-025-02231-w.

[17] W.-T. Lin and J. A. Sauls, *Effects of incipient pairing on nonequilibrium quasiparticle transport in Fermi liquids*, Progress of Theoretical and Experimental Physics **2022**(3), 033I02 (2022), doi:10.1093/ptep/ptac027.

[18] C. Cohen-Tannoudji, J. Dupont-Roc and G. Grynberg, *Processus d'interaction entre photons et atomes*, InterEditions et Éditions du CNRS, Paris (1988).

[19] J. H. Van Vleck, *On σ-Type Doubling and Electron Spin in the Spectra of Diatomic Molecules*, Phys. Rev. **33**, 467 (1929), doi:10.1103/PhysRev.33.467.

[20] J. R. Schrieffer and P. A. Wolff, *Relation between the Anderson and Kondo Hamiltonians*, Phys. Rev. **149**, 491 (1966), doi:10.1103/PhysRev.149.491.

[21] F. Wegner, *Flow-equations for Hamiltonians*, Annalen der Physik **506**(2), 77 (1994), doi:https://doi.org/10.1002/andp.19945060203.

[22] C. P. Heidbrink and G. S. Uhrig, *Landau's quasiparticle mapping: Fermi liquid approach and luttinger liquid behavior*, Phys. Rev. Lett. **88**, 146401 (2002), doi:10.1103/PhysRevLett.88.146401.

[23] F. Mohling and J. C. Rainwater, *Quasiparticle scattering in Fermi fluids*, Journal of Low Temperature Physics **20**(3), 243 (1975), doi:10.1007/BF00117796.

[24] J. C. Rainwater and F. Mohling, *Transport properties of Fermi fluids at finite temperatures*, Journal of Low Temperature Physics **23**(5), 519 (1976), doi:10.1007/BF00116293.

[25] E. Lipschitz and L. Pitaevskii, *Physical Kinetics*, In *Landau and Lifshitz Course of Theoretical Physics*, vol. 9. Pergamon Press, New York (1981).

[26] A. Sommer, M. Ku, G. Roati and M. W. Zwierlein, *Universal spin transport in a strongly interacting Fermi gas*, Nature **472**(7342), 201 (2011), doi:10.1038/nature09989.

[27] E. Vogt, M. Feld, B. Fröhlich, D. Pertot, M. Koschorreck and M. Köhl, *Scale Invariance and Viscosity of a Two-Dimensional Fermi Gas*, Phys. Rev. Lett. **108**, 070404 (2012), doi:10.1103/PhysRevLett.108.070404.

[28] S. Trotzky, S. Beattie, C. Luciuk, S. Smale, A. B. Bardon, T. Enss, E. Taylor, S. Zhang and J. H. Thywissen, *Observation of the Leggett-Rice Effect in a Unitary Fermi Gas*, Phys. Rev. Lett. **114**, 015301 (2015), doi:10.1103/PhysRevLett.114.015301.

[29] X. Li, J. Huang and J. E. Thomas, *Universal density shift coefficients for the thermal conductivity and shear viscosity of a unitary Fermi gas*, Phys. Rev. Res. **6**, L042021 (2024), doi:10.1103/PhysRevResearch.6.L042021.

[30] S. Huang, Y. Ji, T. Repplinger, G. G. T. Assumpção, J. Chen, G. L. Schumacher, F. J. Vivanco, H. Kurkjian and N. Navon, *Emergence of Sound in a Tunable Fermi Fluid*, Phys. Rev. X **15**, 011074 (2025), doi:10.1103/PhysRevX.15.011074.

[31] E. Egilsson and C. J. Pethick, *The transition from first sound to zero sound in a normal Fermi liquid*, Journal of Low Temperature Physics **29**(1), 99 (1977), doi:10.1007/BF00659091.

[32] P. Taillat and H. Kurkjian, *Exact perturbative expansion of the transport coefficients of a low-temperature normal fermi gas with contact interactions*, Phys. Rev. Lett. (2025), doi:10.1103/c6fd-x57s.

[33] D. Einzel and P. Wölfle, *Transport and relaxation properties of superfluid 3He. I. Kinetic equation and Bogoliubov quasiparticle relaxation rate*, Journal of Low Temperature Physics **32**(1), 19 (1978), doi:10.1007/BF00116904.

[34] D. Vollhardt and P. Wolfle, *The Superfluid Phases of Helium 3*, Taylor & Francis, London (1990).

[35] A. Abrikosov and I. Khalatnikov, *Concerning a Model for a Non-Ideal Fermi Gas*, Sov. Phys. JETP **6**, 888 (1958 [ZhETF, **33**, 1154]).

[36] J. R. Engelbrecht, M. Randeria and L. Zhang, *Landau f function for the dilute Fermi gas in two dimensions*, Phys. Rev. B **45**, 10135 (1992), doi:10.1103/PhysRevB.45.10135.

[37] L. Gor'kov and T. Melik-Barkhudarov, *Contribution to the theory of superfluidity in an imperfect Fermi gas*, Zh. Eksp. Teor. Fiz. **40**(5), 1452 (1958), [Sov. Phys. JETP, **13**, 1018 (1958)].

[38] G. Baym and C. Pethick, *Landau Fermi-liquid theory*, Wiley-VCH (1991).

[39] D. J. Griffiths and D. F. Schroeter, *Introduction to Quantum Mechanics*, Cambridge University Press (2004).

[40] I. Shavitt and L. T. Redmon, *Quasidegenerate perturbation theories. A canonical van Vleck formalism and its relationship to other approaches*, The Journal of Chemical Physics **73**(11), 5711 (1980), doi:10.1063/1.440050.

[41] M. Rigol, V. Dunjko and M. Olshanii, *Thermalization and its mechanism for generic isolated quantum systems*, Nature **452**(7189), 854 (2008).

[42] Y. Castin, *Basic Theory Tools for Degenerate Fermi Gases*, In M. Inguscio, W.Ketterle and C. Salomon, eds., *Ultra-cold Fermi Gases*. Società Italiana di Fisica, Bologna (2007).

[43] F. Chevy, *Universal phase diagram of a strongly interacting Fermi gas with unbalanced spin populations*, Phys. Rev. A **74**, 063628 (2006), doi:10.1103/PhysRevA.74.063628.

[44] V. M. Galitskii, *The energy spectrum of a non-ideal Fermi gas*, Zh. Eksp. Teor. Fiz. **34**, 151 (1958), [Sov. Phys. JETP, **7**, 104 (1958)].

[45] V. Belyakov, *The momentum distribution of particles in a dilute Fermi gas*, Zh. Eksp. Teor. Fiz. **40**, 1210 (1961), [Sov. Phys. JETP, Vol. 13, No. 4, p. 850 (1961)].

[46] R. Sartor and C. Mahaux, *Self-energy, momentum distribution, and effective masses of a dilute Fermi gas*, Phys. Rev. C **21**, 1546 (1980), doi:10.1103/PhysRevC.21.1546.

[47] S. Tan, *Large momentum part of a strongly correlated Fermi gas*, Annals of Physics **323**(12), 2971 (2008), doi:https://doi.org/10.1016/j.aop.2008.03.005.

[48] T. Repplinger, *Density wave in a Fermi gas: phonon and plasmon, from hydrodynamic to collisionless regime*, Ph.D. thesis, Université de Toulouse (2024).

[49] I. Khalatnikov and A. Abrikosov, *Dispersion of Sound in a Fermi Liquid*, Sov. Phys. JETP **6**(1), 84 (1958 [ZhETF, 33, 1, 110]).

[50] T. Repplinger, S. Huang, Y. Ji, N. Navon and H. Kurkjian, *Dispersion of First Sound in a Weakly Interacting Ultracold Fermi Liquid*, Annalen der Physik p. e00181 (2025), doi:https://doi.org/10.1002/andp.202500181.

[51] V. N. Popov, *Bose spectrum of superfluid Fermi gases*, In *Functional Integral and Collective Excitations*, chap. III, section 14. Cambridge University Press, Cambridge (1987).

[52] V. N. Popov, *Perturbation theory for superconducting Fermi systems*, In *Functional Integral and Collective Excitations*, chap. III, section 10. Cambridge University Press, Cambridge (1987).

[53] N. Masuhara, B. C. Watson and M. W. Meisel, *Direct Measurement of the Energy Gap of Superfluid* ^{3}He $-B$ *in the Low-Temperature Limit*, Phys. Rev. Lett. **85**, 2537 (2000), doi:10.1103/PhysRevLett.85.2537.

[54] A. Schirotzek, Y.-i. Shin, C. H. Schunck and W. Ketterle, *Determination of the Superfluid Gap in Atomic Fermi Gases by Quasiparticle Spectroscopy*, Phys. Rev. Lett. **101**, 140403 (2008), doi:10.1103/PhysRevLett.101.140403.

[55] M. J. H. Ku, A. T. Sommer, L. W. Cheuk and M. W. Zwierlein, *Revealing the Superfluid Lambda Transition in the Universal Thermodynamics of a Unitary Fermi Gas*, Science **335**(6068), 563 (2012), doi:10.1126/science.1214987, http://www.sciencemag.org/content/335/6068/563.full.pdf.

[56] H. Heiselberg, C. J. Pethick, H. Smith and L. Viverit, *Influence of Induced Interactions on the Superfluid Transition in Dilute Fermi Gases*, Phys. Rev. Lett. **85**, 2418 (2000), doi:10.1103/PhysRevLett.85.2418.

[57] Q. Chen, *Effect of the particle-hole channel on BCS–Bose-Einstein condensation crossover in atomic Fermi gases*, Scientific Reports **6**(1), 25772 (2016), doi:10.1038/srep25772.

[58] L. Pisani, P. Pieri and G. C. Strinati, *Gap equation with pairing correlations beyond the mean-field approximation and its equivalence to a Hugenholtz-Pines condition for fermion pairs*, Phys. Rev. B **98**, 104507 (2018), doi:10.1103/PhysRevB.98.104507.

[59] I. M. Khalatnikov, *An Introduction to the Theory of Superfluidity*, Perseus Publishing, Cambridge, Massachusetts (2000).

[60] A. Camacho-Guardian and G. M. Bruun, *Landau Effective Interaction between Quasiparticles in a Bose-Einstein Condensate*, Phys. Rev. X **8**, 031042 (2018), doi:10.1103/PhysRevX.8.031042.

[61] H. Hu, B. C. Mulkerin, J. Wang and X.-J. Liu, *Attractive fermi polarons at nonzero temperatures with a finite impurity concentration*, Phys. Rev. A **98**, 013626 (2018), doi:10.1103/PhysRevA.98.013626.

[62] I. S. Gradshteyn and I. M. Ryzhik, *Tables of Integrals, Series, and Products*, Academic Press, San Diego (1994).